INSTITUTO POLITÉCNICO DE BRAGANÇA
Escola Superior de Tecnologia e de Gestão

Computational Model for Timber Connections Exposed to High Temperatures

Abderrahim Aissa

Final Thesis Report Presented to:

Escola Superior de Tecnologia e Gestão

Instituto Politécnico de Bragança

Thesis submitted to fulfil the requirements of Ms.C degree in:

Construction Engineering

Supervised by:

Professor Elza Maria Morais Fonseca

Professor Belkacem Lamri

June 2017

Acknowledgements

To begin, I would like to express my deepest gratitude to my thesis supervisors, Prof. Elza Fonseca and Prof. Belkacem Lamri, for their orientation, trust, availability and encouragement throughout the writing of this work.

More, I must express my very profound gratitude to '**My Family**' and **Aisha** for providing me with unfailing support and continuous encouragement throughout my period of study and through the process of researching and writing this thesis. This accomplishment would not have been possible without them. Thank you.

Finally, I also would like to thank all those who participated in one way or another to the realization of this work.

Computational Model for Timber Connections Exposed to High Temperatures

By:

Abderrahim Aissa

Thesis submitted to fulfill the requirements of MSc degree in:

Construction Engineering

Supervised by:

Prof. Elza Maria Morais Fonseca

Prof. Belkacem Lamri

Abstract:

The aim of this work is to present an approach for wood-wood-wood connections design in double shear at ambient and high temperatures, using dowelled connectors. For each situation, all calculations will be performed to determine the cross-section and the number of dowels. A procedure will be presented to calculate the load carrying capacity per shear plane and per steel fastener, using a glued laminated in birch W-W-W timber GL28h.

The designed connection will be considered unprotected at ambient temperature, and protected for high temperatures. In this study, it is important to determine the type of insulation material and the correct dimension for guarantee a fire resistance time.

All developed study will contribute to the knowledge in these connections, where the wood material represents a complex behaviour in fire situations and the combination with steel dowels intensify the heat conduction inside the material. All proposed methodologies (analytical and numerical) could be used to study W-W-W connections with or without insulation material to assess and contribute for a safe design, at ambient and high temperatures. For mechanical analysis, the obtained numerical results were greater than the analytical results according the Eurocode. For thermal analysis, gypsum plasterboard can be considered as the best insulation material for the connection in study.

Keywords:
W-W-W connections, dowels, insulation, thermal analysis, mechanical analysis.

Modelo computacional para ligações em madeira expostas a altas temperaturas

Abderrahim Aissa

Dissertação para obtenção do grau de Mestre em:

Engenharia da Construção

Realização sobre a supervisão de:

Prof. Doutora Elza Maria Morais Fonseca

Prof. Doutor Belkacem Lamri

Resumo

O objetivo deste trabalho é apresentar uma abordagem para o projeto de ligações em madeira (W-W-W) com cavilhas, submetidas a corte duplo, à temperatura ambiente ou a elevadas temperaturas. Para cada situação em estudo, serão apresentados os cálculos para o projeto da ligação tipo cavilha, avaliando a seção transversal da ligação e o número de elementos de fixação necessários. É apresentado o procedimento para o cálculo da carga resistente no plano de corte e de cada elemento de ligação em aço. A ligação W-W-W é em madeira laminada colada do tipo madeira de bétula, com resistência GL28h.

O projeto da ligação tipo cavilha será considerada não protegida à temperatura ambiente e protegida a altas temperaturas. Neste estudo, é importante determinar o tipo de material de isolamento e a dimensão correspondente para garantir um tempo de resistência ao fogo.

O estudo desenvolvido contribuirá para o conhecimento deste tipo de ligações, uma vez que a madeira apresenta um comportamento complexo em situações de incêndio e a combinação com cavilhas metálicas intensificam a condução de calor para o interior do material. As metodologias propostas (analítica e numérica) podem ser utilizadas para a garantia no projeto com segurança, deste tipo de ligações com cavilha com ou sem material de isolamento, à temperatura ambiente ou temperatura elevada. Na análise mecânica, os resultados numéricos obtidos foram superiores aos resultados analíticos obtidos de acordo com as regras do Eurocódigo. Na análise térmica, a colocação de placas de gesso pode ser considerada como o melhor material de isolamento na ligação de madeira em estudo.

Palavras-chave:
Ligações W-W-W, cavilhas, isolamento, análise térmica, análise mecânica.

Contents

Index of Figures

Index of Tables

Chapter 1

Introduction

1. Introduction

The use of wood, as a structural material, continues to grow far beyond traditional application. As a consequence, it is important to improve the knowledge of the connection behaviour under fire conditions by the continuously increasing demand for timber constructions. Connections, indeed, are often considered as the critical point of timber structures because their resistance and durability mainly depend on the connections joining design of the different structural elements, and because they find themselves subject to localized stresses and strains, and may expose the overall stability of the structure, [1]. Figure 1 shows different connections for several structural members (beam to column) used in construction.

Figure 1: Typical connections by URJURO@URJURO_MEXICO

The main condition for the use of wood in buildings is the adequate fire safety. Wood is one of the combustible building materials who burn on their surface, release energy and thus contribute to fire propagation and the smoke development in case of fire. Also in the presence of fire, timber has a surrounding char layer. This layer has the function of delaying the propagation process temperature to its interior, which can be considered as an insulator, [1].

The high timber vulnerability, due to accidental situation, requires the rigour and the accuracy of the thermal and mechanical assessment and their determination. During an accidental situation, the combustion and the chemical phenomena developed in this type of material are a complex study issue. When timber structures are exposed to high temperatures, the burned wood is transformed in a char layer, which loses all strength, and insulates the core of the element, [2].

When choosing the most appropriate method of timber connections, the most relevant is to consider the quality of joint and the strength requirements.

Traditional and popular connectors or joints are obtained by glue, dowels, nails, screws, bolts and steel plates. These methods have been developed through the time and many different systems using combinations of the various connectors. According this, different connections

types have been developed to be used in building construction, as roof trusses, laminated beams (glued, nailed or a combination of both), wall and portal frames.

Timber must be able to make strong joints as well as having strong spanning ability. This condition is determined by the strength developed parallel or perpendicular to wood grain. If one direction is weaker than the other, then joint strength is reduced. Splitting may occur if the connectors are placed too close to the edge or too close to each other.

The analysis of connections (timber and steel) under fire or high temperatures can be a challenge due their complexity, due various connections types, different geometries, fastener arrangements and also the most important the great variability of the material properties. Wood and steel are materials with characteristics strongly temperature dependent. In this work, using a numerical program based on the finite element method it will become possible to calculate the thermal and mechanical resistance of the timber connections, as an important parameter in compliance with safety rules and design.

In 2013, C. Maraveas, worked with timber connections exposed to fire, verifying performance in connections design and concluding about which are typically the weakest zones in timber construction, determining the overall fire resistance of the structure. Experimental and numerical studies on the fire resistance of typical components, as wood-wood-wood (WWW), wood-steel-wood (WSW) and steel-wood-steel (SWS) connections, were presented and studying the effect of several parameters. Results show that timber connections are extremely vulnerable to fire. The fire rating of unprotected joints loaded axially is typically less than 30 min. So, the most effective solution is the application of fire protection, [3]. Figure 2 shows different types of double-shear timber connections, as referred before.

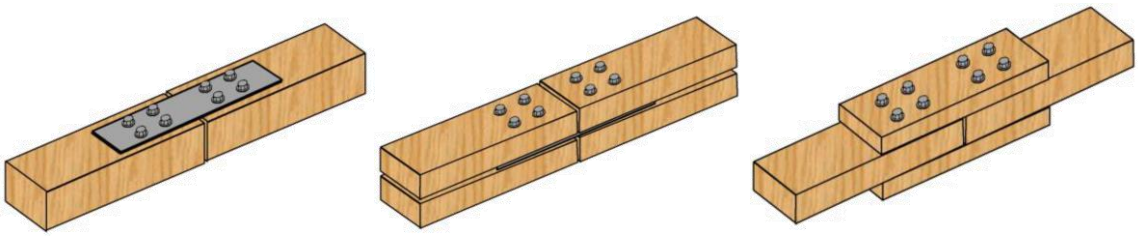

(a) (b) (c)

Figure 2: Double-shear timber connections: (a) steel-wood-steel connection; (b) wood-steel-wood connection; (c) wood-wood-wood connection, [4]

In 2006, J. Branco, P. Cruz and M. Piazza aim to highlight the importance of knowledge of the stiffness and strength of the connections in traditional wood beams. Original connections,

not reinforced, were subjected to static and cyclic testing. Among the unreinforced connections, they are also assessed the influence of the level of pre-compression of the member. The tests in specimens were preceded by an adequate characterization of the wood used in the connections construction. The results of the experimental tests show that capacity depends on the level of compressive stress on the member, however, parameters such as the angle of the components, the width of the connected elements and the friction coefficient are typical conditions to have in attention, [5].

In 2014, L. Dias, also made a study who consists to know the way that traditional joint of roof timber structures act with emphasis to the joint with a single tooth and with two teeth. The main results obtained in this study are that the geometry has a big influence in the transmitted loads, and the critical points of the notch vary the amplitude of the angle between the member and the row of wood, also a larger free end of the wooden truss line allows a decrease in the stress on the edge notch. So, the solutions needed to strengthen this type of slots may be different from each case due the critical sections geometries, [6].

In November 2014, L. Dias, S. Teixeira, E. M. M. Fonseca, presented some different construction solutions with the use of wooden beams in steel profiles sections under fire. The main objective was to study the temperature evolution in transient field in these constructive solutions and choose the best or worst behaviour. They use a numerical program and concluded about the performance as a thermal insulation using wooden beams in the upper profile side, verifying a higher thermal resistance inside in the steel profile, [6].

In 2015, S. I. F. Barbosa, prepared a research in order to understand the mechanisms and factors that influence the global behaviour of the traditional timber connections and evaluate the same connections with reinforced, as metal parts or composite materials. The author observed that the crushing of the fibers in the groove surface was almost common failure mode in all tests, and the deformations in the areas in contact were higher. This phenomenon could introduce a question about its feasibility when applied to a structure. The analytical approaches studied, although they are different when compared to the results of tests, offer very conservative values of the maximum load capacity of connection with single tooth, [7].

Figure 3: Single tooth and two teeth joints, [7]

For timber members and structures, it is possible to use the Eurocode 5, that applies basic rules to the design of buildings and engineering construction. It complies with the principles and requirements for the safety and serviceability of structures and the basis of design, concerning the requirements for mechanical resistance, durability and fire resistance of timber structures, [8].

P.B. Cachim et al., applied the simplified and advanced methods proposed in Eurocode 5 on traditional wood connections under fire action and they observe a good agreement between the analytical calculations and the experimental results. The results showed that the rounding of the cross-sections corners appears to be more pronounced where there is an oldest wood material (with less dense material). And also, the heat flow is perpendicular to the faces tangentially to wood fibers, and the metal screws conduct heat into the section causing an enlargement of the holes, which leads to serious consequences on the performance of connections, [9].

The general objectives of fire protection are to limit risks with respect to the individual and society, neighbouring property, and where required, environment or directly exposed property, in the case of fire, [10]. The construction works must be designed and built in such a way, that in the event of an outbreak of fire:

- the load bearing resistance of the construction can be assumed for a specified period,
- the generation and spread of fire and smoke within the works are limited,
- the spread of fire to neighbouring construction works is limited,
- the occupants can leave the works or can be rescued by other means,
- the safety of rescue teams is taken into consideration.

A structural fire design analysis should consider the following steps as relevant:

- selection of the relevant design fire scenarios (to identify the accidental design situation, the relevant design fire scenarios and the associated design fires should be determined based on a fire risk assessment),
- determination of the corresponding design fires (the design fire should be applied only to one fire compartment of the building at a time, unless otherwise specified in the design fire scenario),
- calculation of temperature evolution within the structural members (the position of the design fire in relation to the member shall be considered, with a nominal temperature-

time curve, the temperature analysis of the structural members is made for a specified period, without any cooling phase, and with a fire model, the temperature analysis of the structural members is made for the full duration of the fire, including the cooling phase),

- calculation of the mechanical behaviour of the structure exposed to fire (it shall be performed for the same duration as used in the temperature analysis, and verification of fire resistance should be in the time, strength or in temperature domain).

In an attempt to present the fire behaviour and resistance of unprotected hybrid connection systems, S. B. A. Boadi (2015) created a system with different materials which are involved in its construction with varying ambient and thermal properties must perform together to ensure a safe and stable structural system. Three different shear double connection systems were studied for two load ratios of 60% and 100%, figure 4. The connection types with side plates (Seated and Exposed Connection Assembly) recorded an average charring rate of 1.09 mm/min as compared to 2.0 mm/min for the other connection type. This confirms the contribution of the slotted in steel plate in advancing the char front to the inner core of the beam at the connections, [11].

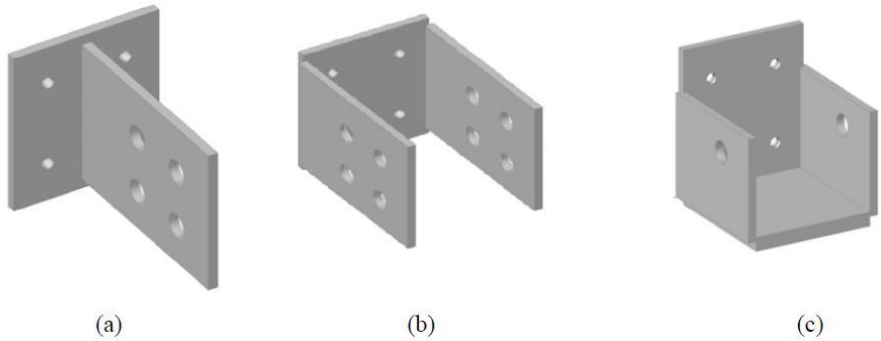

Figure 4: Different connections considered: (a) CN, (b) EX, (c) SE, [11]

In 2014, A. Akotuah Ohene, also considered a typical steel-timber hybrid system. He studied the fire resistance of the connections using a finite element model and compared with the full-scale experimental fire resistance tests which had been conducted earlier in a separate project. The variation between the test and the numerical model results was within a ±11%. The important specifications which were valued in the individual connections were the heat transfer, the temperature development, charring rate of wood, structural damage and the failure, during the fire exposure. In conclusion, the seated connection had a better fire resistance than both the concealed and exposed connections while the exposed connection performed slightly better than the concealed connection, [12].

In 2009, A. Frangi, C. Erchinger and M. Fontana, had made fire tests to analyse two types of steel-to-timber connections. The results show that the unprotected multiple shear steel-to-timber connections with dowels designed for room temperature reached a fire resistance of about 30min. By increasing the side timber members as well as the end distance of the dowels by 40mm, the connections reached a fire resistance of more than 70min. And the unprotected connections with steel side plates and annular ring nails failed after about 12min with large deformations of the nails. And other hand, by protecting the steel side plates using an intumescent paint, the fire resistance of the connections was increased to around 30min, [13].

In 2013, M. Audebert et al, developed a three-dimensional numerical model to simulate the thermo-mechanical behaviour of dowelled and bolted timber to timber connections loaded in tension parallel to grain. The comparison between modelled and experimental nonlinear load–displacement curves reveals that modelling gives satisfactory results regarding the global nonlinear behaviour of the connections. But the comparison under fire exposure presents similar trends, the fire resistance times achieved with the numerical model are always shorter than those observed experimentally with an average relative deviation of 33%, [14].

Lei Peng et al, considered existing calculation models developed in prediction of the fire resistances of double-shear timber connections. A three-dimensional finite-element thermal model was employed to analyse heat transfer within bolted wood-wood-wood (WWW), wood-steel-wood (WSW) and steel-wood-steel (SWS) connections. Comparison with experimental results showed that the method could reasonably predict the fire resistances of WWW and WSW connections with an accuracy of about ± 15% and the method could predict the fire resistances of SWS connections with an accuracy of about ± 10%. In addition, the method can be modified by introducing safety factors to ensure the predictions on the conservative side, [4].

Other typical connections used in construction are two separate pieces of wood and joint up considered to be a joint. There are many possible ways to obtain the joint up of two wood pieces. Some are more applicable to various scenarios than others. Generally, there is three types of timber joints: traditional connections, bonded connections and mechanical connections.

The carpentry joints (traditional) are connected timber elements, usually subjected to compressive axial loads, often without any other devices but notches in the connected members, as represented in figure 5. The carpenter connections are not included in Eurocode 5 and only national regulations are applied. These joints rely on the compression internal forces to keep facing surfaces in close contact.

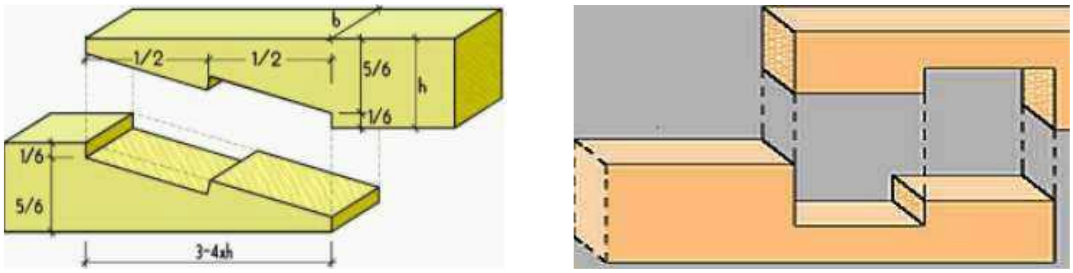

Figure 5: Examples of traditional joints, [16].

Other joints are the glued connections (Bonded), commonly used for connecting new and reinforcing existing members in timber structures represented in figure 6. There are three types of bonded joints: scarf, lateral finger and vertical finger joints. This type of glued connections follows national regulations in design construction.

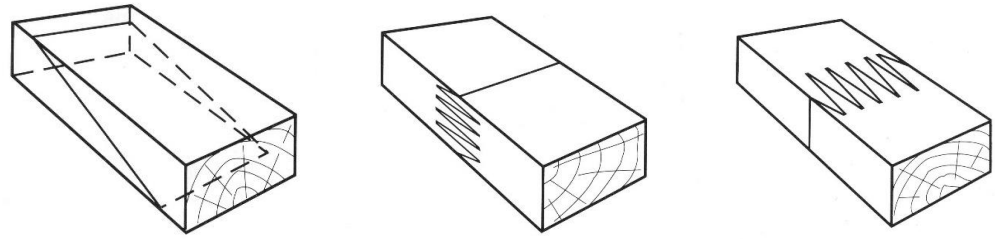

(a) (b) (c)

Figure 6: Types of bonded joints: (a) Scarf joint; (b) Lateral finger joint; (c) Vertical finger joint, [15].

Their main advantage is that the glued in steel rods connection is hidden itself within the timber member, effectively providing the joint with a higher fire rating as well as a more aesthetically pleasing “look” in comparison with traditional dowel-type connections, as shown in figure 7.

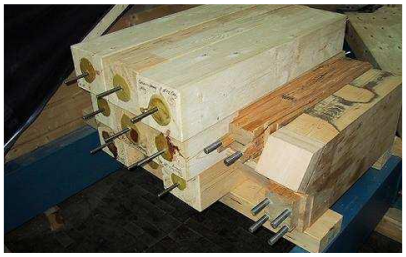

Figure 7: Glued in steel rods joints, [16].

The mechanical connections used in wood buildings can be classified into three major categories: dowel, metal connector plates with integral teeth or shear, and split-rings. Connections with metal fasteners follow the rules according Eurocode 5. There are also a number of patented connections that combine characteristics of each of these types.

Wood members connected with dowel-type fasteners are probably the most common mechanical connections type because they are effective at transferring loads while also being relatively simple and efficient to install. They come in many forms and their strength properties can be calculated using the National Design Specification (NDS) for Wood Construction. Dowelled connections transfer the load between members through a combination of dowel bearing and bending of the dowel fastener. Nails are generally used when loads are relatively light, as in multi-family and light commercial buildings, figure 8. Staples can be used in place of nails, but equivalent capacities need to be determined as the NDS doesn't publish design values for staples.

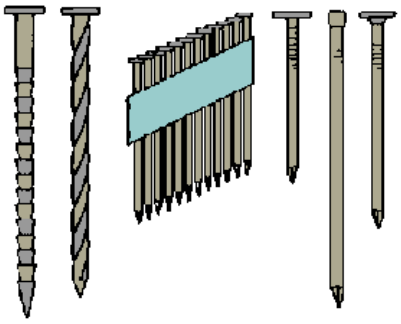

Figure 8: Nails < 8 mm (NF EN14592) definition profiled nails, [16].

Screws may be more satisfactory than nails under certain conditions (such as exposure to moisture) since they have less tendency to work loose and generally have high wind withdrawal resistance under severe wind events, figure 9.

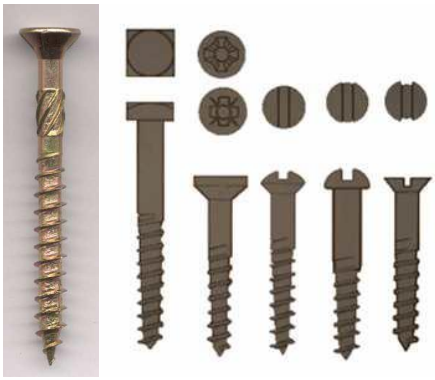

Figure 9: Example of screws, [16].

Bolt design values are tabulated in the NDS for five diameters (1/2 in., 5/8 in., 3/4 in., 7/8 in. and 1 in.). Diameters greater than 1 in. are not permitted as they can initiate localized stresses in the wood member, which can cause splitting or other brittle wood failures. Bolts are inserted in pre-drilled holes 1/32 in. to 1/16 in. larger than the bolt diameter. Dowels are usually round,

fitting into holes in two adjacent pieces to prevent their slipping or to align them, and used to reinforce. Figure 10 represents typical examples of bolts and dowels.

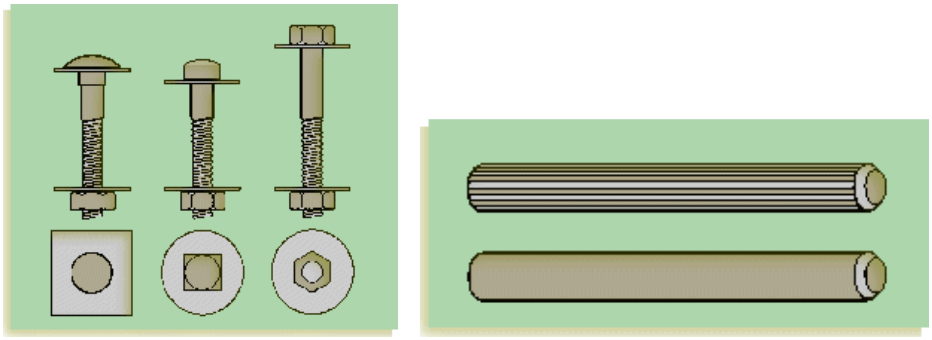

Figure 10: Example of bolts and dowels, [16].

Shear connectors, sometimes referred to as bearing connectors, are typically used to accommodate heavier loads. They include split rings, shear plates and toothed shear plates. They are usually made from cast iron or light metals, and are capable of transmitting the load relying solely on bearing and shear resistance of the wood in the direction parallel or perpendicular to the grain. They can be used to connect wood to wood members or wood to steel, and may be hidden or visible, represented in figure 11.

Figure 11: Punched metal plate fasteners, [16].

Profiled using special machining tools, split rings are usually fitted in a circular groove on the assembly side of the timber members. The split in the steel rings allows the gap in the ring to close or open if the wood members shrink or swell to ensure that the wood members and split ring remain in contact, figure 12. A bolt is installed through the centre to hold the joint assembly together.

Figure 12: Split-ring connectors with (64- 104 mm) diameter and Bolts (M12 to M20), [16].

Numerical models of different timber connections (S-W-S, W-S-W, W-W-W) were analyzed and compared with experimental tests by C. Austruy. Numerical results give an acceptable prediction of the fire resistance of timber connections. Even if the temperature obtained with numerical program are very different of the experimental temperature, the thermal parameters determined give acceptable predictions of fire resistance. The aim of the numerical study was to determine in the future the fire resistance of all types and sizes of connections during a standard fire from numerical temperatures because it cannot be done with tests as too many would be needed. But the differences between the numerical and experimental results are too variable to be trusted, [17].

1.1. Objectives

The main objective of this work is to present a methodology for wood-wood-wood connections design in double shear, following the rules presented in Eurocodes 3 and 5. Also, a comparison of results with a numerical program based on finite element method will be used.

This type of connections W-W-W will be designed at room and high temperatures using dowelled connectors. For each situation, all calculations will be performed to determine the cross-section and number of dowels. A procedure will be presented to calculate the load carrying capacity per shear plane per steel fastener in a typical glued laminated in birch timber GL28h. The timber and steel material properties at room and high temperatures will be presented, according the standards, and considering the orthotropic wood.

The W-W-W designed connection will be considered unprotected at room temperature, and protected for high temperatures. In this study, it is relevant to determine the type of insulation material and thickness dimension for guarantee a fire time resistance.

All developed study will contribute to the knowledge in these connections, where the wood material represents a complex behaviour in fire situations and the combination with steel dowels intensify the heat conduction inside the material. All proposed methodologies could be used to

study W-W-W connections with or without insulation material to assess and contribute for a safe design.

1.2. Summary of the chapters

More six chapters will be presented in this report with all described work and steps to concretize the final Master thesis.

Chapter 2 express the mechanical and thermal performances of the materials. The behaviour of the mechanical properties of wood and steel under ambient and high temperatures are described. Also, the thermal and physical properties of wood and steel are illustrated specifically, the thermal conductivity, specific heat and density.

In **Chapter 3**, wood-wood-wood (W-W-W) connections are calculated according standards (Eurocode 5 Part 1-1), [23]. As well as, defining the mechanical properties of the adopted materials (yellow birch GL28h for wood and hot-rolled low carbon S275 for steel).

The **Chapter 4** describes the finite element method (FEM) used for the numerical model with the equations for the equivalent stress calculation. Also, this chapter presents the shape functions of the finite element for 3D meshes and explain the procedure used in FEM program to solve the mechanical problem under an incremental applied loading condition and discuss the different results obtained from the simulation.

In **Chapter 5**, W-W-W connections are designed unprotected and protected with different insulation materials, according standards (Eurocode 5 Part 1-2), [23]. The thermal properties of the assumed materials are presented.

Chapter 6 presents the numerical model under thermal transient analysis with a description of the shape functions of the finite element for 2D meshes. The equations used for the heat transfer and the general boundary conditions will be exposed. The results from the thermal analysis will be discussed.

The last two chapters are related with the ‘’Conclusions and Future Work’’, and the ‘’References’’ that supports the state of the art of this report.

Chapter 2

Material Properties

2. Material Properties

2.1. Wood material

2.1.1. Wood classification

Wood is a heterogeneous, hygroscopic, cellular and anisotropic material. Wood is classified into two main groups, softwoods and hardwoods. It is overly simple to think of hardwoods as being hard and durable compared to soft and workable softwoods. This happens to be generally true, but there are exceptions, such as in the cases of wood from yew trees (a softwood that is relatively hard), and wood from balsa trees (a hardwood that is softer than softwoods), [18].

Hardwood comes from flowering plants (angiosperm) such as oak, maple, or walnut, that are not monocots. Softwood comes from nonflowering plants (gymnosperm), usually evergreen conifers, like pine or spruce, [18], [19].

Hardwood has vessel elements that transport water throughout the wood; under a microscope, these elements appear as pores. Softwood usually have needles and cones. Medullary rays and tracheids transport water and produce sap. Softwoods have no visible pores because of tracheids, as it is shown if figure 13, [20].

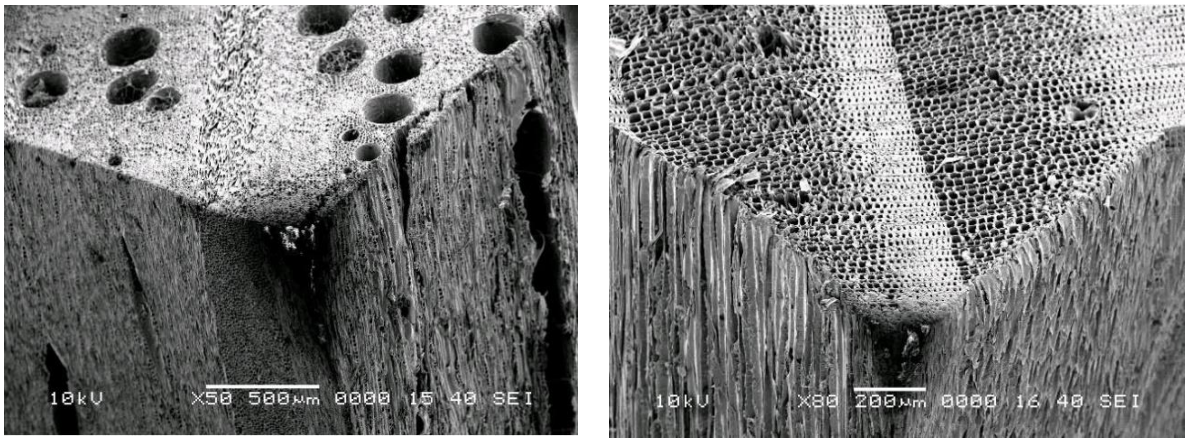

Figure 13: Presence of pores in hardwoods (oak, on the left) and the absence of pores in softwoods (pine, on the right), [18].

Generally, though, softwoods are cheaper, less resistant under fire conditions and easier to work with than hardwoods. As such, they make up the bulk of all wood used in the world, with about 80% of all timber being a softwood. This is impressive considering hardwoods are much more common in the world than softwoods. Softwoods have a wide range of applications and are found in building components (e.g., windows, doors), furniture, medium-density fibreboard (MDF), paper, Christmas trees, and much more. Pines are one of the most commonly used

softwoods, [18]. Though hardwoods are often more expensive, also more resistant under fire conditions and sometimes more challenging to work with, their upside is that most - though not all - are denser, meaning many hardwoods will last longer than softwoods. For this reason, hardwoods are more likely to be found in high-quality furniture, decks, flooring, and the construction that needs to last [18]. The denser a wood is, the harder, stronger, and more durable it is. Most hardwoods have a higher density than most softwoods, [21].

2.1.2. Mechanical properties of wood

Wood may be described as an orthotropic material, that is, it has unique and independent mechanical properties in the directions of three mutually perpendicular axes: longitudinal, radial, and tangential, as represented in figure 14. The longitudinal axis L is parallel to the fiber (grain), the radial axis R is normal to the growth rings (perpendicular to the grain in radial direction), and the tangential axis T is perpendicular to the grain and tangent to the growth rings, [22].

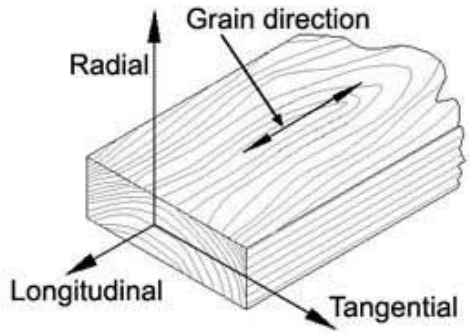

Figure 14: Three principal axes of wood with respect to grain direction and growth rings, [22].

The following values have been obtained by tests carried out on samples of relatively small timber, without disturbing thread without knots, etc. The test conditions are controlled and wood humidity is between 12% and 15% "dry air". For higher moisture content, the modulus of elasticity and resistance drop considerably, [22].

Mechanical properties of timber at ambient temperature

Young´s modulus

Elasticity is a property of an object or material which will restore it to its original shape after distortion. This restoring force is in general proportional to the stretch described by Hooke's Law [24]. The Hook’s law is a relation used for tensile stress σ, proportional to its fractional normal strain ε by the modulus of elasticity E which can be expressed as:

$$\sigma = E \times \varepsilon \quad (1)$$

Elasticity or Young's Modulus is a measure of the material stiffness. It is used to describe the elastic properties of the material when they are in tensile or compression. Table 1 shows the modulus of elasticity of some wood species, [24].

Wood Species	**Modulus of elasticity** [MPa]
Basswood (American)	7200 … 10100
Birch (Yellow)	10300 ... 13900
Cherry tree (Black)	9000 ... 10300
Chestnut (American)	6400 ... 8500
Oak (Pin)	9100 ... 11900
Douglas Fir (Coast)	10800 ... 13400
Maple (Red)	9600 ... 11300
Hemlock (Eastern)	7400 ... 8300
Larch (Western)	10100 ... 12900
Walnut (Black)	9800 ... 11600
Elm (American)	7700 … 9200
Pear tree	7500 ... 8500
Pine (Eastern White)	6800 ... 8500
Lime Tree	7000 ... 11000
Alder (Red)	8100 … 9500
Beech (American)	9500 … 11900
Cedar (Yellow)	7900 … 9800
Hickory (True Mockemut)	10800 … 15300
Redwood (Young-growth)	6600 … 7600
Spruce (Red)	9200 … 11100

Table 1: The elastic modulus of some types of wood at room temperature, [22], [25], [26].

Yield strength

The yield strength is defined in engineering as the amount of stress (Yield point) at which a material stops deform elastically (elastic deformation), reversible and therefore begins to deform irreversibly (plastic deformation). Strength may also be defined as the ability to resist an applied stress: the greater the resistance, the stronger the material. Resistance may be measured in several ways: the maximum stress that the material can suffer before failure occurs; the deformation that results from a given level of stress before total failure. Table 2 shows the yield and the ultimate stress for some wood spices, [28].

Material	**Yield Stress** [MPa]	**Ultimate Stress** [MPa]
Ash	40-70	50-100
Douglas Fir	30-50	50-80
Oak	40-60	50-100
Southern Pine	40-60	50-100

Table 2: The yield and the ultimate stress of some types of wood at ambient temperature, [28].

Poisson's ratio

Poisson's ratio is the ratio between the transverse to longitudinal strain in the direction of the applied load, usually represented as **ν**. Tables 3 and 4 represents some typical values of Poisson's ratio for different types of wood in different orthotropic planes.

Species	ν_{LR}	ν_{LT}	ν_{RT}	ν_{TR}	ν_{RL}	ν_{TL}
Hardwood						
Basswood (American)	0,364	0,406	0,912	0,346	0,034	0,022
Birch (Yellow)	0,426	0,451	0,697	0,426	0,043	0,024
Cherry tree (Black)	0,392	0,428	0,695	0,282	0,086	0,048
Maple (Red)	0,434	0,509	0,762	0,354	0,063	0,044
Maple (Sugar)	0,424	0,476	0,774	0,349	0,065	0,037
Oak (Red)	0,350	0,448	0,560	0,292	0,064	0,033
Oak (White)	0,369	0,428	0,618	0,300	0,074	0,036
Walnut (Black)	0,495	0,632	0,718	0,378	0,052	0,035

Table 3: Poisson's ratios for various hardwood species at approximately 12% moisture content, [22].

Species	ν_{LR}	ν_{LT}	ν_{RT}	ν_{TR}	ν_{RL}	ν_{TL}
Softwood						
Cedar (northern white)	0,337	0,340	0,458	0,345	-	-
Cedar (western red)	0,378	0,296	0,484	0,403	-	-
Douglas Fir (Coast)	0,292	0,449	0,390	0,374	0,036	0,029
Hemlock (Western)	0,485	0,423	0,442	0,382	-	-
Larch (Western)	0,355	0,276	0,389	0,352	-	-
Pine (Western White)	0,329	0,344	0,410	0,344	-	-
Redwood	0,360	0,346	0,373	0,400	-	-
Spruce (Sitka)	0,372	0,467	0,435	0,245	0,040	0,025

Table 4: Poisson's ratios for various softwood species at approximately 12% moisture content, [22].

Wood mechanical properties under high temperatures

Moisture content (MC) and temperature (T) have important effects on mechanical properties of wood. These effects need to be understood and taken into account in the structural use of wood. The mechanical properties of wood increase as moisture content decreases below fiber saturation point, at least down to about 5% MC, and as temperature decreases, [29].

Effect of temperature on modulus of elasticity

The behaviour of the modulus of elasticity under the effect of high temperature is linear and is expressed on two phases, the first between 20 [°C] and 100 [°C] and the second between 100 [°C] and 300 [°C], according Eurocode 5 1-2 [7]. This behaviour is mentioned on figure 15, and also in the table 5 as equations.

$$K_{E,T} = \frac{E_{w,T}}{E_w} \tag{2}$$

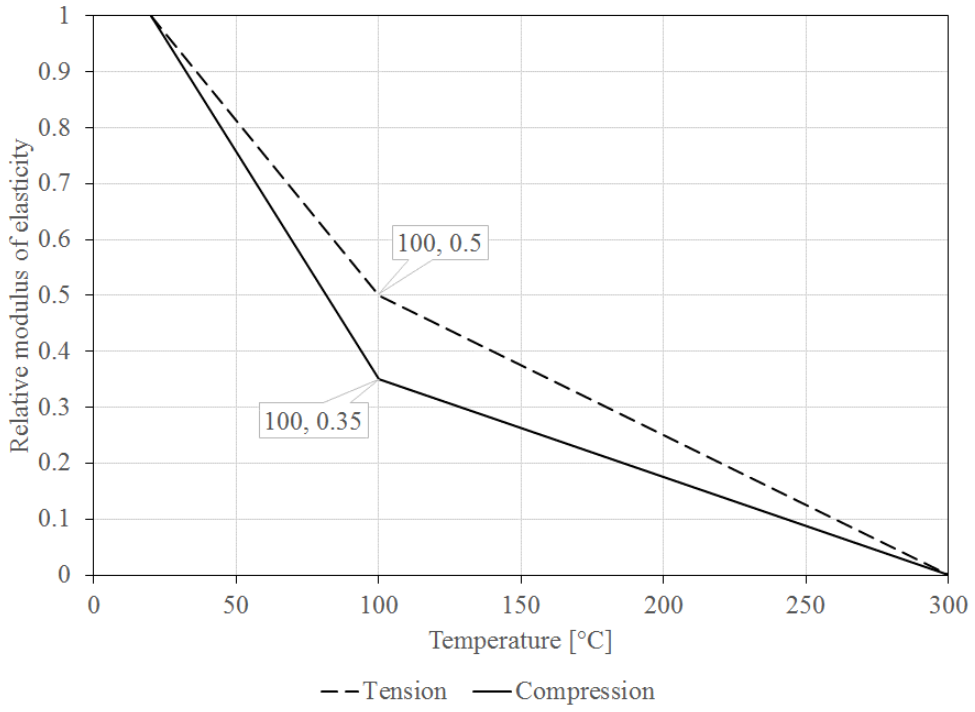

Figure 15: Effect of temperature on modulus of elasticity parallel to grain of softwood, [8].

Temperature [°C]	Relative modulus of elasticity	
	Tensile	Compression
$20 \leq T \leq 100$	$K = \frac{(90 - 0{,}5\,T)}{80}$	$K = \frac{(93 - 0{,}65\,T)}{80}$
$100 \leq T \leq 300$	$K = \frac{(150 - 0{,}5\,T)}{200}$	$K = \frac{(105 - 0{,}35\,T)}{200}$

Table 5: Equations of relative modulus of elasticity of softwood.

Effect of temperature on strength

The figure 16 and the table 6 shows the thermal degradation of bending strength in a linear behaviour, according Eurocode 5 1-2, [8].

$$K_{y,T} = \frac{f_{y,T}}{f_y} \tag{3}$$

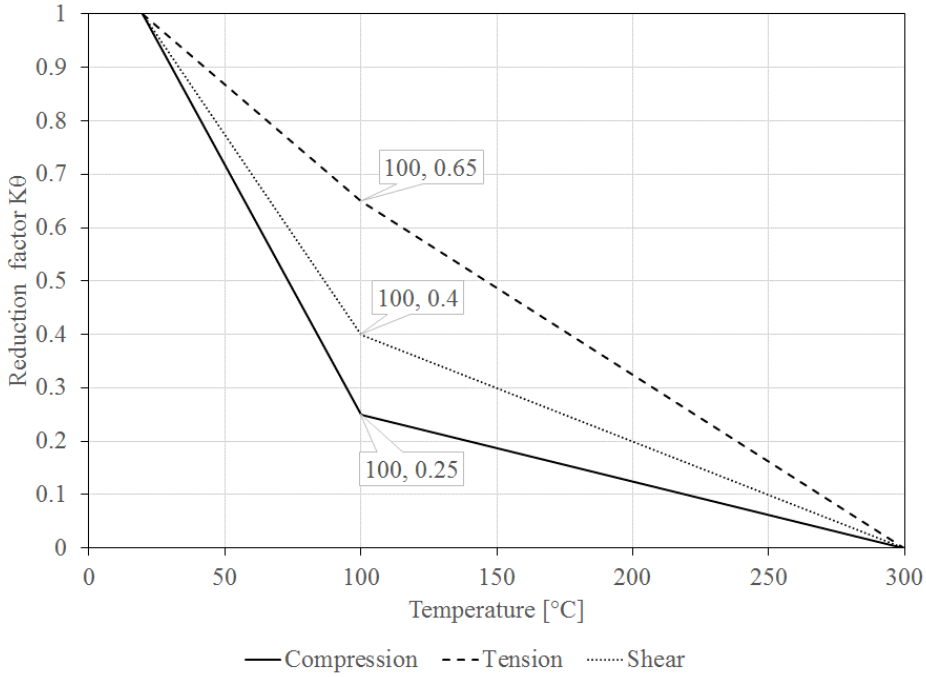

Figure 16: Reduction factor for strength parallel to grain of softwood, [8].

Temperature [°C]	Reduction factor K_θ		
	Tensile	Shear	Compression
$20 \leq T \leq 100$	$K = \frac{(87 - 0{,}35\,T)}{80}$	$K = \frac{(92 - 0{,}6\,T)}{80}$	$K = \frac{(95 - 0{,}75\,T)}{80}$
$100 \leq T \leq 300$	$K = \frac{(195 - 0{,}65\,T)}{200}$	$K = \frac{(120 - 0{,}4\,T)}{200}$	$K = \frac{(75 - 0{,}25\,T)}{200}$

Table 6: Equations of reduction factor for strength of softwood.

2.1.3. Thermal properties of wood

Specific heat

The specific heat is reflected in the required amount of heat so that there is a 1 temperature increase [° C] for 1 [kg] matter. This is independent of the type of wood may vary due to its moisture, [30]. The values of the specific heat are shown in table 7 and figure 17, as referred on Eurocode 5 1-2, [8].

Temperature [°C]	Specific heat [kJ/kg.K]
20	1,53
99	1,77
99	13,60
120	13,50
120	2,12
200	2,00
250	1,62
300	0,71
350	0,85
400	1,00
600	1,40
800	1,65
1200	1,65

Table 7: Temperature - Specific heat capacity relationship for wood, [8].

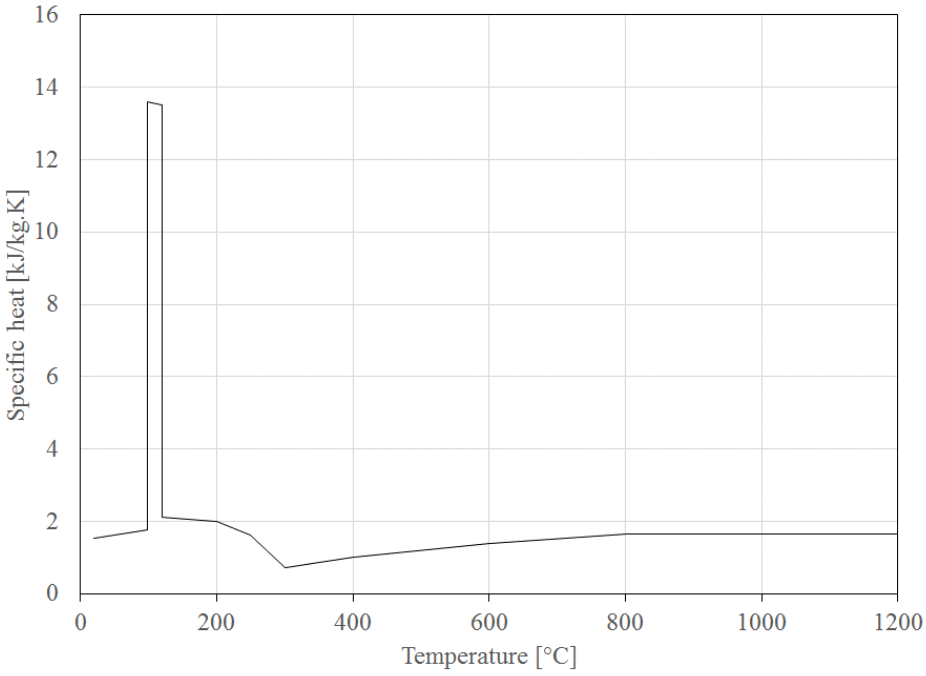

Figure 17: Temperature-specific heat variation for wood, [8].

Thermal conductivity

The thermal conductivity (λ) defined by the speed of the heat that the material can carry, and is assigned to each able to drive this heat material. Wood because of its molecular structure is a poor heat conductor, [30].

Wood material has conductivity values lower than the metals as shown in table 8 and figure 18 according to Eurocode 5 1-2, [8].

Temperature [°C]	Thermal Conductivity [W/m.k]
20	0,12
200	0,15
350	0,07
500	0,09
800	0,35
1200	1,50

Table 8: Temperature - thermal conductivity relationship for wood, [8].

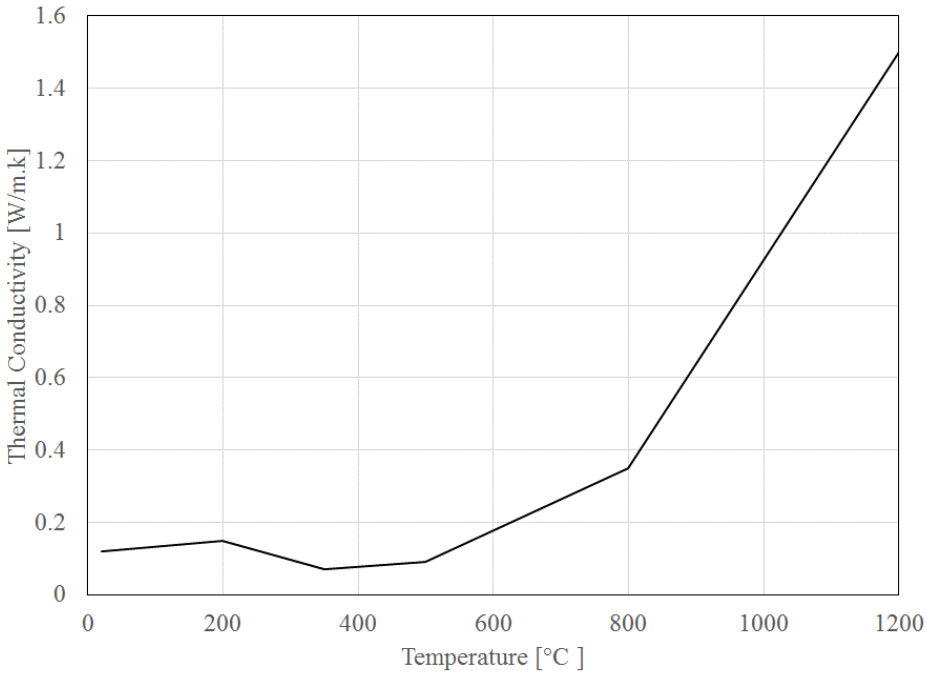

Figure 18: Temperature - thermal conductivity variation for wood, [8].

Density

Wood density is defined according to the moisture, Eurocode 5, [8]. The values, shown in table 9 and figure 19, correspond to a moisture content average 12% (ω).

Temperature [°C]	Density Coefficient
20	1+ ω
99	1+ ω
120	1,00
200	1,00
250	0,93
300	0,76
350	0,52
400	0,38
600	0,28
800	0,26
1200	0,00

Table 9: Temperature - density relationship for wood, [8].

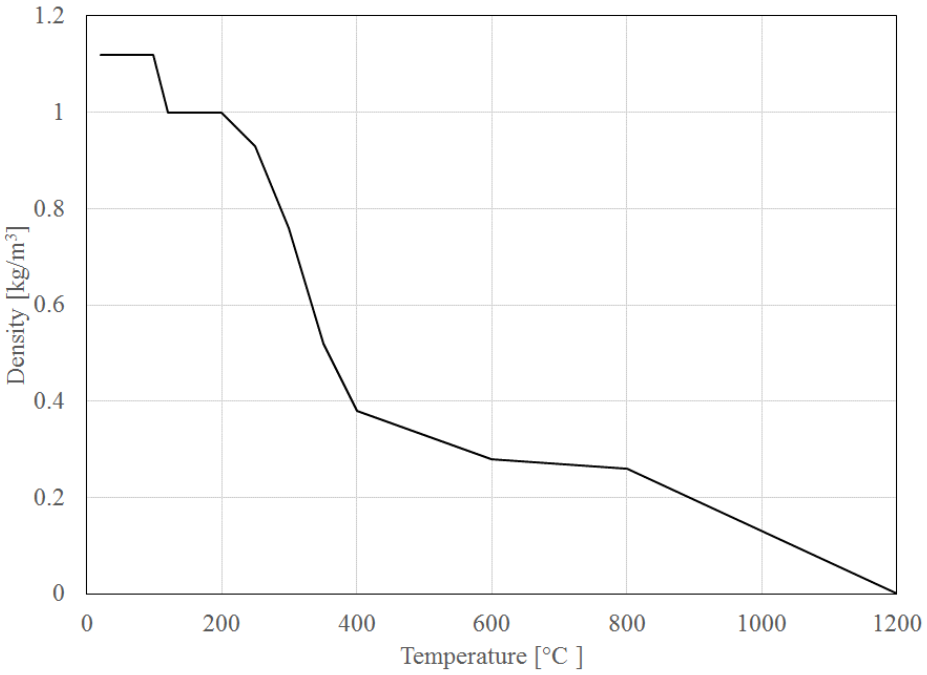

Figure 19: Temperature - density variation for wood, [8].

Table 10, shows the density of some types of wood.

Solid	Density [10^3 kg/m^3]	Solid	Density [10^3 kg/m^3]
Alder	0,4 – 0,7	Hickory	0,83
Ash, white	0,65 – 0,85	Juniper	0,55
Balsa	0,16	Larch	0,5 – 0,55
Basswood	0,3 – 0,6	Maple	0,6 – 0,75
Beech	0,7 – 0,9	Oak	0,6 – 0,9
Birch, British	0,67	Oak, American Red	0,74
Cedar, western red	0,38	Pine, Scots	0,51
Cherry, European	0,63	Pine, yellow	0,42
Douglas Fir	0,53	Redwood, European	0,51
Elm, American	0,57	Spruce	0,4 – 0,7
Hackberry	0,62	Walnut	0,65 – 0,7
Hemlock, western	0,50	Yew	0,67

Table 10: Density of some types of wood, [31].

2.2. Steel material

2.2.1. Steel grades / categories

According to the American Iron & Steel Institute (AISI), steel can be categorized into four basic groups based on the chemical compositions: Carbon Steel, Alloy Steel, Stainless Steel and Tool Steel. Also, there are many different grades of steel that encompass varied properties. These properties can be physical, chemical and environmental. All steel is composed of iron and carbon. It is the amount of carbon, and the additional alloys that determine the properties of each grade. A special classification system is used in the SAE-AISI code for steel. As it's shown in the table 11, the digits 'xx' in the table below represents the carbon content of the metal in hundredths of a percent. The first digit in the number represents the other alloy (if any) added to the steel. The second digit indicates either the percentage of that alloy, or more alloy additives, [32].

AISI / SAE Designation	Major Classifications of Steel	Indicator of the Amount of Carbon
10xx	Carbon steels	Plain carbon, Mn 1.00% max
11xx		Resulfurized free machining
12xx		Resulfurized / rephosphorized free machining
15xx		Plain carbon, Mn 1.00-1.65%
13xx	Manganese steel	Mn 1.75%
23xx	Nickel steels	Ni 3.50%
25xx		Ni 5.00%
31xx	Nickel-chromium steels	Ni 1.25%, Cr 0.65-0.80%
32xx		Ni 1.75%, Cr 1.07%
33xx		Ni 3.50%, Cr 1.50-1.57%
34xx		Ni 3.00%, Cr 0.77%
40xx	Molybdenum steels	Mo 0.20-0.25%
44xx		Mo 0.40-0.52%
41xx	Chromium-molybdenum steels	Cr 0.50-0.95%, Mo 0.12-0.30%
43xx	Nickel-chromium-molybdenum steels	Ni 1.82%, Cr 0.50-0.80%, Mo 0.25%
47xx		Ni 1.05%, Cr 0.45%, Mo 0.20-0.35%
46xx	Nickel-molybdenum steels	Ni 0.85-1.82%, Mo 0.20-0.25%
48xx		Ni 3.50%, Mo 0.25%
50xx	Chromium steels	Cr 0.27-0.65%
51xx		Cr 0.80-1.05%
50xxx		Cr 0.50%, C 1.00% min
51xxx		Cr 1.02%, C 1.00% min
52xxx		Cr 1.45%, C 1.00% min
61xx	Chromium-vanadium steels	Cr 0.60-0.95%, V 0.10-0.15%
72xx	Tungsten-chromium steels	W 1.75%, Cr 0.75%
81xx	Nickel-chromium-molybdenum steels	Ni .30%, Cr 0.40%, Mo 0.12%
86xx		Ni .55%, Cr 0.50%, Mo 0.20%
87xx		Ni .55%, Cr 0.50%, Mo 0.25%
88xx		Ni .55%, Cr 0.50%, Mo 0.35%
93xx	Nickel-chromium-molybdenum steels	Ni 3.25%, Cr 1.20%, Mo 0.12%
94xx		Ni 0.45%, Cr 0.40%, Mo 0.12%
97xx		Ni 0.55%, Cr 0.20%, Mo 0.20%
98xx		Ni 1.00%, Cr 0.80%, Mo 0.25%

Table 11: Indication of AISI/SAE steel numbers, [31].

Carbon steel: Carbon Steel is the type of steel used in our case studies, and it can be segregated into three main categories: Low carbon steel (sometimes known as mild steel), Medium carbon steel, and High carbon steel, [32].

- Low Carbon Steel (Mild Steel): Typically contain 0.04% to 0.30% carbon content. This is one of the largest groups of Carbon Steel. It covers a great diversity of shapes, from Flat Sheet to Structural Beam. Depending on the desired properties needed, other elements are added or increased. For example: Drawing Quality (DQ) - The carbon level is kept low and Aluminium is added, and for Structural Steel the carbon level is higher and the manganese content is increased.
- Medium Carbon Steel: Typically has a carbon range of 0.31% to 0.60%, and a manganese content ranging from 0.60% to 1.65%. This product is stronger than low carbon steel, and it is more difficult to form, weld and cut. Medium carbon steels are quite often hardened and tempered using heat treatment.
- High Carbon Steel: Commonly known as "carbon tool steel" it typically has a carbon range between 0.61% and 1.50%. High carbon steel is very difficult to cut, bend and weld. Once heat treated it becomes extremely hard and brittle.

Alloy steel: Alloy steel is a steel that has had small amounts of one or more alloying elements (other than carbon) such as such as manganese, silicon, nickel, titanium, copper, chromium and aluminium added. This produces specific properties that are not found in regular carbon steel. Alloy steels are workhorses of industry because of their economical cost, wide availability, ease of processing, and good mechanical properties. Alloy steels are generally more responsive to heat and mechanical treatments than carbon steels, [32].

Stainless steel: Stainless steel metal is a versatile material offering corrosion resistance, strength, good pricing, and a wide range of shapes. Stainless steel is generally formable and wieldable, making it a popular choice in both structural and design applications, [32].

Tool steel: Tool steel is a term used for a variety of high-hardness, abrasion resistant steels. Specific tool applications are dies (stamping or extrusion), cutting, mold-making, or impact applications like hammers (personal or industrial). It is also a common material used to make knives. Tool Steels are extremely hard and are quite often used to form other metal products. It is available in a wide variety of shapes including rounded bar, flat bar, square bar and more, [32].

2.2.2. Mechanical properties of steel

Ambient temperature of steel mechanical properties

Tables 12 and 13 present the yield strength, f_y, and the ultimate tensile strength, f_u, for hot rolled structural steel and structural hollow sections at ambient temperature are given in the product standards EN 10025, EN 10210 and EN 10219 respectively. Simplifications are given in Tables C.1 and C.2, which are taken from EN 1993-1-1.

Standard and steel grade	Nominal thickness of the element t [mm]			
	$t \leq 40\ mm$		$40\ mm < t \leq 80\ mm]$	
	$f_y\ [N/mm^2]$	$f_u\ [N/mm^2]$	$f_y\ [N/mm^2]$	$f_u\ [N/mm^2]$
EN 10025-2				
S235	235	360	215	360
S275	275	430	255	410
S355	355	490	335	470
S450	440	550	410	550
EN 10025-3				
S275 N/NL	275	390	255	370
S355 N/NL	355	490	335	470
S420 N/NL	420	520	390	520
S460 N/NL	460	540	430	540
EN 10025-4				
S275 M/ML	275	370	255	360
S355 M/ML	355	470	335	450
S420 M/ML	420	520	390	500
S460 M/ML	460	540	430	530
EN 10025-5				
S235 W	235	360	215	340
S355 W	355	490	335	490
EN 10025-6				
S460 Q/QL/QL1	460	570	440	550

Table 12: Nominal values of yield strength f_y and ultimate tensile strength f_u for hot rolled structural steel, [33].

Standard and steel grade	Nominal thickness of the element t [mm]			
	$t \leq 40\ mm$		$40\ [mm] < t \leq 80\ mm$	
	$f_y\ [N/mm^2]$	$f_u\ [N/mm^2]$	$f_y\ [N/mm^2]$	$f_u\ [N/mm^2]$
EN 10025-2				
S235 H	235	360	215	340
S275 H	275	430	255	410
S355 H	355	490	335	490
S275 NH/NLH	275	390	255	370
S355 NH/NLH	355	490	335	470
S420 NH/NLH	420	540	390	520
S460 NH/NLH	460	560	430	550
EN 10025-3				
S235 H	235	360		
S275 H	275	430		
S355 H	355	510		
S275 NH/NLH	275	370		
S355 NH/NLH	355	470		
S460 NH/NLH	460	550		
S275 MH/MLH	275	360		
S355 MH/MLH	355	470		
S420 MH/MLH	420	500		
S460 MH/MLH	460	350		

Table 13: Nominal values of yield strength f_y and ultimate tensile strength f_u for structural hollow sections, [33].

The material coefficients and the elastic constants used at ambient temperature to be adopted in calculations for the steel design parts of this work covered by the first Eurocode 3 Part should be taken as follows:

- Modulus of elasticity: $E = 210000\ MPa$
- Shear modulus: $G = \frac{E}{2(1+\nu)} \approx 81000\ MPa$
- Poisson's ratio in elastic stage: $\nu = 0{,}3$
- Coefficient of linear thermal expansion: $\alpha = 12{\times}10^{-6}\ perK$ $(T \leq 100\ ℃)$

Steel mechanical properties under high temperatures

The reduction factors for the effective yield strength, the proportional limit and the slope of the linear elastic range is shown in table 14. And it can be also illustrated in figure 20.

Steel temperature θ_a [°C]	Reduction factors at temperature θ_a relative to the value of f_y or E_a at 20 [°C]		
	Reduction factor (relative to f_y) for effective yield strength $K_{y,\theta} = f_{y,\theta}/f_y$	Reduction factor (relative to f_p) for proportional limit $K_{p,\theta} = f_{p,\theta}/f_p$	Reduction factor (relative to E_a) for the slop of the linear elastic range $K_{E,\theta} = E_{a,\theta}/E_a$
20	1	1	1
100	1	1	1
200	1	0.807	0.9
300	1	0.613	0.8
400	1	0.42	0.7
500	0.78	0.36	0.6
600	0.47	0.18	0.31
700	0.23	0.075	0.13
800	0.11	0.05	0.09
900	0.06	0.0375	0.0675
1000	0.04	0.025	0.045
1100	0.02	0.0125	0.0225
1200	0	0	0

Table 14: Reduction factors for stress-strain relationship of carbon steel at elevated temperatures, [33].

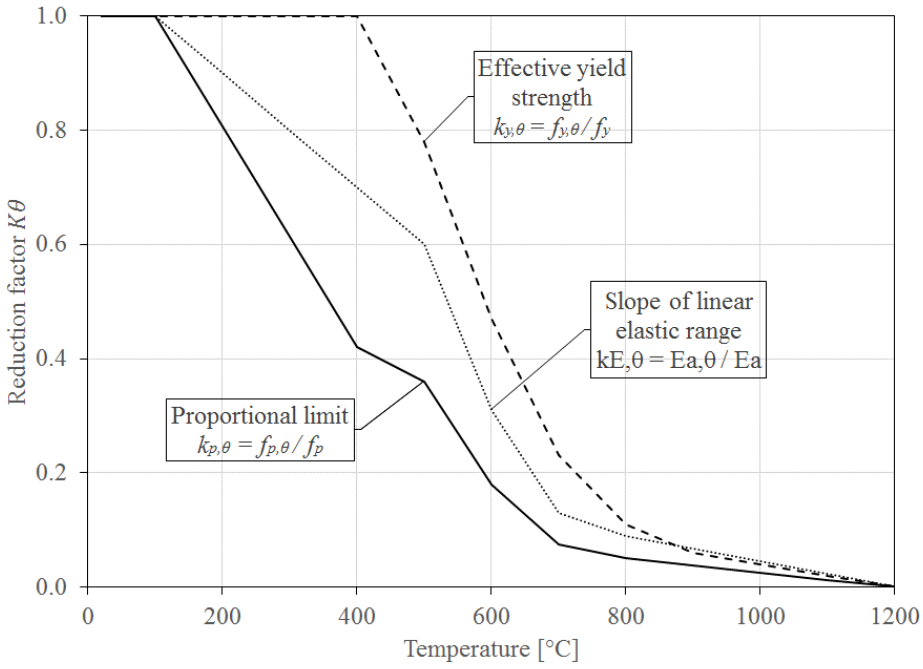

Figure 20: Reduction factors for the stress-strain relationship of carbon steel at elevated temperatures, [33].

2.2.3. Thermal properties of steel

Thermal elongation

When an object is heated or cooled, its length changes by an amount proportional to the original length and the change in temperature. The relative thermal elongation of steel $\Delta l / l$ should be determined from the following:

– For $20℃ \leq \theta_a < 750℃$:

$$\Delta l/l = 1{,}2 \times 10^{-5}\, \theta_a + 0{,}4 \times 10^{-8}\, {\theta_a}^2 - 2{,}416 \times 10^{-4} \quad (4)$$

– For $750℃ \leq \theta_a < 860℃$:

$$\Delta l/l = 1{,}1 \times 10^{-2} \quad (5)$$

– For $860℃ \leq \theta_a < 1200℃$:

$$\Delta l/l = 2 \times 10^{-5}\, \theta_a - 6{,}2 \times 10^{-3} \quad (6)$$

where: l is the length at $20\,℃$; Δl is the temperature induced elongation; θ_a is the steel temperature [℃].

The variation of the relative thermal elongation with temperature can be explained in the figure 21.

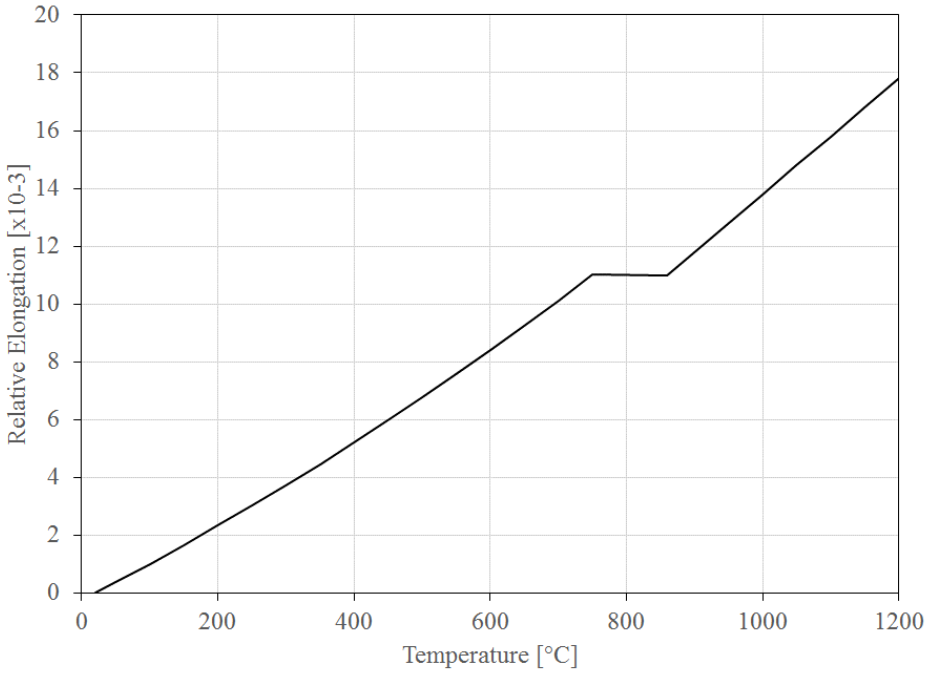

Figure 21: Relative thermal elongation of carbon steel as a function of the temperature, [27].

Specific heat

The specific heat of steel c_a should be determined from the following equalizations:

- For $20℃ \leq \theta_a < 600℃$:

$$c_a = 425 + 7{,}73 \times 10^{-1}\,\theta_a - 1{,}69 \times 10^{-3}\,{\theta_a}^2 + 2{,}22 \times 10^{-6}\,{\theta_a}^3\ [J/kg.K] \quad (7)$$

- For $600℃ \leq \theta_a < 735℃$:

$$c_a = 666 + \frac{13002}{738 - \theta_a}\ [J/kg.K] \quad (8)$$

- For $735℃ \leq \theta_a < 900℃$:

$$c_a = 545 + \frac{17820}{\theta_a - 731}\ [J/kg.K] \quad (9)$$

- For $900℃ \leq \theta_a < 1200℃$:

$$c_a = 650\ [J/kg.K] \quad (10)$$

where: θ_a is the steel temperature [℃].

The variation of the specific heat with temperature can be displayed in the figure 22.

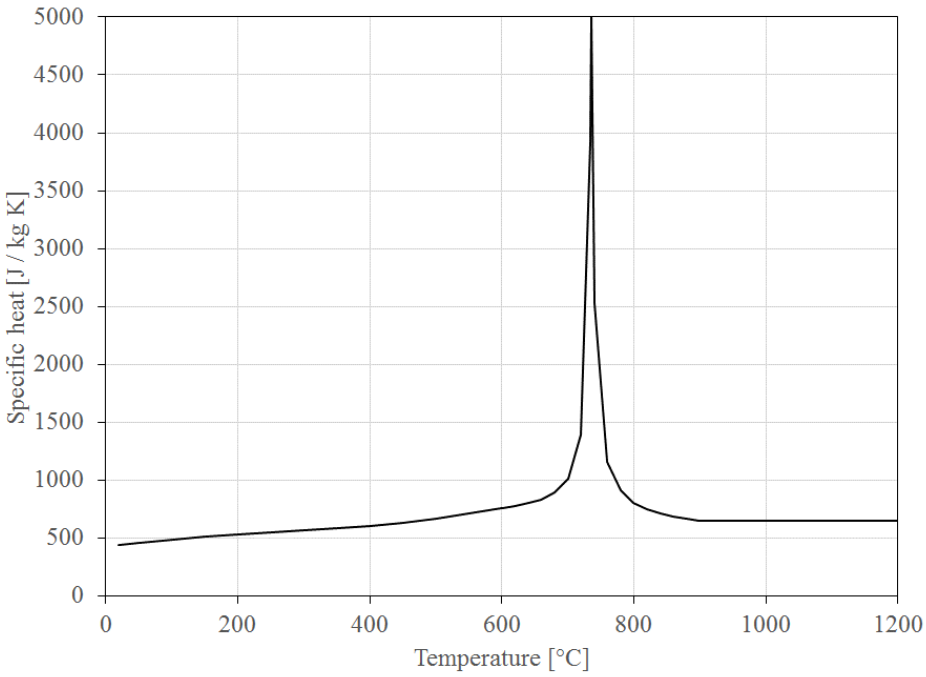

Figure 22: Specific heat of carbon steel as a function of the temperature, [27].

Thermal conductivity

The thermal conductivity of steel λ_a should be determined from equations 11 and 12:

– For $20°C \leq \theta_a < 800°C$:

$$\lambda_a = 54 - 3{,}33 \times 10^{-2}\, \theta_a \; [W/m.K] \tag{11}$$

– For $800°C \leq \theta_a < 1200°C$:

$$\lambda_a = 27{,}3 \; [W/m.K] \tag{12}$$

where: θ_a is the steel temperature [°C].

The variation of the thermal conductivity with temperature can be illustrated in the figure 23.

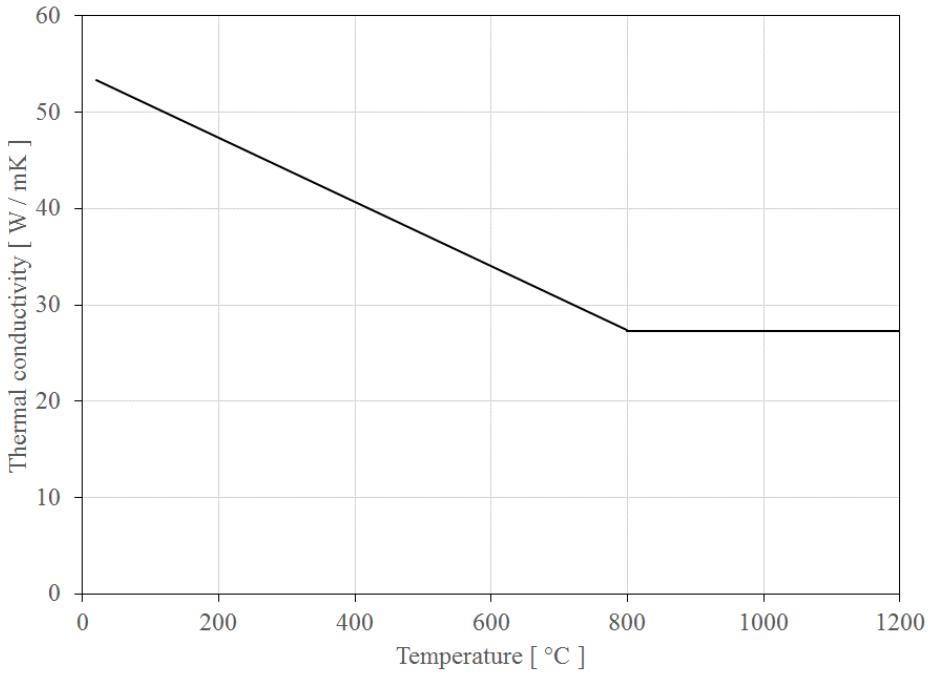

Figure 23: Thermal conductivity of carbon steel as a function of the temperature, [27].

Chapter 3

Design of W-W-W Connection at Ambient Temperature

3. Design of W-W-W Connection at Ambient Temperature

3.1. Introduction

In this work, typical wood-wood-wood (W-W-W) connections will be calculated according standards to be used in building construction. The wood material used is Glue Laminated Timber (GLULAM or GL) as a construction material with significant attributes: strength, stiffness and density, [34]. The mechanical properties are placed in categories in order to distinguish the quality of structural timber. These categories are called quality grades, [34], identified according numbers.

For the wooden plates in this study, a typical yellow birch wood type GL28h (Homogeneous Glue Laminated Timber) with 28 [MPa] bending strength will be used, figure 24. The W-W-W connection will be submitted to an external tensile force equal to 100 [kN], in direction parallel to the grain. The fasteners used in W-W-W connection will be a steel dowels with a diameter equal to ϕ12 [mm] and a grade steel material as S275.

Figure 24: Yellow birch wood. (http://www.wood-database.com/yellow-birch/)

3.2. Properties for GL28h as yellow birch and steel material at ambient temperature

Table 15 presents values of strength, stiffness and density of the laminated timber GL28h used in W-W-W connection.

Strength Class	**GL28h**	
	Designation	Value
Strength [*MPa*]		
Bending strength	$f_{m,\,k}$	28
Tension parallel to the fibers	$f_{t,0,\,k}$	19,5
Tension perpendicular to the fibers	$f_{t,90,\,k}$	0,5
Pressure parallel to the fibers	$f_{c,0,\,k}$	26,5
Pressure perpendicular to the fibers	$f_{c,90,\,k}$	3,0
Stiffness [*MPa*]		
Modulus of elasticity parallel to the fibers	$E_{0,\,mean}$	12600
Modulus of elasticity perpendicular to the fibers	$E_{90,\,mean}$	420
Shear modulus	G_{mean}	780
Density [kg/m^3]		
Density	ρ_k	410

Table 15: Values of strength, stiffness and density of GL28h at ambient temperature, [34].

Considering the values of strength and stiffness for GL28h, a typical yellow birch could be used. Tables below (table 16 and 17) give the properties for this spice as an orthotropic material, that is, it has unique and independent mechanical properties in the directions of three mutually perpendicular axes: longitudinal or parallel to the fiber or grain (L), radial normal to the growth rings (R) and tangential perpendicular to the grain but tangent to the growth rings (T). The strength in the longitudinal direction is the greatest usually about 10 times the other directions. Tables 16 and 17 represents the material properties at ambient temperature for this spice.

Specie	E_T / E_L	E_R / E_L	G_{LR} / E_L	G_{LT} / E_L	G_{RT} / E_L
Birch, yellow	0,050	0,078	0,074	0,068	0,017

Table 16: Elastic ratios at approximately 12% moisture content, [22].

Specie	μ_{LR}	μ_{LT}	μ_{RT}	μ_{TR}	μ_{RL}	μ_{TL}
Birch, yellow	0,426	0,451	0,697	0,426	0,043	0,024

Table 17: Poisson ratios at approximately 12% moisture content, [22].

Table 18 presents the strength properties of timber material at ambient temperature.

Common species names		**Unit**	**Birch Yellow**
Moisture content		[%]	12
Specific gravity		-	0,62
Static bending	Modulus of rupture	[*kPa*]	114000
	Modulus of elasticity	[*MPa*]	13900
	Work to maximum load	[kJ/m^3]	143
Impact bending		[*mm*]	1400
Compression parallel to grain		[*kPa*]	56300
Compression perpendicular to grain		[*kPa*]	6700
Shear parallel to grain		[*kPa*]	13000
Tension perpendicular to grain		[*kPa*]	6300
Side hardness		[*N*]	5600

Table 18: Strength properties of yellow birch material at ambient temperature, [22].

Table 19 presents the values of strength, stiffness and density for steel material used in dowels connections at ambient temperature. Steel is an isotropic material, and hot-rolled low carbon or mild carbon is often used in timber connections as fasteners and connectors.

Steel grade	**S275**	
	Designation	Value
Strength [*MPa*]		
Characteristic value of strength at the max load	$f_{u,k}$	400
Yield strength	f_y	275
Ultimate tensile strength	f_u	430
Stiffness [*GPa*]		
Modulus of elasticity	E	210
Poisson's Ratio		
Poisson's ratio	υ	0,3
Density [kg/m^3]		
Density	ρ_s	7850

Table 19: Values of strength, stiffness and density of the steel at ambient temperature, [33].

3.3. W-W-W configuration at ambient temperature

To determine the configuration in study, W-W-W connection at ambient temperature, all requirements according standards will be conducted under a report guide from, [35]. The final W-W-W configuration with all dimensions is presented in figure 25. The proposed model is calculated in cross-section size, number of dowels and spacing between dowels, due to an applied tensile force.

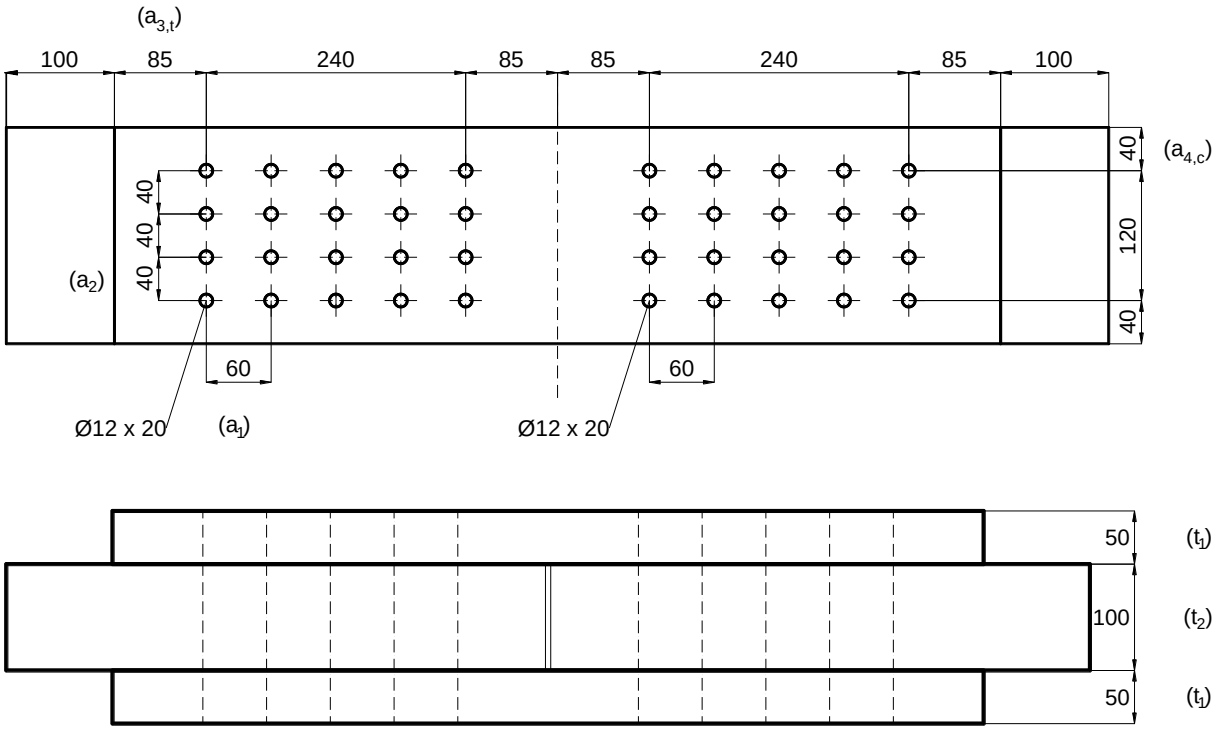

Figure 25: W-W-W connection in study.

According the standards, all rules will be conducted to establish the correct procedure for the design of W-W-W connection. The following steps will be used for this type of connection.

The ultimate limit state in the connection needs to be controlled, using the expression of the tension parallel to the grain, EN 1995-1-1, [23]:

$$\sigma_{t,0,d} \leq f_{t,0,d} \tag{13}$$

where: $\sigma_{t,0,d}$: the design tensile stress along the grain and $f_{t,0,d}$: the design tensile strength along the grain. For normal design tensile stress, the calculation is given by:

$$\sigma_{t,0,d} = \frac{F_d}{A_s} \tag{14}$$

where: F_d is the applied design force equal to 100 $[kN]$ and A_s the cross-section of the W-W-W connection.

Design tensile strength is obtained according EN 1995-1-1, [23] considering the following expression:

$$f_{t,0,d} = \frac{k_{mod} \times f_{t,0,k}}{\gamma_M} \tag{15}$$

Where: k_{mod} is the modification factor taking into account the effect of the duration of load and moisture content, from the table 3.1 EN 1995-1-1, [23], and for short term action k_{mod} is equal to 0,9. $f_{t,0,k}$ is the tension parallel to the fibers, for laminated timber GL28h equal to 19,5 MPa. γ_M is the partial safety factor equal to 1,25.

With all considerations, the calculated design tensile strength is:

$$f_{t,0,d} = \frac{0{,}9 \times 19{,}5}{1{,}25} = 14{,}04\ [MPa]$$

$$\sigma_{t,0,d} = \frac{F_d}{A_s} \leq f_{t,0,d} \iff A_s \geq \frac{F_d}{f_{t,0,d}} \iff A_s \geq \frac{100 \times 10^3}{14{,}04}$$

$$A_s \geq 7122{,}507\ [mm^2]$$

And inverting the equation it is possible to determine the minimum cross-section for W-W-W connection. The chosen cross-section for the timber plates of W-W-W connection is:

$$\left\{\begin{matrix} Center: 200 \times 100 = 20000 \\ Lateral: 200 \times 50 = 10000 \end{matrix}\right\}$$

$$total: 20000 + 2 \times 10000 = 40000\ [mm^2] \geq 7122{,}5\ [mm^2]$$

According the EN 1995-1-1, [23] and the used report guide [35], the characteristic load-carrying capacity for dowels per shear plane per fastener, and for fasteners in double shear, should be taken as the minimum value found from the following expressions:

$$F_{v,Rk} = min \begin{cases} f_{h,1,k} \cdot t_1 \cdot d & (a) \\ 0{,}5 \cdot f_{h,2,k} \cdot t_2 \cdot d & (b) \\ 1{,}05 \frac{f_{h,1,k} \cdot t_1 \cdot d}{2+\beta} \left[\sqrt{2\beta\,(1+\beta) + \frac{4\beta\,(2+\beta)\,M_{y,Rk}}{f_{h,1,k} \cdot d \cdot {t_1}^2}} - \beta \right] + \frac{F_{ax,Rk}}{4} & (c) \\ 1{,}15 \sqrt{\frac{2\beta}{1+\beta}} \cdot \sqrt{2 \cdot M_{y,Rk} \cdot f_{h,1,k} \cdot d} + \frac{F_{ax,Rk}}{4} & (d) \end{cases} \quad (16)$$

$$\beta = \frac{f_{h,2,k}}{f_{h,1,k}}$$

where:

$F_{v,Rk}$: is the characteristic load-carrying capacity per shear plane per fastener,

t_i: is the timber or board thickness or penetration depth, with *i* either 1 or 2 (t_1=50 [mm] and t_2=100 [mm]),

$f_{h,i,k}$: the characteristic embedment strength in timber member *i*, at an angle 0° to the grain, for Laminated veneer lumber (LVL) and a diameter between 6 $[mm] \leq d \leq 30$ $[mm]$,

d: is the fastener diameter equal to 12 [mm],

$M_{y,Rk}$: is the characteristic fastener yield moment, for rounded nails,

β: is the ratio between the embedment strength of the members, the characteristic embedment strength parallel to the grain in all members is equal $f_{h,1,k} = f_{h,2,k} \implies \beta = 1$.

$F_{ax,Rk}$: is the characteristic axial withdrawal capacity of the dowels equal to 0%.

$$f_{h,0,k} = 0{,}082\,(1 - 0{,}01 \times d) \cdot \rho_k \quad (17)$$

$$f_{h,0,k} = 0{,}082\,(1 - 0{,}01 \times 12) \times 410 = 29{,}5856\ [MPa]$$

$$M_{y,Rk} = 0{,}3 \cdot f_u \cdot d^{2,6} \quad (18)$$

$$M_{y,Rk} = 0{,}3 \cdot f_u \cdot d^{2,6} = 0{,}3 \times 400 \times 12^{2,6} = 76745{,}4\ \text{[kN.m]}$$

After replacing all the previous values in equation (16), it is possible to obtain the following:

$$\begin{cases} f_{h,1,k} \,.\, t_1 \,.\, d = 29{,}5856 \times 50 \times 12 = 17751{,}36 & (a) \\ 0{,}5 \,.\, f_{h,2,k} \,.\, t_2 \,.\, d = 0{,}5 \times 29{,}5856 \times 100 \times 12 = 17751{,}36 & (b) \\ 1{,}05 \, \dfrac{f_{h,1,k} \,.\, t_1 \,.\, d}{2+\beta} \left[\sqrt{2\beta \, (1+\beta) + \dfrac{4\beta \, (2+\beta) \, M_{y,Rk}}{f_{h,1,k} \,.\, d \,.\, {t_1}^2}} - \beta \right] + \dfrac{F_{ax,Rk}}{4} = & \\ 1{,}05 \times \dfrac{29{,}5856 \,.\, 50 \,.\, 12}{2+1} \left[\sqrt{2 \times 1 \, (1+1) + \dfrac{4 \times 1 \, (2+1) \, 76745{,}4}{29{,}5856 \,.\, 12 \,.\, 50^2}} - 1 \right] = 7731{,}81 & (c) \\ 1{,}15 \sqrt{\dfrac{2\beta}{1+\beta}} \,.\, \sqrt{2 \,.\, M_{y,Rk} \,.\, f_{h,1,k} \,.\, d} + \dfrac{F_{ax,Rk}}{4} = & \\ 1{,}15 \sqrt{\dfrac{2 \times 1}{1+1}} \,.\, \sqrt{2 \times 76745{,}4 \times 29{,}5856 \times 12} = 8489{,}26 & (d) \end{cases}$$

The characteristic load-carrying capacity is the minimum value between all four equations. The result obtained should be multiplied by the modification factor which take into account the effect of the load and moisture content duration.

$$F_{v,Rk} = min \begin{cases} 17751{,}36 \\ 17751{,}36 \\ 7731{,}81 \\ 8489{,}26 \end{cases} = 7731{,}81 \; [N]$$

$$F_{v,R,d} = \frac{k_{mod} \times F_{v,R,k}}{\gamma_M} = \frac{0{,}9 \times 7731{,}81}{1{,}25} = 5566{,}90 \; [N]$$

In this study, the load carrying $F_{v,R,d}$ per shear and for each fastener is equal to 5566,9 [N], considering a safe factor equal 1,338 (N=1,25/0,9) where the minimum value of the characteristic load-carrying capacity per shear plane per fastener $F_{v,Rk}$ was determined in previous. According the applied design force F_d, in safe design the number of dowels Nº for the connection in symmetry is given by:

$$N\º = \frac{F_d}{F_{v,R,d}} = \frac{100000}{5566{,}90} \geq 18 \qquad (19)$$

In the W-W-W connection in study, a total of 20 dowels will be considered (in 4 lines and 5 columns) with a symmetrical distribution. According the EN 1995-1-1, [23], the minimum spacing and edge, and end distances between the dowelled connections are presented in figure 26, considering the calculation in table 20. In nailed timber-to timber connections the definitions

used are: a_1 represents the spacing of nails within one row parallel to grain; a_2 the spacing of rows of nails perpendicular to grain; $a_{3,t}$ the distance between nail and loaded end and $a_{4,c}$ the distance between nail and unloaded edge.

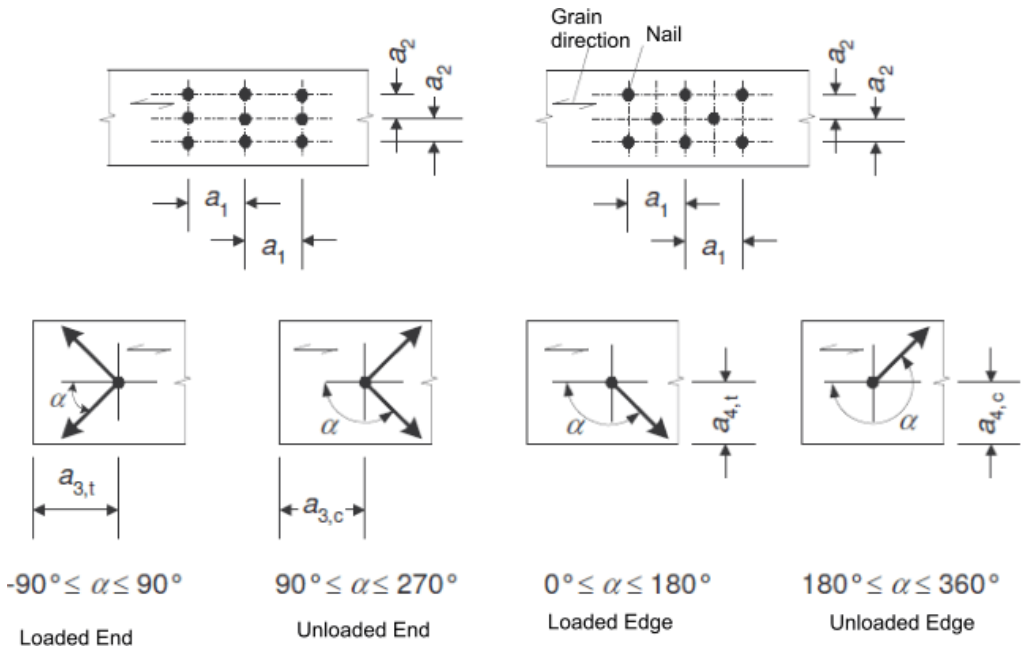

Figure 26: Spacing and end and edge distances, [23].

Spacing and edge / end distances	Angle	Minimum spacing or edge / end distance	Value
a_1 (Parallel to grain)	$0° \le \alpha \le 360°$	$(3 + 2\lvert\cos \propto\rvert).d$	$(3 + 2\lvert\cos 0\rvert).12 = 60\ [mm]$
a_2 (Perpendicular to grain)	$0° \le \alpha \le 360°$	$3\ .d$	$3 \times 12 = 36\ [mm] \Rightarrow 40\ [mm]$
$a_{3,t}$ (loaded end)	$-90° \le \alpha \le 90°$	$\max(7.d\ ;\ 80\ mm)$	$\max(7\times12\ ;\ 80\ mm) = \max(84\ ;\ 80\ ) = 84\ [mm] \Rightarrow 85\ [mm]$
$a_{3,c}$ (unloaded end)	$90° \le \alpha \le 150°$ $150° \le \alpha \le 210°$ $210° \le \alpha \le 270°$	$\max\left((a_{3,t}\lvert\sin \propto\rvert).d\ ;\ 3.d\right)$ $3.d$ $\max\left((a_{3,t}\lvert\sin \propto\rvert).d\ ;\ 3.d\right)$	-
$a_{4,t}$ (loaded edge)	$0° \le \alpha \le 180°$	$\max([2 + 2\sin \propto].d\ ;\ 3.d)$	-
$a_{4,c}$ (unloaded edge)	$180° \le \alpha \le 360°$	$3\ .d$	$3 \times 12 = 36\ [mm]$ $40\ [mm]$

Table 20: Minimum spacing and edge and end distances for dowels, [23].

Chapter 4

FEM Analysis of W-W-W Connection at Ambient Temperature

4. FEM Analysis of W-W-W Connection at Ambient Temperature

4.1. Introduction

The finite element method (FEM) is a numerical procedure that can be used to obtain solutions to a large class of engineering problems involving stress analysis, heat transfer, electromagnetism, fluid flow, … [36]. Today the finite element method is considered as one of the well-established and convenient technique for the computer solution of complex problems in different fields of engineering as civil engineering, mechanical engineering, etc. From other side, FEM can be examined as a powerful tool for the approximate solution of differential equations describing different physical processes, [36].

In this work ANSYS will be used as a finite element analysis software applicable in all fields of engineering such as structural, thermal, fluid (including computational fluid dynamics), electrical, electrostatics and electromagnetics. The structural analysis is employed to determine the displacements, deformations, strains and stresses. Coupled-field analysis considers the mutual interaction between two or more fields such as thermal-stress analysis. The fact that each depends upon another makes it is impossible to solve each separately, therefore the program that can solve both physics problems by combining them, [37]. The design is modelled using discrete elements, and each element has exact equation that describe how it responds to a certain load, and the sum of the response of all elements in the model gives the total response of the problem. The thermal analysis is used to determine the temperature distribution in the problem in study. Other quantities of interest include amount of heat lost or gained, thermal gradients, and thermal flux. All three primary heat transfer modes can be simulated: conduction, convection, radiation, [37].

In FEM analysis, continuous models are approximated using a finite number of discrete elements, as called ‘discretization’. Interpolation within the elements is achieved through typical shape functions. The shape function is the equation which interpolates the solution between the discrete values obtained at the nodal elements. Therefore, appropriate functions must be used and, as already mentioned, low order polynomials are typically chosen as shape functions, [37]. In this work, linear shape functions are used.

In all simulations, SOLID185 is used for the three-dimensional modelling, represented in figure 27. The element is defined by eight nodes having three degrees of freedom at each node: translations in the nodal x, y, and z directions.

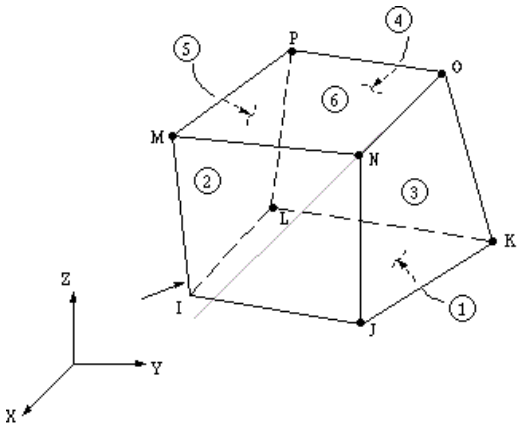

Figure 27: SOLID185 3-D Structural Solid.

In this study, the main objective is the use of FEM analysis to obtain the maximum critical load applied to the W-W-W connection and to determine the maximum capacity of the connection. The numerical results will be compared with the analytical previous calculation. The numerical results for stresses are according the applied generalized Hooke law. Also, the von Mises equivalent stress is a measure that accounts for all six components of a general 3D state of stress. von Mises stress σ_{vm}, can be expressed either by six stress components as:

$$\sigma_{vm} = \sqrt{0{,}5\left[\left(\sigma_x - \sigma_y\right)^2 + \left(\sigma_y - \sigma_z\right)^2 + \left(\sigma_z - \sigma_x\right)^2\right] + 3\left(\tau_{xy}{}^2 + \tau_{yz}{}^2 + \tau_{zx}{}^2\right)} \quad (20)$$

Or expressed function of their principal stresses as:

$$\sigma_{vm} = \sqrt{0{,}5\left[(\sigma_1 - \sigma_2)^2 + (\sigma_2 - \sigma_3)^2 + (\sigma_3 - \sigma_1)^2\right]} \quad (21)$$

Notice that von Mises stress is a non-negative, scalar stress measure. von Mises stress is commonly used to present results because the structural safety for many engineering materials showing elastic-plastic properties can be evaluated using this criterion, [38]. In the present study, the von-Mises will be calculated to verify the critical zones in W-W-W connection.

4.2. W-W-W connection at ambient temperature in FEM analysis

In the present work, one model representative of the 4 wooden plates connected to each other by steel dowels, will be reproduced in FEM analysis. The technical drawings of this model are presented in the chapter 3.

Figure 28 represents the entire model developed in the numerical program. Two different material properties are considered, as mentioned in previous chapter. All materials are considered as non-linear with an elastic-plastic behaviour, as a multilinear material. For the

structural analysis, the material strength and elastic properties (isotropic for steel and orthotropic for timber) are the major determining factors to obtain desired results of the structural capacity.

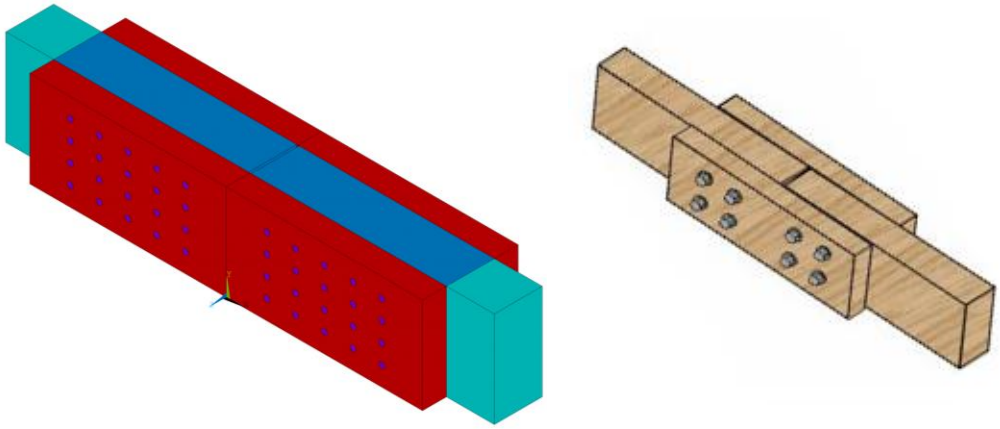

Figure 28: The numerical model representative of the W-W-W connection.

Due the geometric symmetry and loading conditions, only one quarter of the model will be analyzed, figure 29. We can take advantage of simulating the model as half or quarter, due the reduction in time computational processing and memory required. In symmetry, the lines or planes of the model can be simulated by providing proper restraints to the symmetrical boundary conditions. The geometry and the restraints must be symmetric about a plane, and the loads must be either symmetric. By taking advantage of symmetry, the size of the analysis domain can be reduced, at least by a factor of two. Or, a thinner mesh can be used in the reduced domain resulting in a more accurate analysis than a coarsely meshed in full model.

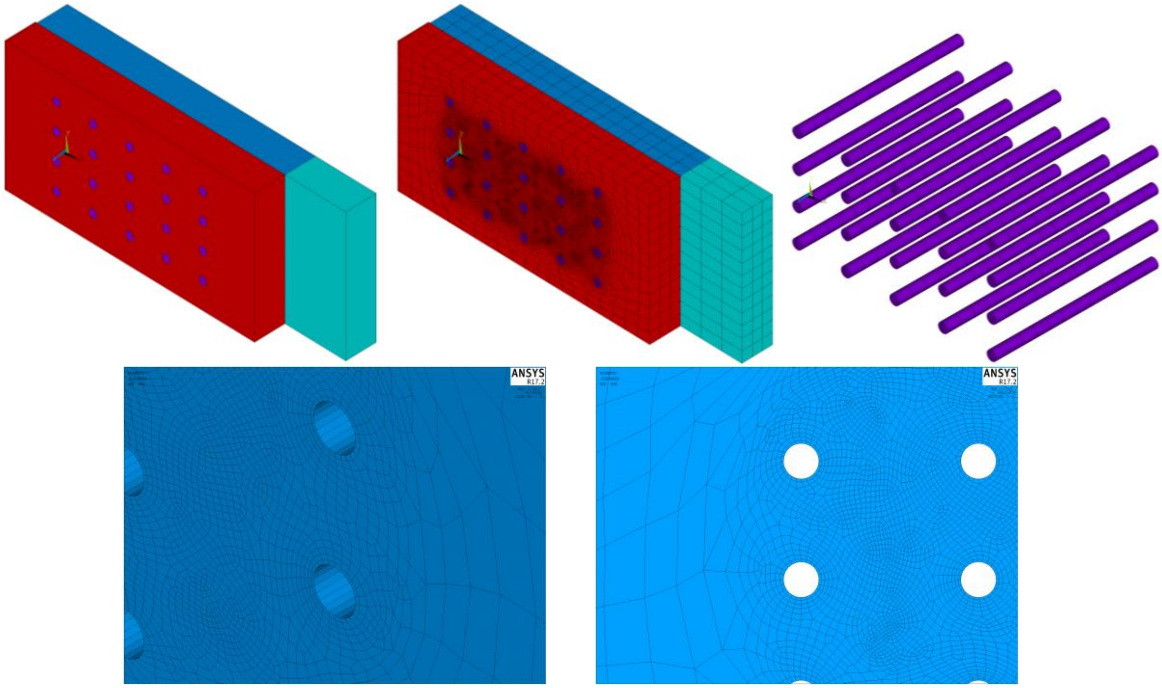

Figure 29: The reduced model, one quarter of the entire model. Mesh for reduced model and for dowels.

An automatic mesh was used in FEM program. The mesh is more refined near of the holes being less discretized in the remain cross-section of the connection.

In this assembly, many contacts occur between surfaces such as, the dowels hole, wood-wood plates and wood-dowels interactions. Contact elements and contact algorithms are needed to predict the discontinuities in the model. In the program introduces these contact elements and algorithms through the contact interaction and interaction properties features, with pairs of surfaces known as ‘’contact pairs’’, generated automatically. In this study, the contact pair are defined as Targe170 and Conta174. A static friction coefficient of 0,3 was used for the tangential behaviour, based on the friction Coulomb’s law. Also, figure 29 shows the global mesh, produced automatically, of the steel part of the model (the dowels) and which present the connection elements between the timber plates, also the mesh in timber plates.

In FEM structural analysis, an incremental and linear tensile load P_{inc} will be implemented from 0 to 100000 [N] (between 0 to 100 [s]) in the lateral right edge, representing a half of the applied load in W-W-W connection ($^{P}/_{2}$). The program conducts an analysis in steps and applies the load in increments in order to obtain a converged solution. In this side, the load will be distributed in 33 nodes, proportional to the step time increment [($^{P}/_{2}$)./ 33 nodes]. Each analysis step contains a procedure to solve the numerical problem within a certain time frame known as ‘’step time’’. This concept of time increments and the proportional applied load was used to estimate the load to cause ultimate failure or damage in the wood material during the analysis. The time step size chosen is equal to 5 [s].

The main objective of the numerical analysis is to determine the maximum capacity of the connection, until end of the running structural problem. The ultimate capacity of the connection leads to a failure mode, as maximum stresses reached in the glulam W-W-W in the parallel direction to wood grain. According the obtained numerical results, the estimation of the ultimate capacity from the structural W-W-W model will be calculated as the following and compared with the ultimate load capacity recorded from the analytical solution.

The predicted ultimate load from the model is 132 [kN] and permits to calculate a load carrying $F_{v,R,d\ (numerical)}$ per shear and for each fastener (20 dowels) equal to 6,6 [kN] for the numerical W-W-W connection. The calculated load carrying $F_{v,R,d}$ per shear and for each fastener was equal to 5,57 [kN] according standards. The estimated relative error is 18,49% in relation to the calculated $F_{v,R,d}$ value. The numerical value is obtained from a time step equal to 20 [s] which represents 6,6 [kN] in model, as presented in table 21.

For lower time step *t*=15 [s], the ultimate load is lesser than the design load imposed in the model. The numerical value obtained is 4,95 [kN] and the estimated relative error is 11,13% in relation to the $F_{v,R,d}$ value, table 21.

Time step	**Applied incremental tensile force**	**Load carrying per shear and each fastener**		
t, [s]	*P*, [N] (in 33 nodes)	$F_{v,R,d}$, [kN]		|Error|, %
		Numerical	EC5	
15	1500 x 33 x 2 = 99 000	99 / 20 = 4,95	5,57	11,13
20,	2000 x 33 x 2 = 132 000	132 / 20 = 6,60		18,49

Table 21: Load carrying per shear and each fastener calculation.

Figure 30 represents the analysis of equivalent stresses when a load carrying per shear and each fastener reaches 4,95 [kN]. The model doesn't show any damage due the lower equivalent stresses. But, the images show the distribution of the equivalent stress among the model.

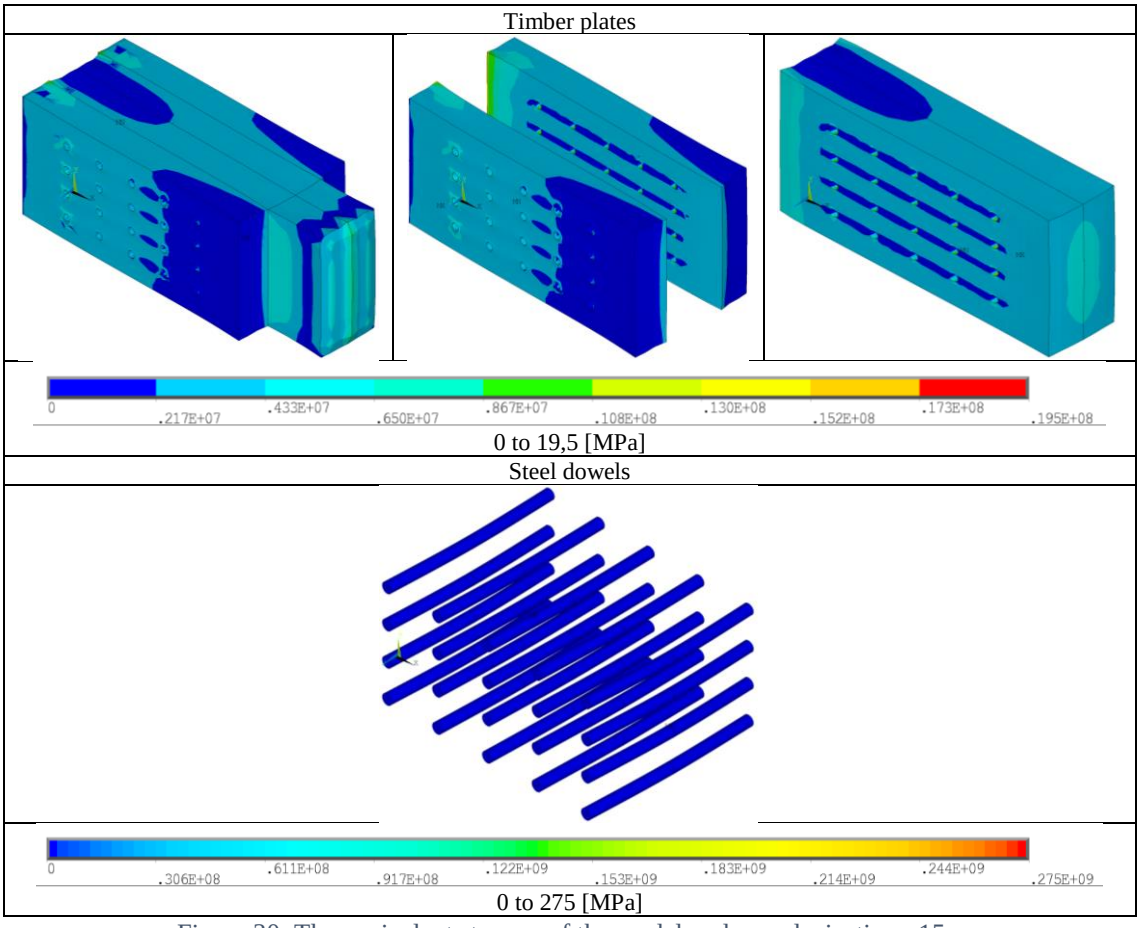

Figure 30: The equivalent stresses of the model under analysis, time=15s.

The last value of the incremental tensile load at 20 [s], when the load carrying per shear and each fastener reaches 6,6 [kN], is compared with the previous time-step, and all timber holes reach the maximum value of yield stress material. As verified, the maximum level of equivalent stresses was obtained in the timber hole near of the middle of connection. Inside the timber holes the level of maximum stresses reaches the maximum value of yield stress material, and due this fact, the damage starts at this point. The steel dowels don't appear any damage due the lower equivalent stresses. But, due the deformed shape, the stresses concentrations are in middle of the dowels.

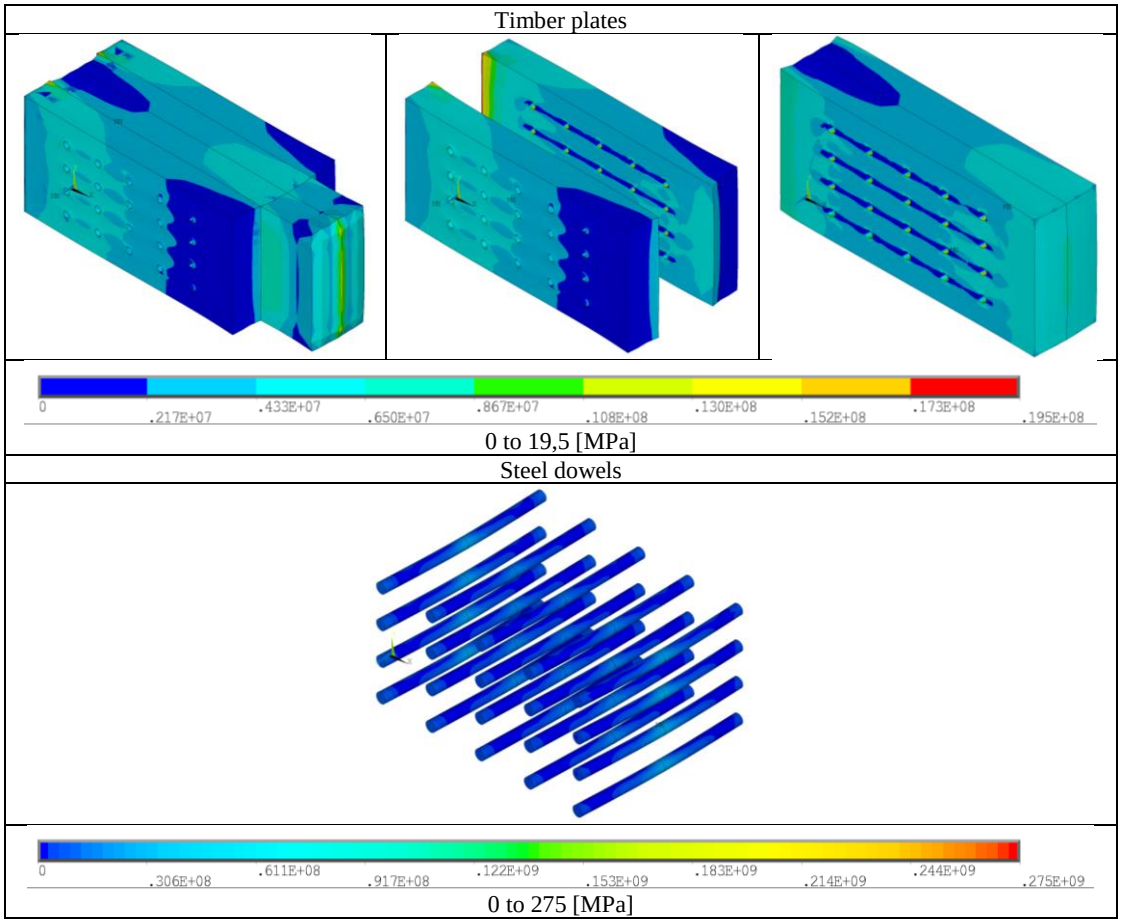

Figure 31: The equivalent stresses of the model under analysis, time=20 [s].

Figure 32 exemplifies the difference between the equivalent stress in the timber holes at 15 and 20 [s] of the FEM analysis. As it can be noticed, the maximum equivalent stress is more concentrated in the lower and higher part of the timber holes.

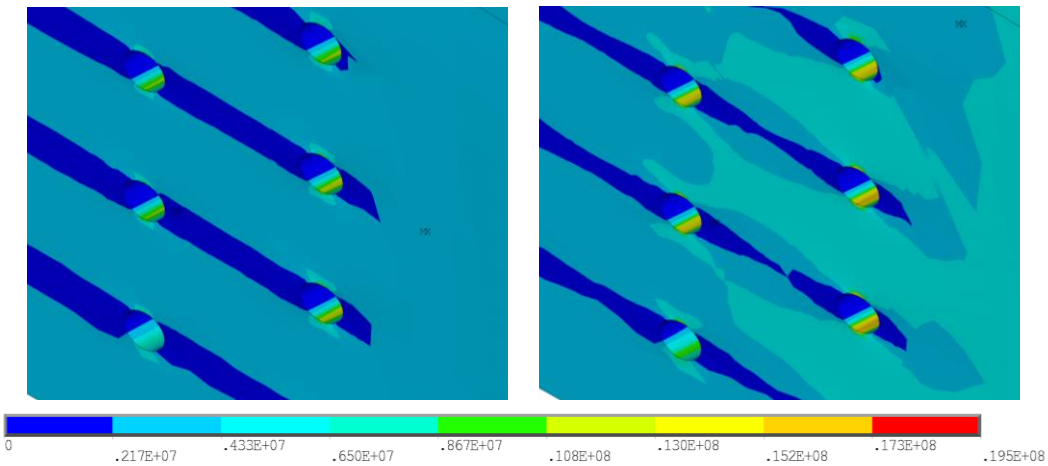

Figure 32: The equivalent stress [Pa] in timber holes at 15 [s] (left) and 20 [s] (right).

Figure 33 represents a time curve history for equivalent stress in different nodal positions at two holes in the W-W-W connection, as an elasto-plastic behaviour. The curve shows an increase of the obtained equivalent stress in upper and lower sides of the timber holes, giving the maximum critical value after 20 [s] where the material reaches the yield stress and the damage surface occurs in timber. This behaviour is the result of the applied tensile load and the effect of the steel dowels in contact with the timber in these locations. In opposite, the hole sides appear with small values of stress as the deformation effect of the timber connection during the same applied load.

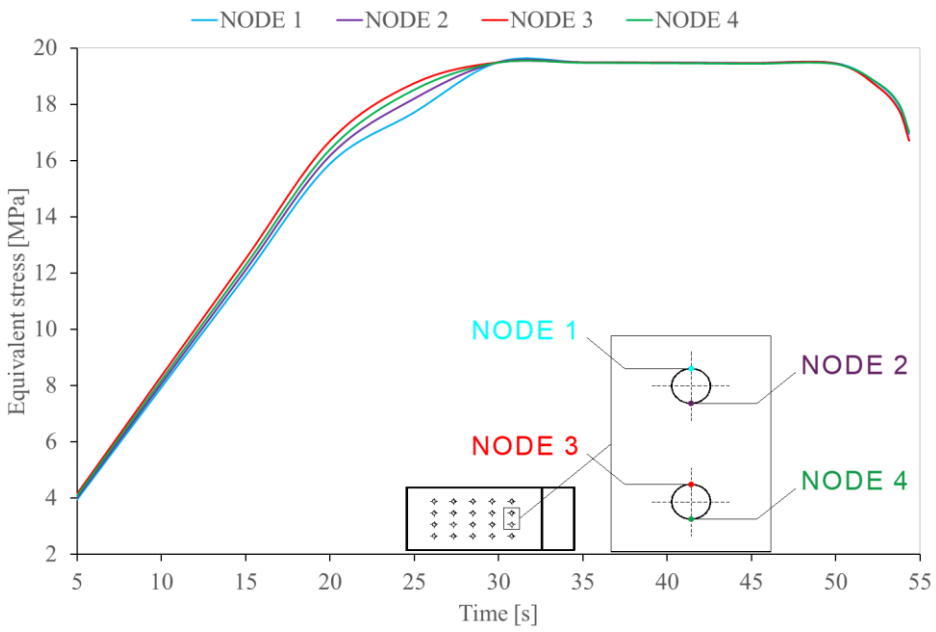

Figure 33: The development of the equivalent stress in upper and lower sides of timber holes.

To exemplify what happen in the particular damage holes, figure 34 shows the numerical values from the W-W-W connection loaded parallel to the grain with the maximum stress

distribution obtained in timber holes along the longitudinal direction (direction of load). Reached value for numerical models is heavily dependent on the orthotropic of timber material for the three principal directions. Figure 34 shows the equivalent stress horizontally to the loading direction (blue color). This tensile load causes the dowel which is pressed into the timber holes and simultaneously occurs the maximum stress in timber perpendicularly to the loading direction (red and yellow color). It can be seen that the stress is symmetrical in value over the load axe. Tensile stress component is trying to pull the timber of the dowel hole and this creates maximum values and move perpendicularly (upper and lower zone of timber holes).

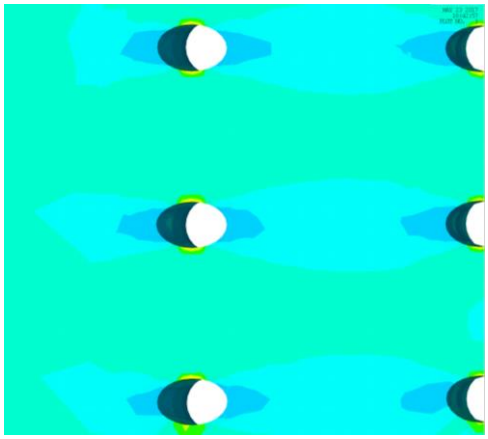

Figure 34: Equivalent stress distribution with the timber holes shape deformation.

In numerical modelling, due to the high computational cost, time steps equal to 5 were used. The numerical solution obtained results up 20 [s]. The proposed numerical simulation can be used for stresses calculation and verification of the field distribution for any materials or components of the model under study, as an accepted methodology to prevent any damage material on the building design. The numerical solution can be improved by using shorter time steps and even using finite elements with higher polynomial shape functions. Nevertheless, the presented solution gives good results and are in accordance with the previous calculated load carrying per shear and by each fastener.

Chapter 5

Design of W-W-W Connection at High Temperatures

5. Design of W-W-W Connection at High Temperatures

5.1. Introduction

Fire safety has always been a major concern in the design of timber construction. Even though wood is a highly combustible material, timber members perform adequately under elevated temperature effects. The thermal response of timber connections, however, is in most cases poor and determination of their fire resistance is usually the crucial factor in evaluating the overall loadbearing capacity of wood structures exposed to fire. The analysis of timber joints under fire conditions can be challenging due to their complexity and variety. After presenting the behaviour of the W-W-W connection with ambient temperature, this chapter reviews the fire performance on this type of connection. The temperature effect is an important factor on the fire resistance of timber connections, which leads to the joint protection, or a redefined size model with non-protected material, [39].

5.2. Charring rate

Application of sufficient heat to wood leads to a process of thermochemical decomposition, called pyrolysis, which results in alteration of its chemical composition and physical appearance (formation of the char layer). This phenomenon is accompanied by mass loss in the material. In timber structural members, charring appears in all exposed surfaces in form of a layer which increases in depth with the fire development. According to EN1995-1-2, [8], the position of the char layer coincides with 300 [°C] isotherm (start of charring time is the time when charring of wood starts behind the cladding). The charred layer cannot carry structural loads (resulting in a reduction of the cross-section) but acts as thermal insulation for the remain cross-section, [40]. The charring rate is defined as the ratio of the char layer depth divided by the duration of fire and it is considered to be constant with time. This is a common assumption for exposure to standard fire and it is based on the principles of one-dimensional heat transfer, which hold true for members used in typical timber construction. The notion of a constant charring rate has been adopted by EN1995- 1-2, [8]. The importance of charring rate in the fire design of timber construction has already been emphasized, [40]. After fire exposure, the wood cross-section given in figure 35 shows different areas:

- An outer part of the wood that is charred,
- A layer with a thickness of about 5 [mm] which is pyrolysis, that the wood is chemically altered by fire but is not yet completely decomposed,

- The heart of the section which consists of intact or normal wood.

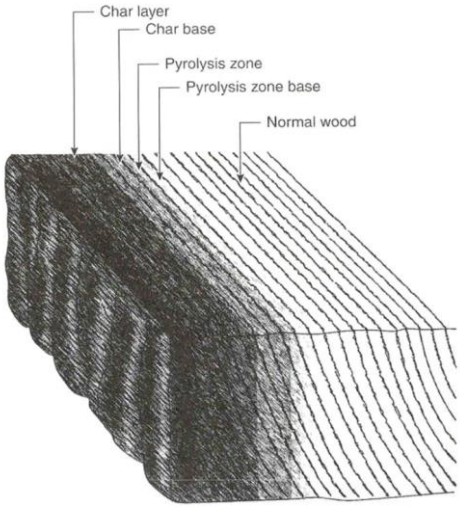

Figure 35: Degradation zones in a wood section, [41].

The char layer depth shall be measured from the outer surface of the element, up to the border between the charring layer and the non-charring part of the element (char-line). The char layer depth can be calculated using the following formulas, [42]:

- for one-dimensional (figure 36)

$$d_{char,0} = \beta_0 \,.\, t \tag{22}$$

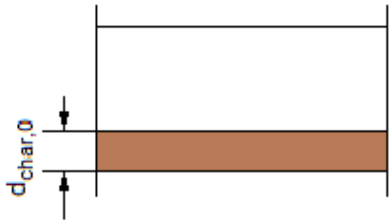

Figure 36: One-dimensional char layer for one fire exposure direction, [42].

- for the notional char layer which incorporates the effect of corner rounding (figure 37)

$$d_{char,n} = \beta_n \,.\, t \tag{23}$$

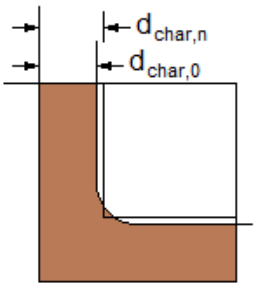

Figure 37: Char layer depth for more than one fire exposure direction, [42].

In previous equations, the variables definitions are according to the following:

$d_{char,0}$: design char layer depth for one-dimensional fire exposure [mm],

$d_{char,n}$: design char layer depth, which incorporates the effect of corner rounding [mm],
β_n: one-dimensional charring rate under standard fire exposure [mm/min],
β_n: design charring rate, which includes the effect of corner rounding and fissures [mm/min],
t: time of fire exposure [min].

5.3. Insulation materials

Insulations are building materials which reduce the heat transfer to other elements. They may be categorized by its composition (natural or synthetic materials), shape (spray foam, panels…), structural effect, functional mode, resistance to heat transfer, environmental impacts, etc. The choice of which insulation material is used depends on a wide variety of factors. The factors affecting the type and amount of insulation to be used in a building include: thermal conductivity, moisture, strength, ease of installation, durability, cost, toxicity, flammability, also environmental impact and sustainability.

There are different insulation materials: Rockwool, ceramic fiber, calcium silicate boards, gypsum boards, intumescent materials, spray-on cement based materials. Depending on the application or in conjunction with other materials, the selection of the insulation material will be the guarantee to produce better thermal performance. To predict the fire resistance of a load-bearing assembly, the temperatures inside the assembly must be determined, as they are critical in assessing the structural behaviour of the assembly. For such calculations, knowledge of the thermal properties that include thermal conductivity, specific heat and density, at ambient and elevated temperatures, of the materials that comprise the assembly, i.e., wood, steel and insulation, is required, [43].

5.3.1. Wood-based panels

Wood-based panels are a general term for a variety of different board products, which have an extraordinary range of physical properties. More precisely, wood-based panels are materials made of wood scraps, bonded with adhesives using pressure and high temperature. They are usually used in construction and in the furniture industry. The advantages of such materials include high strength, durability, stability and easy installation.

There are different types of wood-based panels, [44]:

- Solid wood panel, consisting of pieces of timber glued together on their edges and, if multi-layer, on their faces.
- Laminated veneer lumber (LVL), consisting of wood veneers with fibres primarily in the same direction.
- Plywood, consisting of an assembly of layers glued together with the direction of the grain in adjacent layers usually at right angles.
- Oriented strand board (OSB), as a multi-layered board made from strands of wood of a predetermined shape and thickness together with a binder (strip-shaped wood chips bonded with adhesives).
- Resin-bonded particleboard, is manufactured under pressure and heat from particles of wood and/or other lignocellulose material in particle form with the addition of an adhesive.
- Cement-bonded particleboard (CBPB) or fibreboard, is manufactured under pressure, based on wood or other vegetable particles bonded with cement and additives.

The medium density fibreboard (MDF) is one of the most widely used wood-based panels, it is composed of wood fibers that are mixed with resin and pressed into flat panels under high temperature and pressure, [43].

Figure 38: Medium density fibreboard (MDF), [45].

Table 22 shows the thermal properties of the medium density fiberboard:

Material	**Thermal conductivity**	**Specific Heat**	**Density**	**Emissivity**
	[W/m.°K]	[J/kg.°K]	[kg/m^3]	
Medium Density Fiberboard	0,14	1700	600	0,85

Table 22: Thermal properties of medium density fiberboard, [51].

5.3.2. Gypsum plasterboards

Other typical insulation material is the gypsum plasterboard (also known as drywall). This material is a typical panel that consists of a non-combustible core, made primarily of calcium sulphate dehydrate (gypsum) with or without additives and normally pressed between a facer and a backer (typically thick sheets of paper), back and long edges, used in as several building materials. The plaster is mixed with fiber (typically paper and/or fiberglass), plasticizer, foaming agent, and various additives that can decrease mildew, increase fire resistance, and lower water absorption. Gypsum plasterboard walls and ceilings have different advantages: ease of installation, fire resistance, sound insulation and durability, [47]. As its chemical formula shows (CaSO4 . 2H2O), gypsum contains water (approximately 50% by volume). When gypsum panels are exposed to fire, heat is absorbed as a portion of the combined water is driven off as steam. This chemical process is called calcination, [47].

Figure 39: Gypsum Plasterboards, [50].

Table 23 shows the thermal properties of the gypsum plasterboard:

Material	**Thermal Conductivity**	**Specific heat**	**Density**	**Emissivity**
	[W/m.°K]	[J/kg.°K]	[kg/m^3]	
Gypsum	0,25	1000	900	0,85
Gypsum plasterboard	0,21	1000	700	0,85

Table 23: Thermal properties of gypsum types of insulation material, [46].

5.4. W-W-W configuration at high temperature

To determine the W-W-W connection at high temperature, all requirements according standards will be conducted. For the design of wood connections under high temperature, according to Eurocode 5 1-2, [8], there are two different methods, the simplified method and the load reduction method. In this work, the simplified method will be used, considering two proposed methodologies, for unprotected and protected W-W-W connection at high temperature. The final W-W-W configuration with all dimensions for the unprotected and the

protected connection is presented in figure 40 and figure 41, respectively. The proposed model is calculated in the extra thickness of member to improve the fire resistance for the unprotected connection, and the fire protective panel thickness for the protected connection. In order to evaluate the resistance time of the element in wood exposed to a fire situation, the simplified calculation methodology is presented.

5.4.1. Unprotected connection

The fire resistance time of the type of joint used which is the dowels is $t_{d,f_i} = 20\ [min]$ and the thickness of the side member is $t_1 \geq 45\ [mm]$, [8].

According to Eurocode 5 1-2, [8], and from the report guide, [35], for connections with dowels, the fire resistance period t_{d,f_i} which is greater than 20 [min] but not exceeding 30 [min], $20\ [min] < t_{d,f_i} < 30\ [min]$, may be achieved by increasing the following dimensions by a_{f_i} for the following sides: the thickness of side members; the width of the side members and the end edge distance to dowels.

$$a_{f_i} = \beta_n \,.\, k_{flux} \,.\, \left(t_{req} - t_{d,f_i}\right) \tag{24}$$

where:

β_n: charring rate according the 'table 3.1' of EC5 1-2, [8],

$k_{flux} = 1{,}5$: coefficient that considers increased heat flux through the dowels,

t_{req}: required standard fire resistance period,

t_{d,f_i}: fire resistance period of the unprotected connection.

For the timber plates, and as it has been already seen in chapter 3, a typical yellow birch wood type GL28h (Homogeneous Glue Laminated Timber, Hardwood) has been used, with a density of $\rho = 410\ [kg/m^3]$.

According to the table 3.1 from EC5 1-2, [8], the design charring rates β_0 and β_n for the glued laminated hardwood with a characteristic density $\geq 410\ [kg/m^3]$:

$\beta_0 = 0{,}50\ [mm/min]$, $\beta_n = 0{,}55\ [mm/min]$.

Then, using equation (24):

$$a_{f_i} = 0{,}55 \times 1{,}5 \times (30 - 20) = 8{,}25\ [mm]$$

For a fire resistance equal to 30 [min], table 24 represents all calculations for W-W-W unprotected connection.

Dimension [mm]	**Initial dimensions** [mm]	$F_{v,Rk}{}^1$ [N]	**Exposure time** [min]	**New dimensions** [mm]	$F_{v,Rk}{}^2$ [N]	η
∅12	$t_1 = 50$ lateral $t_2 = 100$ internal	7731,81	30	$t_1 = 58{,}25$ $t_2 = 100$	8489,26	$\eta = \frac{F_{v,Rk}{}^2}{F_{v,Rk}{}^1}$ $\cong 1{,}1$

Table 24: Fire resistance calculation for 30 [min].

where $F_{v,Rk}{}^1$ is the characteristic load-carrying capacity per shear plane and per fastener, at ambient temperature (from chapter 3) and $F_{v,Rk}{}^2$ the characteristic load-carrying capacity per shear plane per fastener (considering $t_1 = 58{,}25\ [mm]$ in calculation).

According the equation (16):

$$\begin{cases} f_{h,1,k} \,.\, t_1 \,.\, d = 29{,}5856 \times 58{,}25 \times 12 = 20680{,}33 & (a) \\ 0{,}5 \,.\, f_{h,2,k} \,.\, t_2 \,.\, d = 0{,}5 \times 29{,}5856 \times 100 \times 12 = 17751{,}36 & (b) \\ 1{,}05\ \dfrac{f_{h,1,k} \,.\, t_1 \,.\, d}{2+\beta}\left[\sqrt{2\beta\ (1+\beta) + \dfrac{4\beta\ (2+\beta)\ M_{y,Rk}}{f_{h,1,k} \,.\, d \,.\, t_1{}^2}} - \beta\right] + \dfrac{F_{ax,Rk}}{4} = & \\ 1{,}05 \times \dfrac{29{,}5856 \,.\, 58{,}25 \,.\, 12}{2+1}\left[\sqrt{2\times1\ (1+1) + \dfrac{4\times1\ (2+1)\ 76745{,}4}{29{,}5856 \,.\, 12 \,.\, 58{,}25^2}} - 1\right] = 8561{,}06 & (c) \\ 1{,}15\sqrt{\dfrac{2\beta}{1+\beta}} \,.\sqrt{2 \,.\, M_{y,Rk} \,.\, f_{h,1,k} \,.\, d} + \dfrac{F_{ax,Rk}}{4} = & \\ 1{,}15\sqrt{\dfrac{2\times1}{1+1}} \,.\sqrt{2 \times 76745{,}4 \times 29{,}5856 \times 12} = 8489{,}26 & (d) \end{cases}$$

The characteristic load-carrying capacity is the minimum value between all four equations:

$$F_{v,Rk}{}^2 = min\begin{cases} 20680{,}33 \\ 17751{,}36 \\ 8561{,}06 \\ 8489{,}26 \end{cases} = 8489{,}26\ [N]$$

As it can be seen, the new dimensions in W-W-W connection give 10% more mechanical resistance to the connection, at ambient temperature.

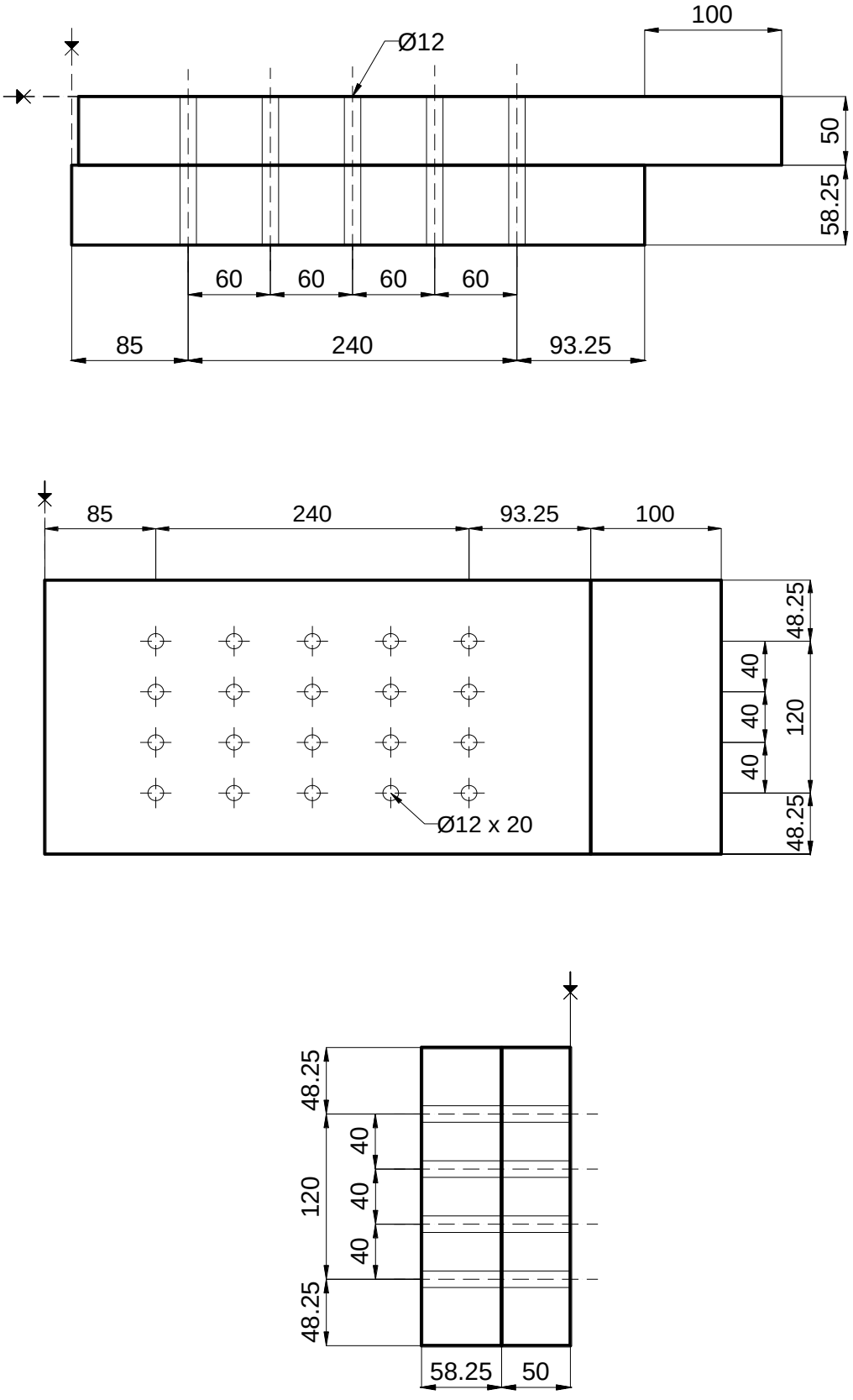

Figure 40: Unprotected connection in study under high temperature.

5.4.2. Protected connection

Also, according to Eurocode 5 1-2, [8], and from the report guide, [35], when the connection is protected by the addition of wood panelling or gypsum plasterboards type A or H, the time until start of charring should be calculated as it is shown in table 25.

	t_{ch} , [min]	h_p , [mm]
Wood panelling	$t_{ch} \geq t_{req} - 0{,}5\ t_{d,f_i}$	$h_p = t_{ch} \times \beta_0$
Gypsum plasterboard Type A / H	$t_{ch} \geq t_{req} - 0{,}5\ t_{d,f_i}$	$h_p = \frac{t_{ch} + 14}{2{,}8}$
Gypsum plasterboard Type F	$t_{ch} \geq t_{req} - 1{,}2\ t_{d,f_i}$	

Table 25: Charring time for different protection options for 30 [min].

where:

t_{ch}: time of start of charring,

h_p: thickness of the panel,

t_{req}: required standard fire resistance period,

t_{d,f_i}: fire resistance period of the unprotected connection.

The fire resistance time of the dowels is $t_{d,f_i} = 20\ [min]$ and the design charring rate β_0 for the hardwood GL28h is $\beta_0 = 0{,}50\ [mm/min]$, [8]. For different required times, table 26 shows the different values of t_{req}, t_{ch} and h_p.

Dowels, ∅12	t_{req} , [min]	t_{ch} , [min]	h_p , [mm]
Gypsum type A	30	20	12,1
	60	50	22,9
Gypsum type F	30	6	7,1
	60	36	17,9
Wood panelling	30	20	10
	60	50	25

Table 26: Values of t_{ch} and h_p depending on the protection type and t_{req}.

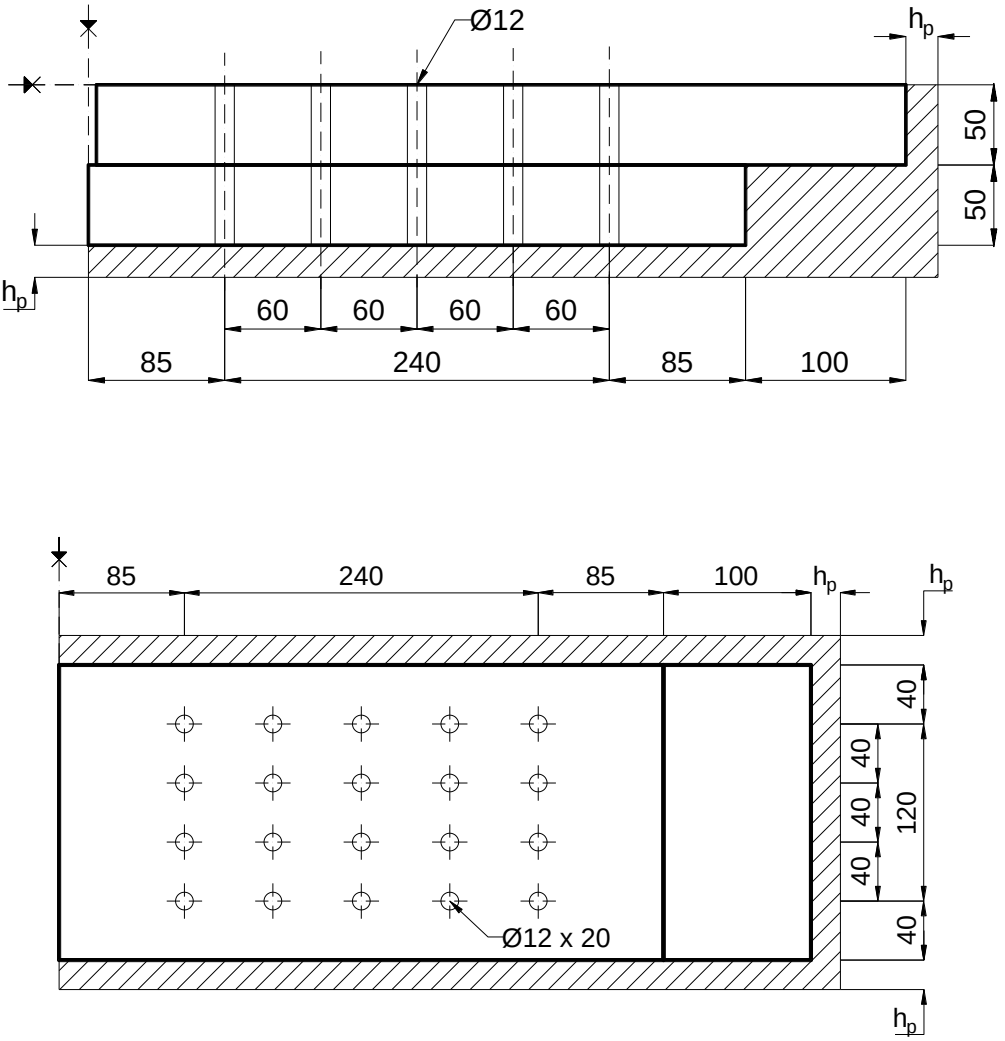

Figure 41: Protected connection in study under high temperature.

Chapter 6

FEM Analysis of W-W-W Connection at High Temperature

6. FEM Analysis of W-W-W Connection at High Temperature

6.1. Thermal introduction

Heat transfer is the science that studies the analysis of heat rate in a system, this transfer is occurring in the direction of areas where the temperature is lower. There are three heat transfer modes in a system: conduction, convection and radiation.

6.2. Conduction

Conduction is the process of heat transmission occurring in the particle with higher temperature for the particle with lower temperature, without occurrence of transport of matter from one region to another. The process of heat transmission occurs mainly in solids and especially in metals, as these are good conductors of heat. In general, a good conductor of electricity is also a good conductor of heat, [48].

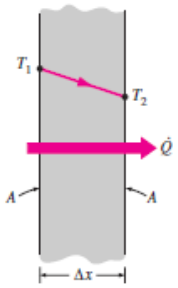

Figure 42: Heat conduction through a large plane wall of thickness Δx and area A, [48].

Fundamental law of conduction - Fourier law

Conduction occurs in stationary materials as a result of the atoms or molecules vibrations in the materials. It is governed by Fourier's law of heat conduction, which in one dimension is written as:

$$\dot{Q} = \lambda \times A \, \frac{T_1 - T_2}{L} \,, \qquad where: \quad q = \frac{\dot{Q}}{A} \tag{25}$$

where the heat flow transmitted per unit time $\dot{Q}, [J/s] = [W]$ is function of the thermal conductivity $\lambda, [W/(mK)]$, heat transfer area $A, [m^2]$, the temperature variation $(T_1 - T_2, [°C])$, and wall thickness ΔL, [m]. The thermal conductivity λ is a proportionality constant that characterizes the heat conduction behaviour for each material and depends on the phase at which this material is: density, porosity, moisture, temperature, etc.

6.3. Convection

Convection is the process of transferring heat between a surface and a fluid motion. Heat transfer occurs if the temperature of the fluid is different from the surface temperature, [49].

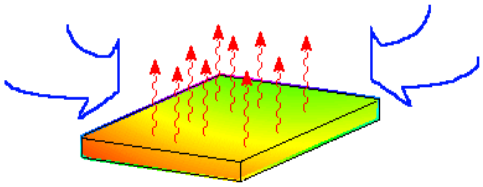

Figure 43: Natural or free convection, [38].

Fundamental law of convection - Newton Fourier's law

Newton's law represents that the rate of heat loss of a body is proportional to the temperature variation between the body and the environment where it is found, expressed in the form:

$$\text{If:} \quad T_s > T_\infty \quad \dot{Q} = h\,A\,(T_s - T_\infty) \tag{26}$$

$$\text{If:} \quad T_s < T_\infty \quad \dot{Q} = h\,A\,(T_\infty - T_s) \tag{27}$$

where the heat flux $\dot{Q}, [W]$, is function of the convection heat transfer coefficient $h, [W/(m^2°\text{C})]$, heat transfer area $A, [m^2]$, and the difference between the surface temperature $T_s, [°\text{C}]$ and ambient / fluid temperature $T_\infty, [°\text{C}]$, if the surface temperature $T_s, [°\text{C}]$ is less than ambient temperature / Fluid $T_\infty, [°\text{C}]$ positions are reversed.

6.4. Radiation

All bodies constantly radiate energy because of their temperature. This process is called thermal radiation, characterized by the process of heat transfer originated by the emission of an electromagnetic radiation (Maxwell's theory) due to the temperature of the bodies. The bodies or the surfaces in addition to emitting, can also receive radiations. For example, exactly as the energy of the sun reaches the earth, [49].

Fundamental law of radiation - Stefan-Boltzmann law

The heat flux that is transmitted in the presence of radiation is obtained by the law of Stefan-Boltzmann (fundamental law of radiation), according to equation 28. This law allows to affirm that, the transmitted heat flow is calculated by the product of the material emissivity in the

surface area, absolute surface temperature transmission area and Stefan-Boltzmann constant, given by equation 28, [40]:

$$\dot{Q} = \varepsilon \times \sigma \times A \times T_s^4 \tag{28}$$

where the flow of heat transferred per unit time $\dot{Q}, [J/s] = [W]$, is due to the emissivity of the surface ε (dimensional 0-1), the Stefan-Boltzmann constant $\sigma, [W/(m^2K^4)] = 5{,}6697 \times 10^{-8}$, heat transfer area $A, [m^2]$, and the absolute surface temperature $T_s, [℃]$, the normal emissivity values of steel and wood are, respectively, $\varepsilon = 0{,}7$ and $\varepsilon = 0{,}8$.

6.5. Equations and boundary conditions for heat transfer

For an isotropic body with temperature-dependent heat transfer, the basic equation of heat transfer has the following form (equation 29):

$$-\left(\frac{\partial q_x}{\partial x} + \frac{\partial q_y}{\partial y} + \frac{\partial q_z}{\partial z}\right) + Q = \rho c \frac{\partial T}{\partial t} \tag{29}$$

where: q_x, q_y and q_z are components of heat flow through the unit area; $Q = Q(x, y, z, t)$ is the inner heat-generation rate per unit volume; ρ is the material density; c is the heat capacity; T the temperature and t is the time. According to Fourier's law the components of heat flow can be expressed as follows, [49]:

$$q_x = -k \frac{\partial T}{\partial x}$$

$$q_y = -k \frac{\partial T}{\partial y} \tag{30}$$

$$q_z = -k \frac{\partial T}{\partial z}$$

Where: k is the thermal conductivity coefficient of the porous media. Substitution of Fourier's relations gives the following basic heat transfer equation:

$$\frac{\partial}{\partial x}\left(k \frac{\partial T}{\partial x}\right) + \frac{\partial}{\partial y}\left(k \frac{\partial T}{\partial y}\right) + \frac{\partial}{\partial z}\left(k \frac{\partial T}{\partial z}\right) + Q = \rho c \frac{\partial T}{\partial t} \tag{31}$$

Using the finite element method to discretize the problem in domain, a weak formulation based in Galerkin method is used, for choosing the weighting functions. This allows the following system of differential equations represented in equation 32 or 33, [43].

$$K_{(\lambda)(T,t)}\, T_{(t)} + C_{(C_p,\rho)}\, \dot{T}_{(t)} = F_{(T,t)(Q,q,h_c,T_p)} \tag{32}$$

$$K\, T + C\, \dot{T} = F \tag{33}$$

Each term of the equation 33 could be represented in terms of the following expressions:

$$K_{lm} = \sum_{e=1}^{E} \int_{\Omega^e} (\nabla N_l\, \lambda\, \nabla N_m)\, d\Omega^e + \sum_{e=1}^{H} \int_{\Gamma_h^e} h_{cr}\, N_l\, N_m\, d\Gamma_q^e \tag{34}$$

$$C_{lm} = \sum_{e=1}^{E} \int_{\Omega^e} \rho\, C_p\, N_l\, \lambda\, N_m\, d\Omega^e \tag{35}$$

$$F_l = \sum_{e=1}^{E} \int_{\Omega^e} N_l\, \dot{Q}\, d\Omega^e - \sum_{e=1}^{Q} \int_{\Gamma_q^e} N_l\, \bar{q}\, d\Gamma_q^e + \sum_{e=1}^{H} \int_{\Gamma_h^e} N_l\, h_{cr}\, \theta_\infty\, d\Gamma_q^e \tag{36}$$

where E is the total number of elements, Q is the number of elements with boundary type Γ_q, H is the number of elements with boundary type Γ_c and / or Γ_r, N_l and N_m are typical shape functions. The boundary conditions are defined as the prescribed quantities on the physical boundary. There are three types of boundary conditions, [49]:

A. Dirichlet boundary condition (condition of first type)

Dirichlet boundary condition may also be referred to as a fixed boundary condition. The temperature on the boundary of the body is prescribed by:

$$T(x,t) = T_w(x,t) \tag{37}$$

Where: T_w is a known function. In a lot of practical applications, T_w is simply a constant.

B. Neumann boundary condition (condition of second type)

Neumann boundary condition specifies the values that the derivative of a solution is to take on the boundary of the domain. If the heat flux $\dot{q_w}$ out of the body (perpendicular to the surface)

is given, then Fourier's law helps us in determining the partial derivative of the temperature with respect to the outward normal vector n:

$$\dot{q_w}(x,t) = -\lambda \frac{\partial T}{\partial n}(x,t) \quad \Rightarrow \quad \frac{\partial T}{\partial n}(x,t) = -\frac{\dot{q_w}(x,t)}{\lambda} \tag{38}$$

Notice that in the special case of perfect insulation ($\dot{q_w} = 0$), the equation to the right becomes a homogeneous Neumann boundary condition:

$$\frac{\partial T}{\partial n}(x,t) = 0$$

C. Cauchy boundary condition (condition of third type)

Cauchy boundary condition specifies both the function value and normal derivative on the boundary of the domain. This corresponds to imposing both a Dirichlet and a Neumann boundary conditions. Very often, there is a thermal interaction between the body and a surrounding fluid of temperature T_f. To quantify this, the boundary of the domain is considered as a control 'volume' for an energy balance. Since the thickness of the boundary is zero, no energy can be stored within. This means that all the heat entering a surface increment from the interior (by conduction) must leave outwards (by convection):

$$-\lambda \frac{\partial T}{\partial n}(x,t) = \alpha\,(T(x,t) - T_f) \tag{39}$$

6.6. Unprotected W-W-W connection at high temperature

6.6.1. Unprotected connection at high temperature in FEM analysis

In the present chapter, the same model of the 4 wooden plates connected to each other by steel dowels will be reproduced in FEM program with a non-linear thermal and transient analysis. The technical drawings of this model were presented in the chapter 5. Figures 46, 47 and 48 represent the front, top and a top cross-section (at the level of the dowels) of the unprotected model developed in the numerical program in 2D. Similar in the chapter 4, and due to the geometric symmetry and loading conditions, only one half of the model will be analyzed. We can take advantage of simulating the model as half, due to the more efficient solution results and reduced computational cost.

The thermal analysis is used to determine the temperature distribution in the problem in study. The boundary conditions used in this analysis are related to the convection and radiation, due the exposed fire in all external surfaces of the connection. Also the initial temperature in the numerical model was considered equal to 20 [ºC]. The environment surface emissivity in wood and steel materials will be taken constant equal to 1, and for insulation materials equal to 0,85. The three sides of the models will be exposed to standard fire curve ISO-834 during 7200 [s]. The convection will be taken equal to 25 [W/m^2.K] in all the exposed faces.

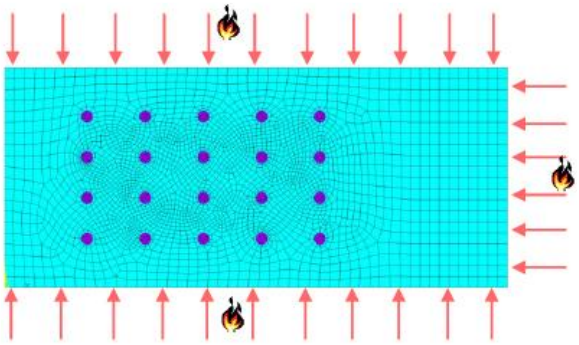

Figure 44: The exposed faces - Boundary conditions.

In all thermal simulations, a non-linear thermal and transient analysis was implemented using a finite element with 8 nodes (PLANE 77) for the two-dimensional modelling, represented in figure 45. The element PLANE 77 has one degree of freedom, temperature, for each node. The 8-node elements have compatible shape functions and are well suited to model curved boundaries.

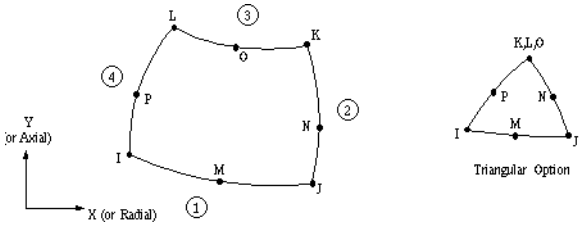

Figure 45: PLANE77 2-D 8-Node Thermal Solid.

As in the mechanical analysis, the used meshes in the numerical models were automatically generated by the FEM program, with a more discretized mesh near of the timber holes.

The main objective of this analysis is to verify the charring rate produced in wood plates through different time instants of the running thermal analysis, and compare it with the theoretical char layer presented in chapter 5. According to the obtained theoretical results using Eurocode 5 1-2, [8], and only for 30 [min], the calculated char layer is 8,25 [mm] and the charring rate is $\beta_0 = 0{,}50\ [mm/min]$.

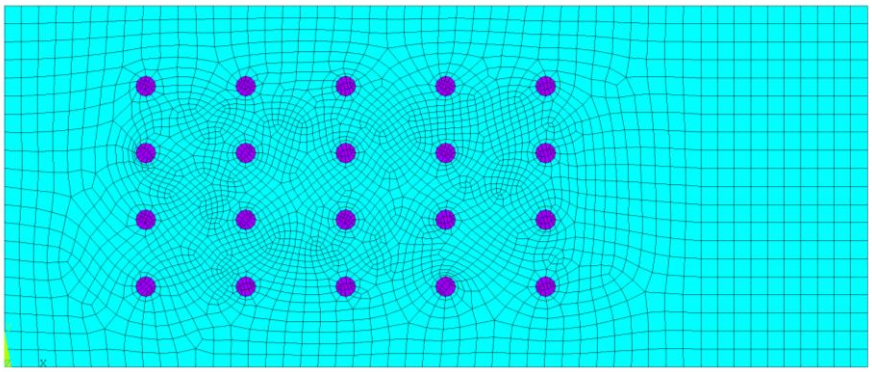

Figure 46: Mesh of half-model, front side of the unprotected W-W-W connection

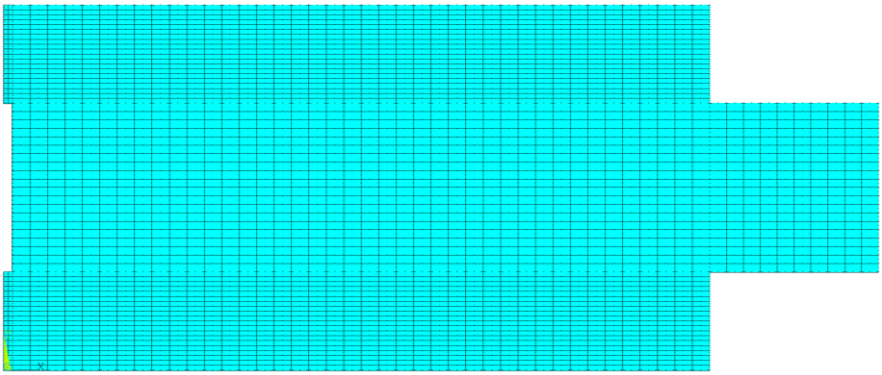

Figure 47: Mesh of half-model, top side of the unprotected W-W-W connection

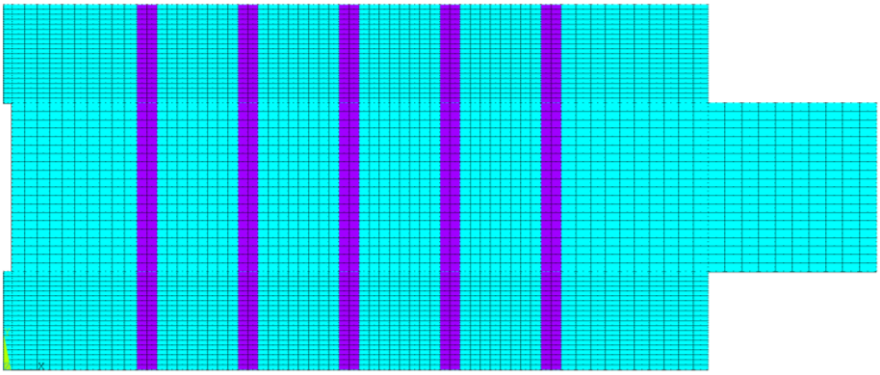

Figure 48: Mesh of half-model, top cross-section at the level of the dowels, unprotected W-W-W connection.

Two different material properties are considered, as mentioned in previous chapters. In the numerical analysis, the non-linear material thermal properties and temperature dependence (wood and timber) are the major determining factors to obtain desired results of the char layer.

For thermal and non-linear transient analysis, all sides of each model will be subjected to fire conditions. An initial temperature in all models were considered equal to 20ºC and the boundary conditions used in the numerical simulations are radiation and convection, according the environment temperature evolution due to fire. According standard curve ISO-834 for fire situation, an incremental temperature will be subjected from 20 to 1049 [°C] (between 0 and 7200s) in all three models. Each analysis step contains a procedure to solve the numerical

problem within a certain time frame known as ‘’step time’’. This concept of time increments and the proportional applied thermal load was used to estimate the temperature to cause a char layer in the wood material during the thermal and transient analysis. For all models, the time step size chosen is equal to 10 [s].

6.6.2. FEM results of the unprotected model at high temperature

The following figures represent the numerical results of the temperature evolution during 120 [min] of fire exposure in three sides of the W-W-W connection.

Figure 49 shows the development of the temperature in function of time, for different nodes in timber material considering the front side of the connection.

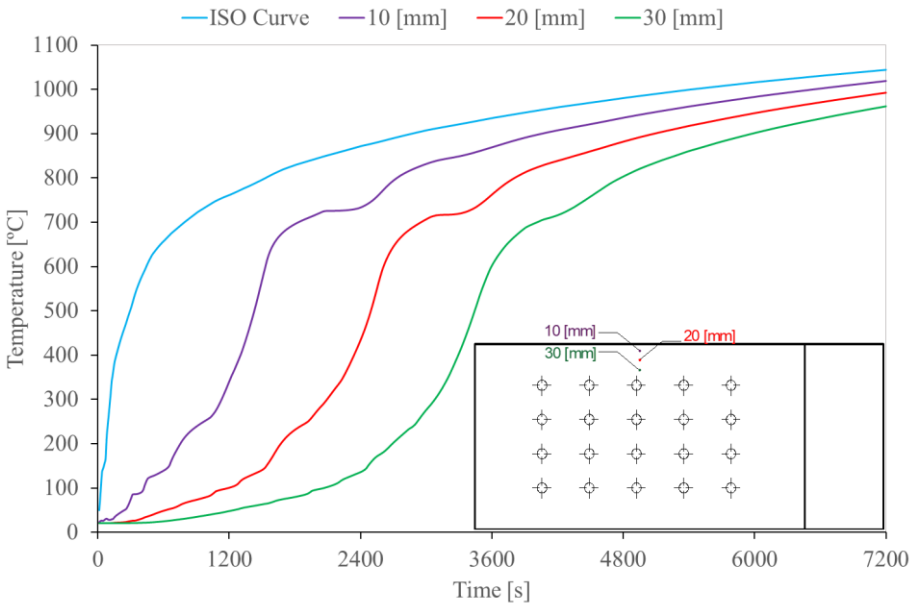

Figure 49: The temperature - time history in 10, 20 and 30 [mm] (front side).

It can be concluded that the deeper is the nodal points selection, the cooler effect of the timber is more pronounced. The first part (20 to 150 [ºC]) of the transient thermal analysis can be slightly sensitive, due to mesh and time step considered in FEM program. The warping in the curves between 650 [ºC] and 800 [ºC] is a result of thermal properties of steel material (dowels), precisely the specific heat effect. The behaviour of the specific heat of steel material under fire can be recognized by the pick at 720 [ºC]. Since, the model analyzed is composed of two different materials (wood and steel) with different properties, remarkably, the nodal point receives the heat effect of the steel, and also, the behaviour from the specific heat is more pronounced in the curve. This behaviour is the reason of the warping illustrated in Figure 48.

Figure 50 shows the temperature evolution, function of time, for different selected nodal positions of the W-W-W connection for the top side.

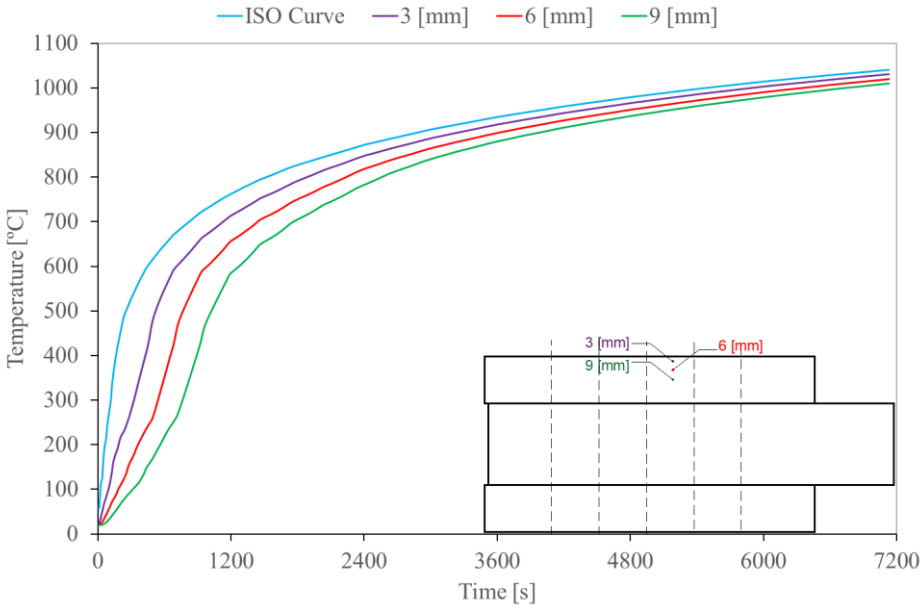

Figure 50: The temperature - time history in 3, 6 and 9 [mm] (top side).

According to the numerical results, it can be concluded that the nodal points are more close comparing with the front model, and the effect of the specific heat of steel dowels on timber members is almost negligible along the thermal analysis.

Figure 51 represents the temperature evolution for different nodal points (timber and steel material) considering the top cross-section side at the level of the dowels. The time-temperature curve of the steel does not manifest the effect of the specific heat, since simultaneously it has a slight cooling of the lateral wood.

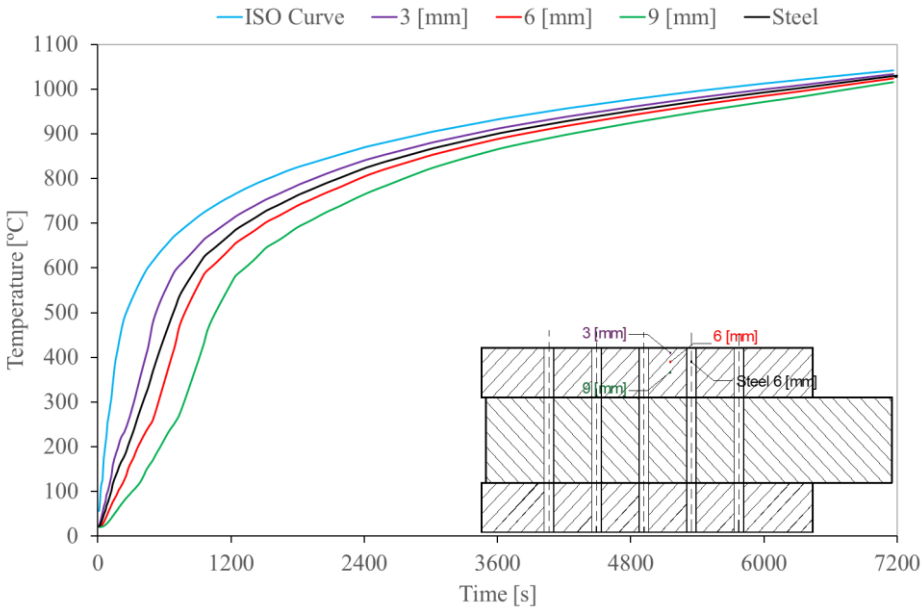

Figure 51: The temperature - time history in 3, 6 and 9 [mm] (top cross-section on level of dowels).

Figures 52, 53 and 54 represent the char layer obtained from the numerical analysis when the temperature reaches a value of 739 [°C], at a time of about 15 [min].

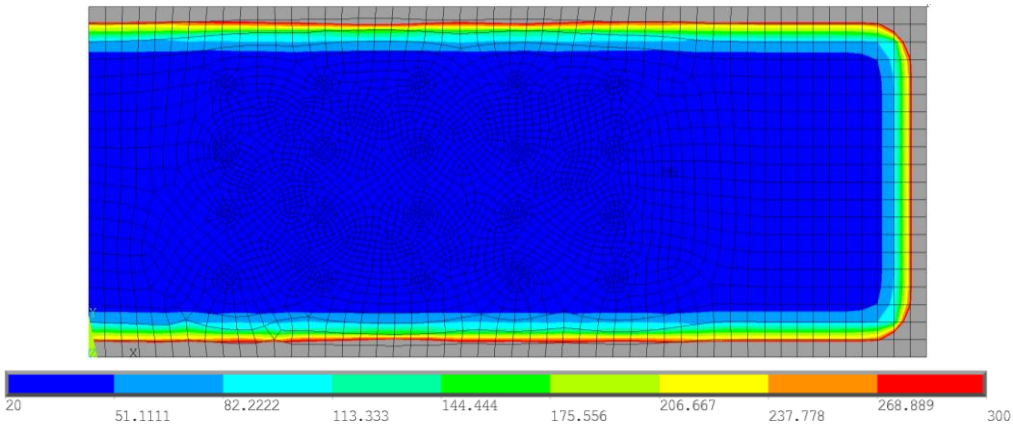

Figure 52: Char layer of the front side at 15 [min], 739 [ºC]

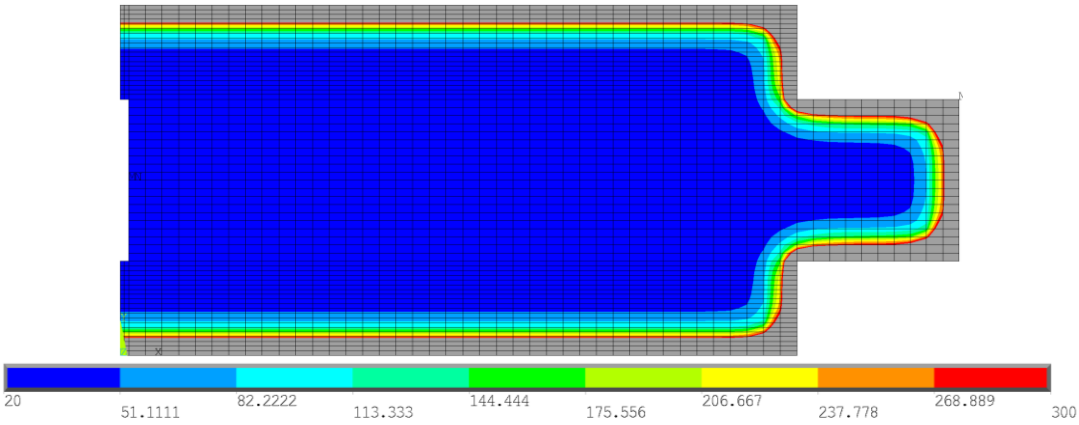

Figure 53: Char layer of the top side at 15 [min], 739 [ºC]

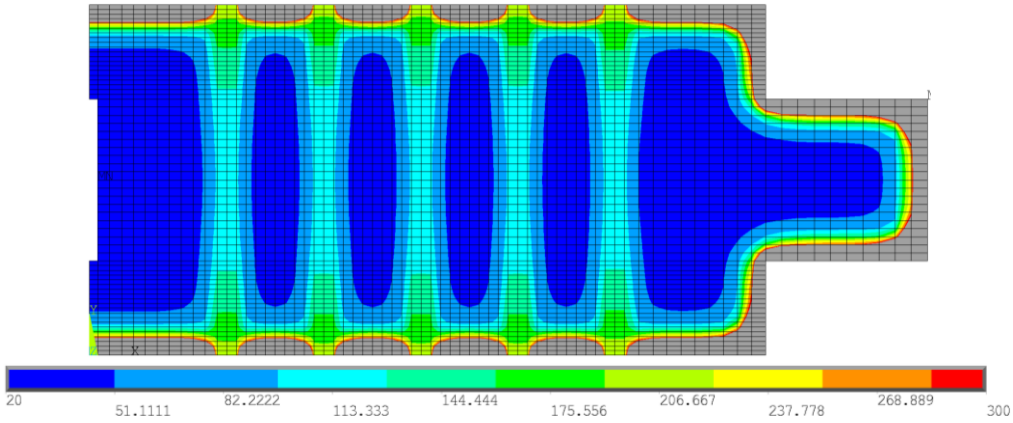

Figure 54: Char layer of the cross-section at the level of the dowels at 15 [min], 739 [ºC]

6.6.3. Conclusions of the FEM analysis results for the unprotected models

The produced charring rate from the different models at different nodal positions and different time instants are shown in tables 27, 28 and 29. The charring rate for a known depth far from the edge at certain time is calculated according the following equation (40):

$$\beta_0 = \frac{d_{[mm]}}{(t_{[s]}/60)} \tag{40}$$

Temperature	[ºC]	280			300		
Depth (d)	[mm]	10	20	30	10	20	30
Time (t)	[s]	1093,7	2023,7	3013,7	1133,7	2093,7	3073,7
Charring rate	β[mm/min]	0,59	0,59	0,60	0,53	0,57	0,59
The average	β[mm/min]	0,59			0,56		

Table 27: Results of the charring rate of the half-model at front side.

Temperature	[ºC]	280			300		
Depth (d)	[mm]	2,9125	5,825	8,7375	2,9125	5,825	8,7375
Time (t)	[s]	300,25	520,25	740,25	320,25	540,25	760,25
Charring rate	β[mm/min]	0,58	0,67	0,71	0,55	0,65	0,69
The average	β[mm/min]	0,65			0,63		

Table 28: Results of the charring rate of the half-model on top side.

Temperature	[ºC]	280			300		
Depth (d)	[mm]	2,9125	5,825	8,7375	2,9125	5,825	8,7375
Time (t)	[s]	305,23	515,23	745,23	325,23	545,23	775,23
Charring rate	β[mm/min]	0,57	0,68	0,70	0,54	0,64	0,68
The average	β[mm/min]	0,65			0,62		

Table 29: Results of the charring rate of the half-model at cross-section at the level of the dowels.

According to all the obtained results from the thermal transient analysis of the unprotected W-W-W connection, it can be concluded that the numerical models are in accordance with the calculations obtained from the (EC5 1-2), [8].

6.7. Protected W-W-W connection at high temperature

6.7.1. Protected connection at high temperature in FEM analysis

This sub-chapter represents the front and a top section of the protected model developed in the numerical program in 2D, considering three different insulation materials (gypsum, gypsum plasterboards and medium density fiberboards or MDF). Identical to the unprotected model, and due to the geometric symmetry and loading conditions, only one half of the model will be analyzed. The main objective of this analysis is to verify the heating effect produced by the fire in the protected wood connection, when different insulation materials are considered, or considering an extra thickness in the wood connection. Also, through different time instants of the thermal analysis, compare the results with the analytical calculations from chapter 5. According to the obtained theoretical results using Eurocode 5 1-2, [7], and for 30 [min] of fire

exposure, the calculated extra thickness for the gypsum, gypsum plasterboards and the medium density fiberboards are 12,1 [mm], 7,1 [mm] and 10 [mm], respectively.

Gypsum:

Figures 55 and 56 shows the front and top cross-section at the level of the dowels, for gypsum with an extra thickness of 12,1 [mm] in red color as presented.

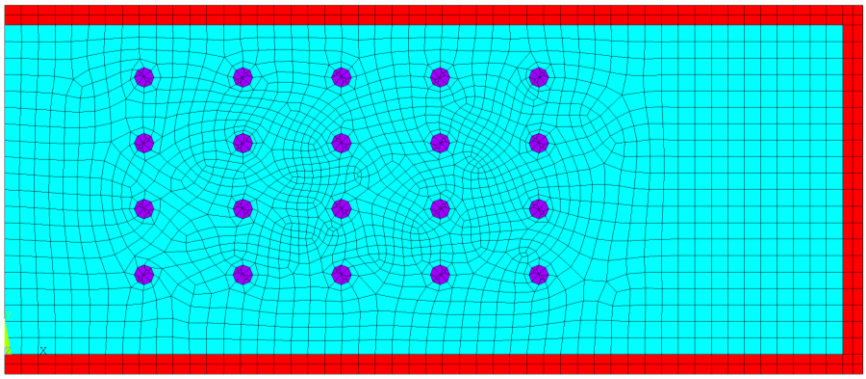

Figure 55: Front model of the protected W-W-W connection with gypsum.

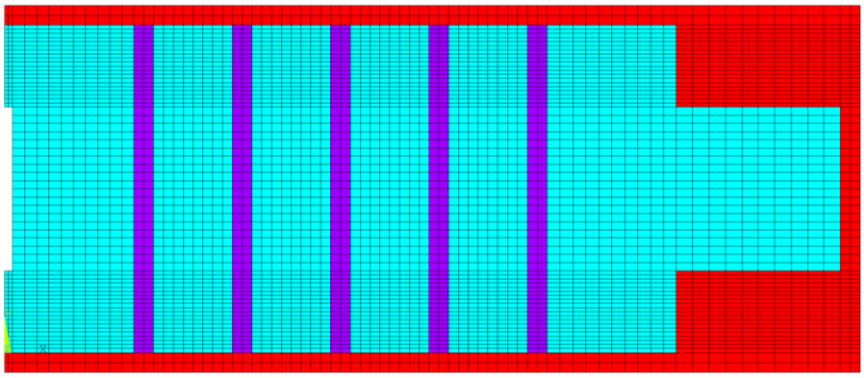

Figure 56: Top cross-section at the level of the dowels of the protected W-W-W connection with gypsum.

Gypsum plasterboards:

Figures 57 and 58 shows the front and top cross-section for gypsum plasterboards with an extra thickness of 7,1 [mm] produced in dark blue color.

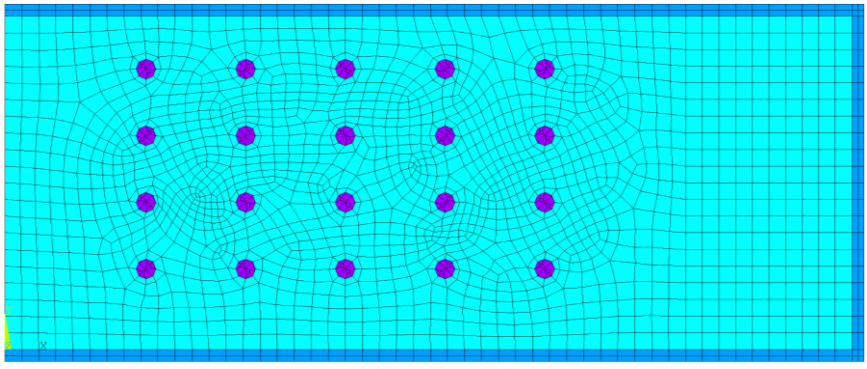

Figure 57: Front model of the protected W-W-W connection with gypsum plasterboards.

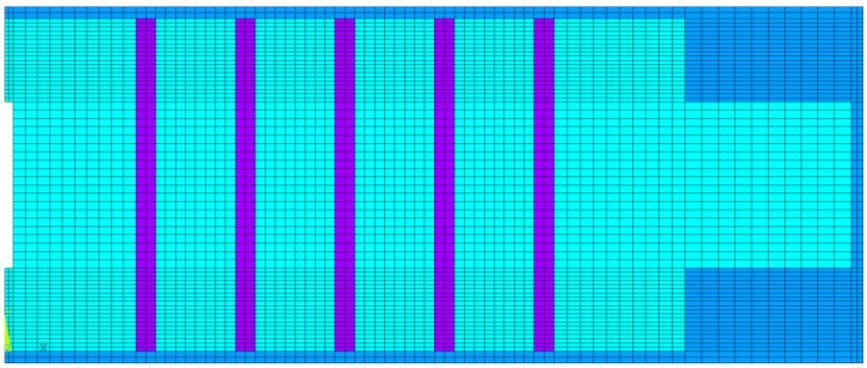

Figure 58: Top cross-section, level of the dowels, protected W-W-W connection with gypsum plasterboards.

Medium density fiberboards (MDF):

Figures 59 and 60 shows the front and top cross-section for medium density fiberboards (MDF), with an extra thickness of 10 [mm], as represented in pink color.

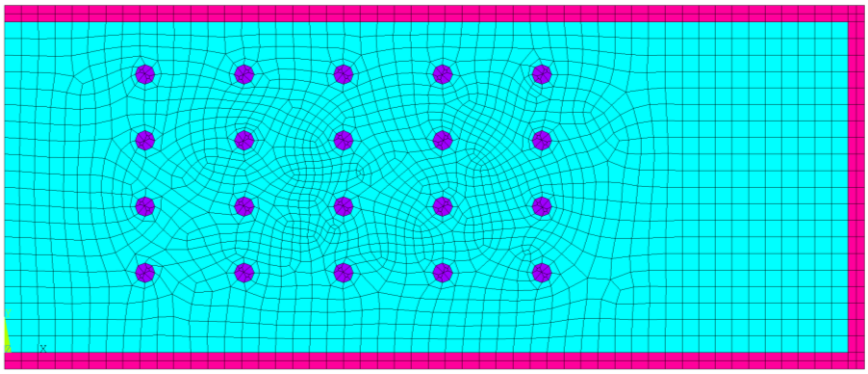

Figure 59: Front model of the protected W-W-W connection with MDF.

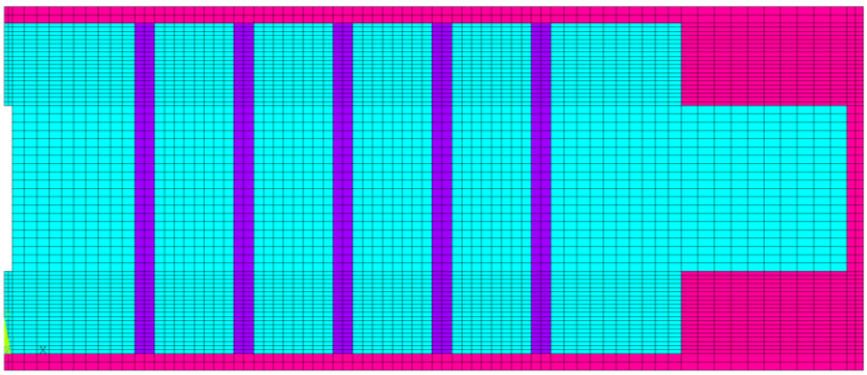

Figure 60: Top cross-section at the level of the dowels, protected connection with MDF.

Five different material properties are considered, as mentioned in previous. In the numerical analysis, the non-linear material thermal properties and temperature dependence (wood, steel and insulation materials) are the major determining factors to obtain desired results of the thermal analysis.

As it was mentioned for the unprotected model, and for thermal and transient analysis, all sides of each model will be subjected to fire conditions. According standard curve ISO-834 for fire situation, an incremental temperature will be subjected from 20 to 1049 [°C] (between 0 and 7200 [s]) in all six presented models, with a time step size equal to 10 [s].

6.7.2. FEM results of the protected model at high temperature

The produced charring rate from the different models with three different insulation materials at different nodal positions and different time instants is presented.

As for the unprotected models, the charring rate for a known depth far from the edge at certain time is calculated according equation (40).

Gypsum:

The melting point of a material is the temperature at which the solid and liquid phases of the substance are in equilibrium at a specified pressure (normally taken to be atmospheric). The melting point of the gypsum material is 1450 [ºC], [51]. Figure 61 and 62 show the time – temperature history for the 2D front model and top-section at the level of the dowels, both covered with gypsum material. Different nodes in steel, timber and gypsum material were selected to verify the evolution of the temperature during 7200 [s].

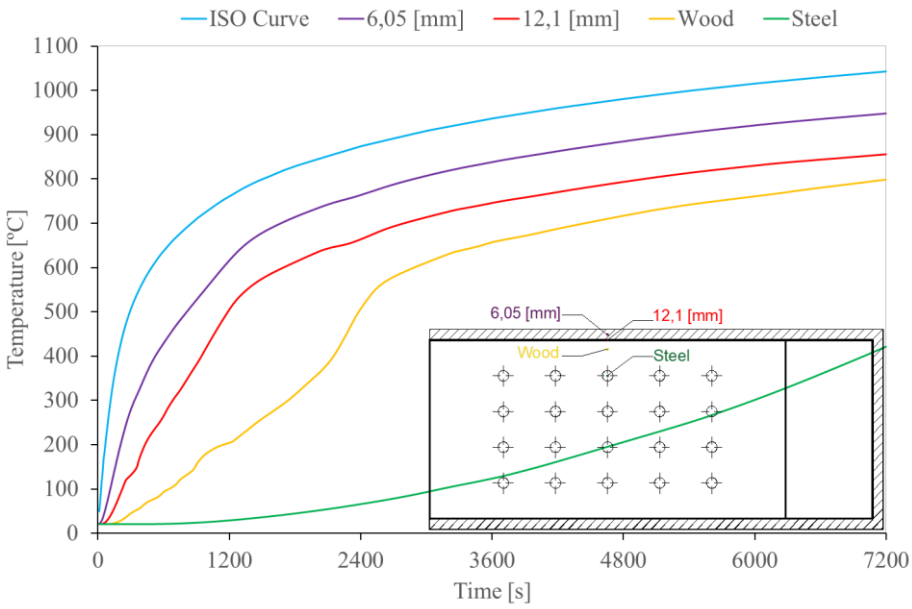

Figure 61: Temperature - time history for the front model with gypsum.

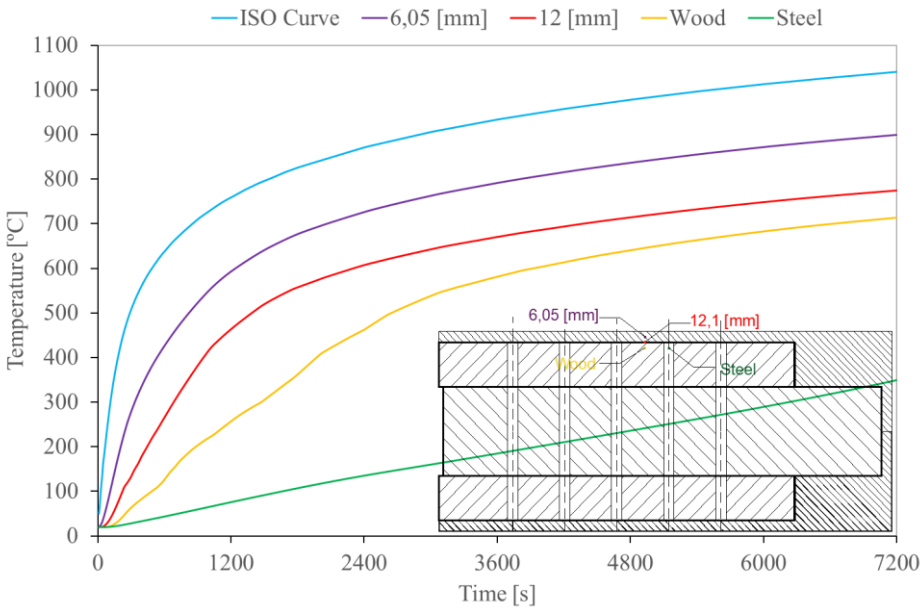

Figure 62: Temperature - time history, top-section at the level of the dowels, protected model with gypsum.

For both numerical representative models of W-W-W connection insulated with gypsum material, the model remains safe after the transient thermal analysis (7200 [s]) by reason of the thermal properties of the gypsum which is considered as one of the first-rated insulation materials in construction field. Steel remains at lower temperature during 7200 [s]. Wood material was more protected with a decrease in temperature evolution when compared with similar thermal analysis without insulation material. For the chosen nodal wood positions, only after more than 1800 [s] the char layer will start.

Figures 63 and 64 represent the layer obtained from the analysis when the temperature reaches a value of 1450 [°C], at a time of about 15 [min] for the W-W-W connection insulated with gypsum material. Both models show the protection in wood plate according the obtained temperature inside the material.

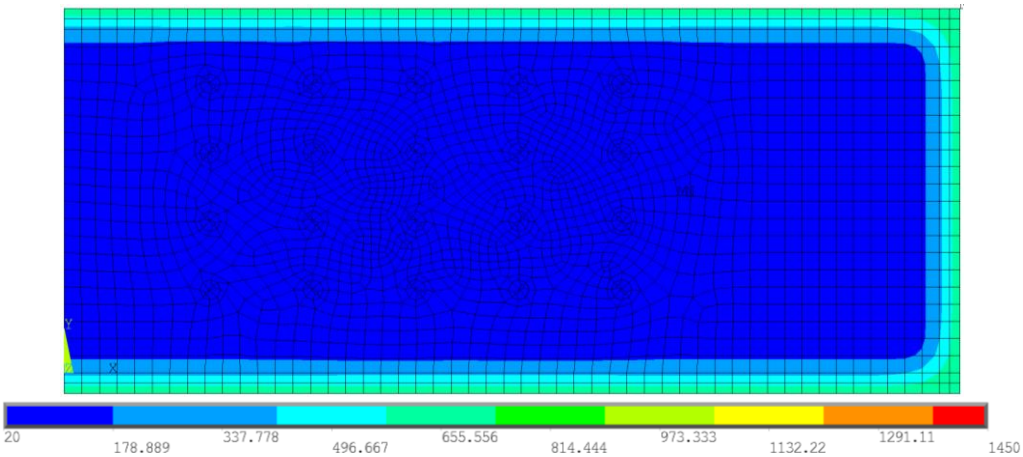

Figure 63: Char layer of the front model protected with gypsum at 15 [min].

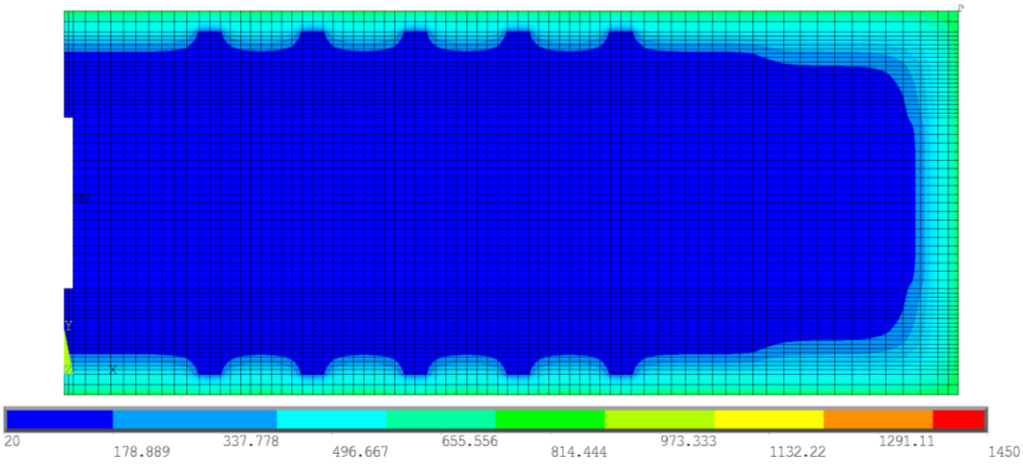

Figure 64: Char layer, top cross-section at the level of the dowels, protected model with gypsum at 15 [min].

Gypsum plasterboards:

Figures 65 and 66 represent the temperature evolution for the 2D models covered with gypsum plasterboard. The melting point of the gypsum plasterboard material is 1450 [ºC], [51].

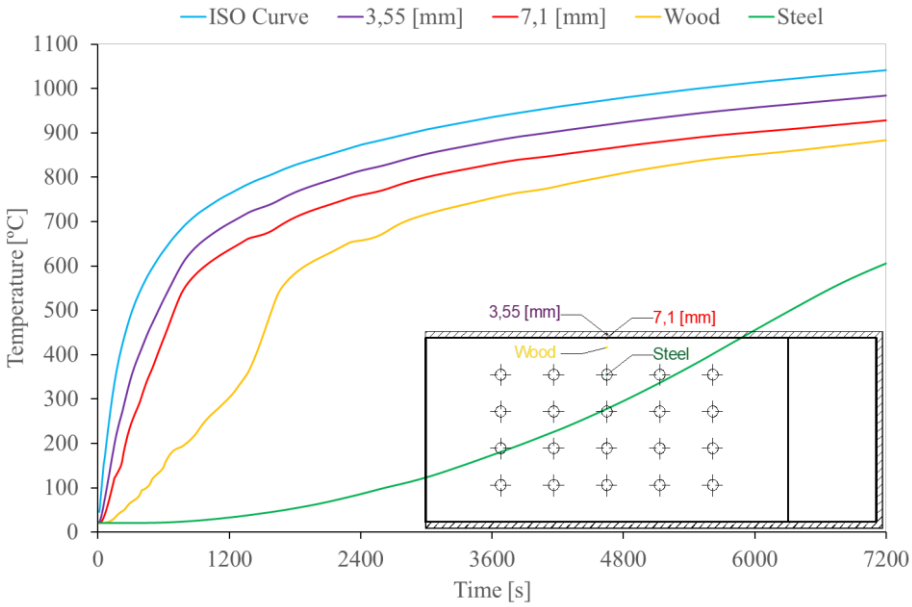

Figure 65: Temperature - time history for the front model with gypsum plasterboard.

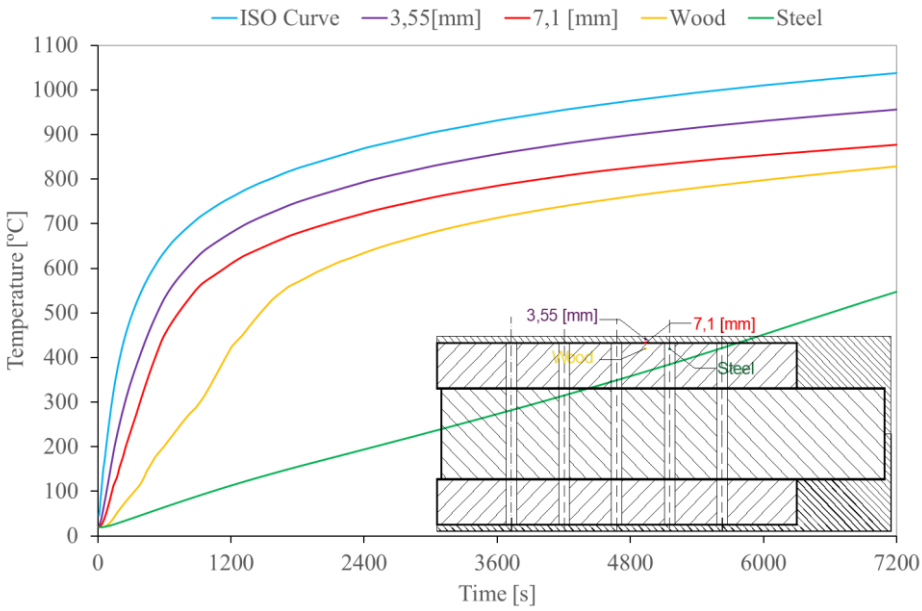

Figure 66: Temperature - time history, top cross-section at the level of the dowels, protected model with gypsum plasterboard.

Again, as well as for the models insulated with gypsum, for both numerical representative models of W-W-W connection insulated with gypsum plasterboard material, the model remains excellent after the analysis due to thermal properties of the gypsum plasterboard which is considered, as for gypsum, first-rated as an insulation material. It can be considered better than gypsum regarding his low thermal conductivity.

Figures 67 and 68 show the layer obtained from the analysis at a time about 15 [min] for the models insulated with gypsum plasterboard material. Wood material remains at lower temperatures.

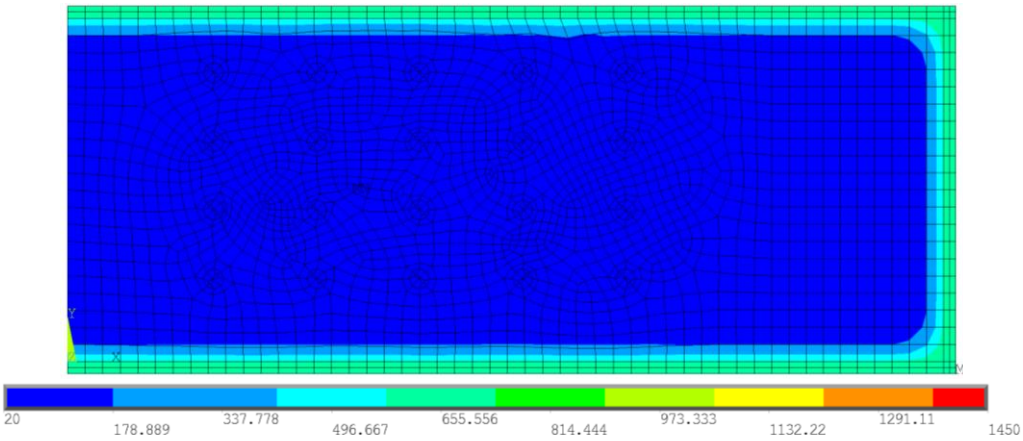

Figure 67: Char layer of the front model protected with gypsum plasterboard at 15 [min].

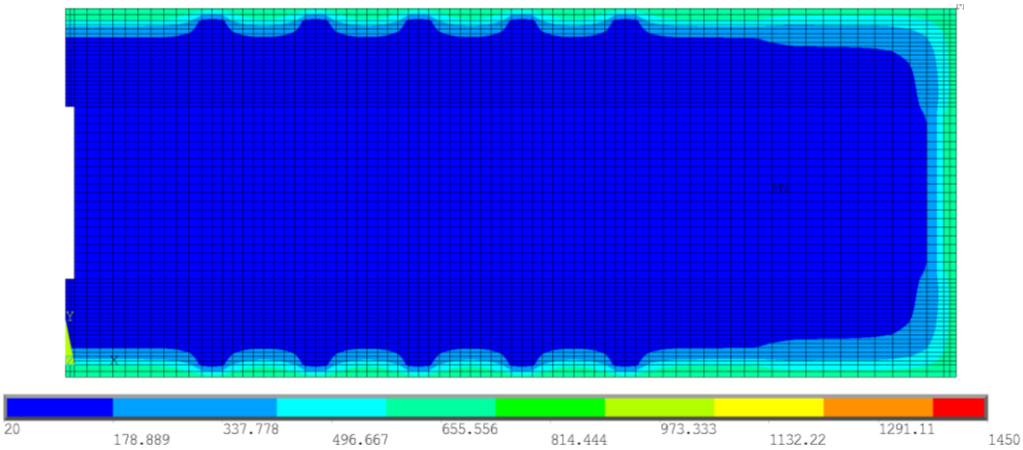

Figure 68: Char layer of top cross-section at level of the dowels, protected with gypsum plasterboard at 15 [min].

Medium density fiberboards (MDF):

Figures 69 and 70 represent the temperature evolution for the 2D models covered with medium density fibreboard (MDF). The melting point of the MDF is 275 [ºC], [51]. As the typical wood material, MDF has the same temperature which the material loses their physical characteristics. According to this effect, tables 30 and 31 represent the calculated charring rate obtained in two different nodal depths from exposure fire in MDF material.

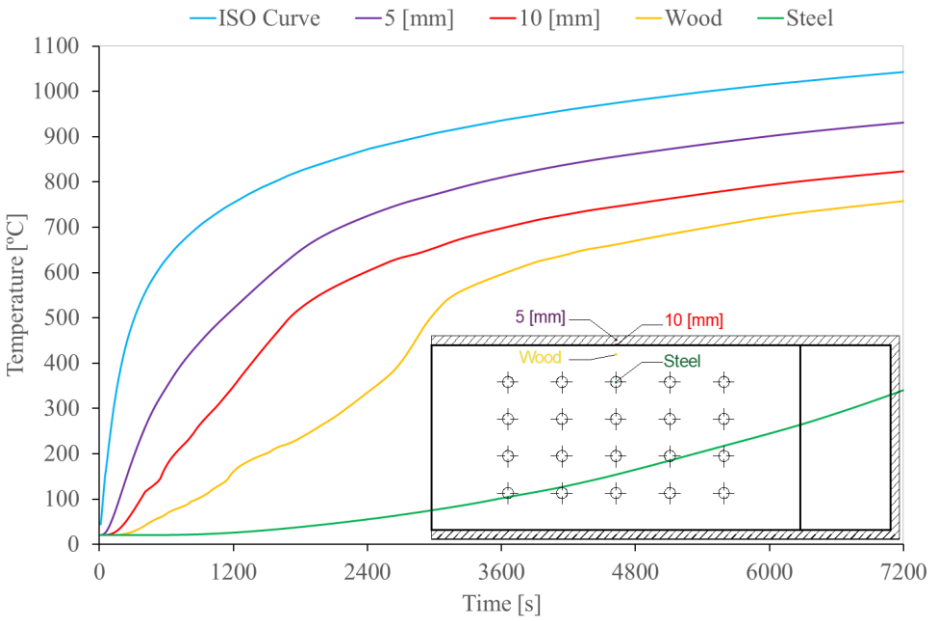

Figure 69: Temperature - time history for the front model with MDF.

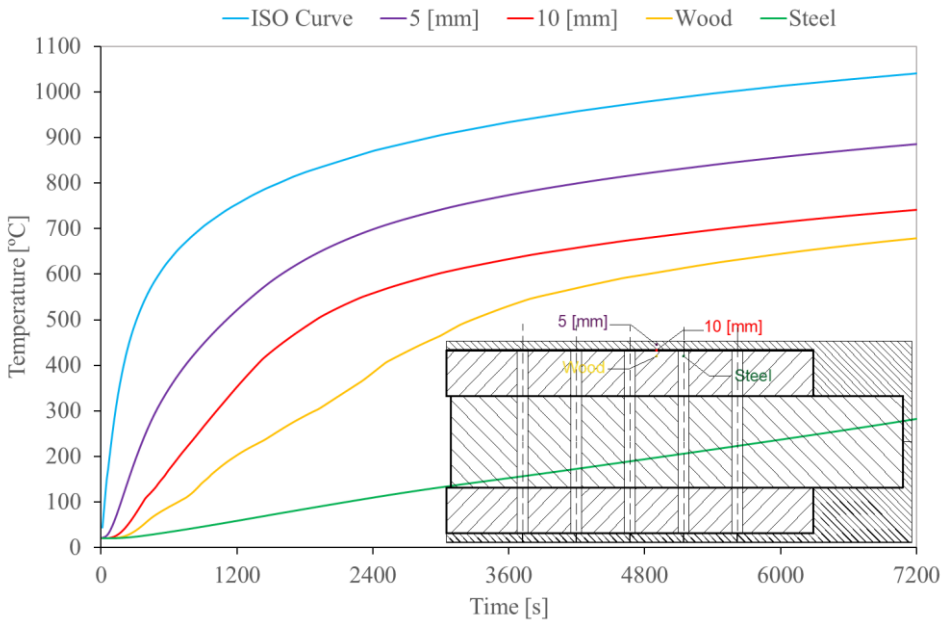

Figure 70: Temperature - time history, top cross-section at the level of the dowels, protected model with MDF.

On the regard of W-W-W connection insulated with MDF under high temperatures, the model remains insulated only for about 900 [s] or 15 [min], as the previous analytical calculation. After that, MDF material starts charring because the melting point for MDF is 275 [ºC]. Due to the thermal properties of MDF and regarding the similar results from the unprotected W-W-W connection, this type of insulation can be considered like a wood, and the layer of MDF can be considered as an extra thickness of timber. The charring rate calculated for two-time instants, according the equation (40), permits to obtain a medium value equal to 0,65 [mm/min].

Temperature	[ºC]	275	
Depth (d)	[mm]	5	10
Time (t)	[s]	447,36	957,36
Charring rate	β[mm/min]	0,67	0,63
The average	β[mm/min]	0,65	
h_p	[mm]	10	

Table 30: Results of the analysis for the front model with MDF.

Temperature	[ºC]	275	
Depth (d)	[mm]	5	10
Time (t)	[s]	437,36	947,36
Charring rate	β[mm/min]	0,69	0,63
The average	β[mm/min]	0,66	
h_p	[mm]	10	

Table 31: Results of the analysis, top cross-section at the level of the dowels, model with MDF.

Due to the thermal properties of MDF and regarding to the similar results from the unprotected W-W-W connection, this type of insulation can be considered like a wood, and the layer of MDF can be considered as an extra thickness of timber.

Figures 71 and 72 show the char layer at 15 [min] for the models insulated with MDF.

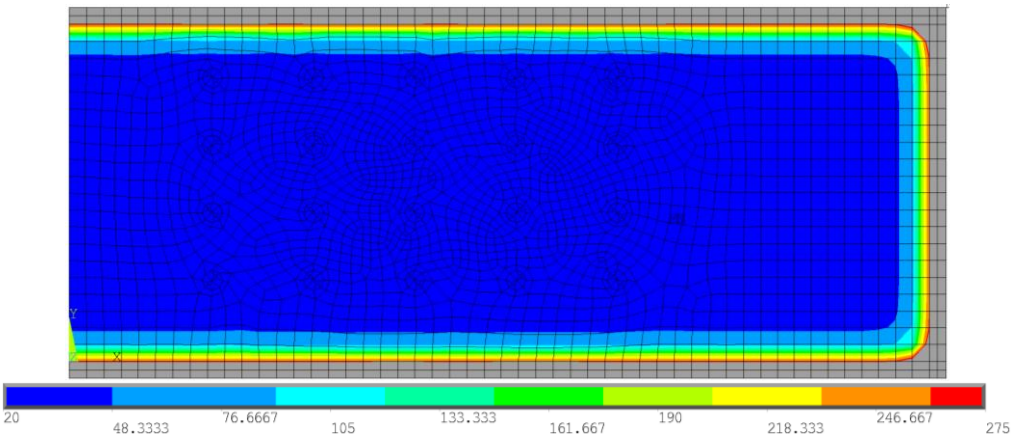

Figure 71: Char layer of the front model protected with MDF at 15 [min].

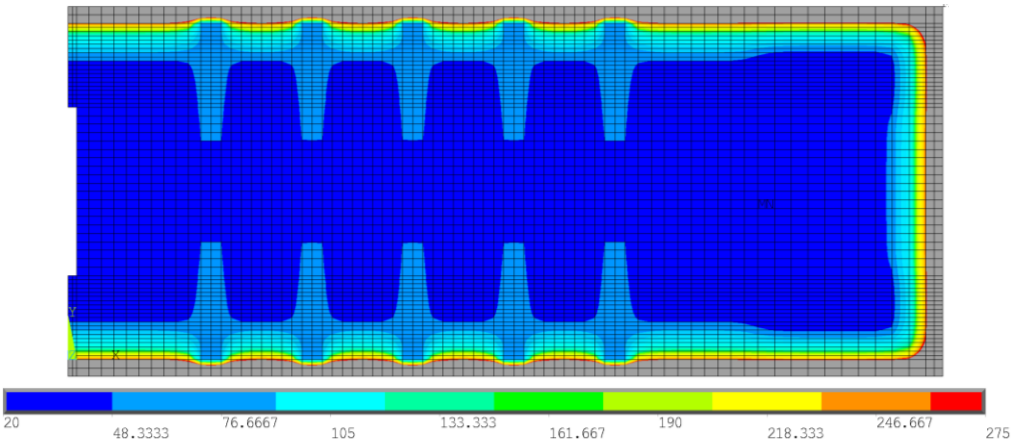

Figure 72: Char layer of the top cross-section, level of the dowels, protected model with MDF at 15 [min].

6.7.3. Conclusions of the FEM analysis results for the protected models

Regarding to the results shown in this previous sub-chapter about the protected models, it can be concluded that the behaviour of the insulation materials under fire depend essentially on their thermal properties. Gypsum plasterboards can be presented as the most insulating and protective material for the W-W-W connection when comparing with gypsum and medium density fiberboards. The numerical analysis finds accordance with the calculations made from standards (EC 5 1-2), [8]. The numerical model also allows to understand better the influence of dowels in the conduction of heat inside the connections, with the temperature profile from the numerical model.

Chapter 7

Conclusions

7. Conclusions

This work present different methodologies applied to the design of a typical W-W-W connection used in building construction. A procedure with all analytical equations were presented to assess the cross-section and all dimensions for an applied tensile load in the connection at ambient and high temperatures. Also, a numerical procedure using the finite element method was implemented to produce different simulations of 3D models focused on mechanical analysis, and 2D models for thermal analysis in transient and non-linear behaviour of the material. The numerical models represent the W-W-W connection with an applied incremental tensile load in mechanical analysis, in order to obtain the maximum critical load applied and to determine the maximum load capacity of each fastener. The same W-W-W connection was subject to fire situations in thermal transient analysis, considered unprotected and protected using different insulations materials (gypsum, gypsum plasterboard and medium density fibreboard (MDF)), allowing to understand the temperature development, the char layer formation and the charring rate calculation.

The comparison of several results obtained by 3D and 2D models showed a favorable accordance with the analytical calculations obtained from standards (EC5 1-1, [23]; EC5 1-2, [8]). These numerical simulations are very relevant, the models can be used for verification in other type of W-W-W connection subjected to fire action and mechanical loading conditions.

Wood material when exposed to fire presents a thermal physical degradation. The predicted ultimate load from the numerical model of W-W-W connection was greater than the calculated load carrying according standards (EC5 1-1, [23]). The model overestimates the resistance with 18,49%. The numerical value is obtained from an analysis with time step equal to 5 [s], more precision results can be reached by decreasing the time step.

In W-W-W connections, the type and the dimensions of timber plates, the number and the position of dowels can limit the use of these constructive elements in terms of fire resistance. Also, the different temperature evolution obtained, is due to the geometry and position of elements. The calculated charring rates are approximately equal to the results from EC5 1-2, [8]. These constructive elements should be chosen before, to prevent and delay the fire damage effect, allowing that the connection could remain in service with more safety and durability. W-W-W connection with an insulation layer of gypsum plasterboard and gypsum (protected) are more stable under fire conditions (more than 120 [min]), when compared with W-W-W

connection with an extra thickness of timber (unprotected) and with an insulation layer of medium density fiberboard MDF (protected) under the same condition (15 [min]).

The use of insulation material increases the fire resistance and the safety of the W-W-W connection, with no flames propagation to the timber plates. The insulating materials are based on the thermal properties which include the density, specific heat and mostly the low thermal conductivity. These parameters determine the temperature distribution in transient conditions and measures the ability of a material to fire resistance, indicating how quickly a material temperature will change. Increasing the thickness of the protection material, will reduce the temperature level around the connection. The use of MDF enables the evolution of heating, when compared with gypsum plasterboard. Also, the temperature degradation of gypsum plasterboard is higher (1450 [ºC]) when compared with MDF (275 [ºC]).

Finally, the results showed in this work, reveal extreme importance because they give great information for designers, more details about the behaviour of the W-W-W connections and the use of insulation materials in simultaneous, in fire situations. This knowledge can be taken into account for the building construction to minimize the failure and increasing the people safety.

Considering the works carried out in this study, some suggestions for future work will be presented, as the following:

- propose a numerical model under coupled mechanical and thermal analysis. The thermomechanical analysis could give different results to compare with the previous investigations,
- perform different experimental tests for both mechanical and the thermal behaviour to correlate the results with the numerical analysis,
- carry out different experimental and numerical tests with other type of connections to be used in timber structures, considering different sizes, geometries and type of connectors.

Chapter 8

Bibliography

8. Bibliography

[1] Diana.C.V. Coelho, Modelo Computacional para Avaliação Térmica e Mecânica de Estruturas em Madeira, Dissertação em Mestrado em Engenharia da Construção, Instituto Politécnico de Bragança, P 08-27, Novembro 2011.

[2] Luísa.M.S. Barreira, Estudo Numérico do Comportamento Térmico e Mecânico de Estruturas em Madeira, Dissertação em Mestrado em Engenharia Industrial (Ramo Engenharia Mecânica), Instituto Politécnico de Bragança, P 27-29, Decembro 2008.

[3] C. Maraveas, K. Miamis and C.E. Mathew, Performance of Timber Connections Exposed to Fire, Fire Technology, School of Mechanical, Aerospace and Civil Engineering, The University of Manchester, UK, Vol. 51, p1401–1432, 2013.

[4] Lei Peng, et al., On the Fire Performance of Double-shear Timber Connections, Canada, Fire Safety Science, Vol. 10, P. 1207-1218, 2011.

[5] J. Branco, P. Cruz, M. Piazza, Comportamento semi-rígido de ligações tradicionais de madeira, 4as Jornadas Portuguesas De Engenharia De Estruturas (JPEE), Laboratório Nacional de Engenharia Civil (LNEC) - Centro de Conferências, Lisboa, Portugal, 13 a 16 de Dezembro de 2006.

[6] L. Dias, S. Teixeira, Elza M. M. Fonseca, Resistência ao Fogo Vigas de Madeira e Secções Perfis em Aço, 4as Jornadas de Segurança aos Incêndios Urbanos, Instituto Politécnico de Bragança, Portugal, 06-07 de Novembro de 2014.

[7] S. I. F. Barbosa, Reforço de Ligações Tradicionais de Madeira, Dissertação em Mestrado em Engenharia Civil, Escola de Engenharia, Universidade do Minho, P 01-22, Novembro 2015.

[8] CEN, EN1995-1-2: Eurocode 5: Design of timber structures. Part 1-2: General Structural fire design, Brussels, 2003.

[9] P.B. Cachim, et al. Aplicação do Eurocódigo 5 na Avaliação de Ligações Tradicionais de Madeira ao Fogo, Departamento de Engenharia Civil & LABEST, Universidade de Aveiro, Mecânica Experimental, Vol. 20, P. 41-49, 2012.

[10] CEN, EN1991-1-2: Eurocode 1: Actions on structures. Part 1-2: General actions - Actions on structures exposed to fire, Brussels, 2002.

[11] S. B. A. Boadi, Full Scale Tests on the Performance of Hybrid Timber Connections in Real Fires, Master Dissertation of Applied Science in Civil Engineering, Department of Civil and Environmental Engineering, Carleton University, Ottawa, Ontario, P 01-39 / P 147-149, 2015.

[12] A. Akotuah Ohene, Modelling the Fire Performance of Hybrid Steel-Timber Connections, Master Dissertation of Applied Science in Civil Engineering, Department of Civil and Environmental Engineering, Carleton University, Ottawa, Ontario, P 01-56 / P 140-143, 2014.

[13] A. Frangi, C. Erchinger, M. Fontan, Experimental Fire Analysis of Steel-to-Timber Connections Using Dowels and Nails, Institute of Structural Engineering IBK, Zurich, Switzerland, Fire and Materials, Vol. 34, P. 01-19, January 2010.

[14] M. Audebert, D. Dhima, M. Taazount, A. Bouchair, Thermo-Mechanical Behaviour of Timber-to-Timber Connections Exposed to Fire, Clermont University, Clermont-Ferrand, France, Fire Safety Journal, Vol. 56, P. 52-64, February 2010.

[15] C. Grunwald, et al., Adhesively bonded timber joints, Germany, International Journal of Adhesion and Adhesives, Vol. 55, P. 12-17, December 2014.

[16] Ad. Leijten, Timber Connections (EN1995-1-1: Section 8 - Connections), Dissemination of Information Workshop, Brussels, 18-20 February 2008.

[17] C. Austruy, et al., Experimental Testing and Analytical Prediction of the Behaviour of Timber Bolted Connections Subjected to Fire, Journal of Fire Technology, DOI: 10.1007/s10694-009-0096-6, P46-129, January 2010.

[18] N. Jasuja, S. Gauri, S. Pooja, B. Rupal, T. Kate, Hardwood vs Softwood, Diffen.com, Diffen LLC, n.d. Web. (2016, Oct 19), Retrieved from: 'http://www.diffen.com/difference /Hardwood_vs_Softwood'.

[19] BS 350-2:1994, Durability of Wood and Wood - based Products - Natural Durability of Solid Wood -, Part 2: Guide to Natural Durability and Treatability of Selected Wood Species of Importance in Europe, British Standard Institution 'BSI', May 1994 Revised 1999.

[20] Wood Figure and Grain Terms, hobbithouseinc.com, (2016, Oct 18), Extracted from: 'http://hobbithouseinc.com/personal/woodpics/_figureandgrainterms.htm', (Hobbit House Glossary).

[21] Densities of Wood Species, Engineeringtoolbox.com, (2016, Oct), Retrieved from: 'http://www.engineeringtoolbox.com/wood-density-d_40.html'.

[22] D.W. Green, Mechanical Properties of Wood, Department of Agriculture, Forest Service, Forest Products Laboratory, Chapter 4: P 01-26, 1999 Revised June 2002.

[23] CEN, EN1995-1-1: Eurocode 5: Design of timber structures. Part 1-1: General - Common rules and rules for buildings, Brussels, 2008.

[24] Modulus of Elasticity or Young's Modulus - and Tensile Modulus for common Materials, Engineeringtoolbox.com, (2016, Nov 08), Retrieved from: 'http://www.engineering toolbox.com/young-modulus-d_417.html'.

[25] Mechanical Properties of Wood, (2016, Nov), Retrieved from: 'Lignum Journal'.

[26] Wood Density Chart, Workshop, (2016, Nov 19), Extracted from: 'https://cedarstripkayak .wordpress.com/lumber-selection/162-2/'.

[27] CEN, EN1993-1-2: Eurocode 3: Design of steel structures. Part 1-2: General rules - Structural fire design, Brussels, 2005.

[28] Wood Strengths, Woodworkweb.com, Web. (2016, Nov), Source: U.S. Forest Products Laboratory and Chris Messier – Messman, Canada, Retrieved from: 'http://www.wood workweb.com/woodwork-topics/wood/146-wood-strengths.html'.

[29] C. C. Gerhards, Effect of Moisture Content and Temperature on The Mechanical Properties of Wood: An Analysis of Immediate Effects, Forest Products, U.S. Department of Agriculture, (Received: 15 of November 1980), Wood and Fiber, Vol. 14 (01), P. 04-36, January 1982.

[30] R. C. Zeller, R. O. Pohl, Thermal Conductivity and Specific Heat of Non-Crystalline Solids, Laboratory of Atomic and Solid-State Physics, Cornell University, New York, USA, Physical Review B, Vol. 4, P 2029, 15 September 1971.

[31] Wood Strength, Workshopcompanion.com, (2016, Nov 09), Extracted from: 'http://workshopcompanion.com/KnowHow/Design/Nature_of_Wood/3_Wood_Strength/3_ Wood_Strength.htm'.

[32] AISI / SAE Steel – Numbering System, Engineeringtoolbox.com, (2016, Oct 23), Retrieved from: 'http://www.engineeringtoolbox.com/aisi-sae-steel-numbering-systemd_1449 .html'.

[33] CEN, EN1993-1-1: Eurocode 3: Design of steel structures. Part 1-1: General rules and rules for buildings, Brussels, 2005.

[34] DIN 1052: 2004-08, Design of timber structures – General rules and rules for buildings, Deutsche Norm, Deutsche Institut fur Normung (Normenausschuss Bauwesen), August 2004.

[35] Ruben F P Silva, Cálculo ao Fogo de Ligações de Madeira, Dissertação para obtenção do Grau de Mestre em Engenharia Civil, Universidade de Aveiro, 2009.

[36] Saeed Moaveni, Finite Element Analysis (Theory and Application with ANSYS, Minnesota State University, Mankato, 1999.

[37] M. Kaloop, Advanced Materials, Structures and Mechanical Engineering, Incheon National University, Department of Civil and Environmental Engineering, South Korea, P 61-62, 2016.

[38] P. M. Kurowski, Engineering Analysis with SolidWorks Simulation, SDC Publications, Department of Mechanical & Materials Engineering, Western University, Ontario, Canada, 2016.

[39] Maraveas, C., Miamis, K. and Mathew, C.E., Performance of Timber Connections Exposed to Fire, Fire Technology, DOI: 10.1007/s10694-013-0369-y, Vol. 51(6), P1-32, November 2013.

[40] Peng L, Hadjisophocleous G, Mehaffey J, Mohammad M., Fire Performance of Timber Connections, Part 1: Fire Resistance Tests on Bolted Wood-Steel-Wood and Steel-Wood-Steel Connections, Journal of Structural Fire Engineering, DOI: 10.1260/2040- 2317.3.2.107, Vol. 3(2), P107-131, June 2012.

[41] P. J. Moss, A. H. Buchanan, M. Fragiacomo, P. H. Lau and T. Chuo, Fire Performance of Bolted Connections in Laminated Veneer Lumber (LVL), MEFE Thesis, Department of Civil Engineering, University of Canterbury, Auckland, New Zealand, Fire and Materials, Fire Mater, DOI: 10.1002/fam.999, Vol. 33, P. 223-243, 20 April 2009.

[42] F. Ewelina, Fire properties of Wood-based Panels, Annals of Warsaw University of Life Sciences - SGGW, Fire Research Department of Building Research Institute, Forestry and Wood Technology, Vol. 86, P. 109-113, 2014.

[43] J. Haddad, Numerical Analysis of Wooden Slabs with Perforations Under Fire Conditions, Master Dissertation in Construction Engineering, Instituto Politécnico de Bragança, P 32-34, Julio 2016.

[44] BSI EN 13986:2004, Wood-based Panels for Use in Construction - Characteristics, Evaluation of Conformity and Marking, ICS 83.140.99, British Standards Institution, London, 2004.

[45] Medium Density Fiberboard, Robelbois.com, Web. (2017, Mar), France, Retrieved from: 'https://www.robelbois.com/en/mdf/'.

[46] ISO/FDIS 10456:2007(E), Building Materials and Products - Hygrothermal Properties - Tabulated Design Values and Procedures for Determining Declared and Design Thermal Values, January 2007.

[47] A. Just, J. Schmid, J. König, Gypsum Plasterboards Used as Fire Protection - Analysis of a Database, SP Technical Research Institute of Sweden, Stockholm, Sweden, 2010.
[48] F. S. Óscar, A. G. Paulo, Comportamento ao Fogo de Ligações de Aço em Estruturas de Madeira, Dissertação em Licenciatura em Engenharia Mecânica, Instituto Politécnico de Bragança, P 17-21, Julho 2016.
[49] Bastian Pentenrieder, Finite Element Solution of Heat Conduction Problems in Complicated 3D Geometries Using the Multigrid Method, Dissertation in Mathematics, Technical University of Munich, Faculty of Mathematics, Munich, Germany, 29 July 2005.
[50] Lide D.R. (editor), CRC Handbook of Chemistry and Physics, 71st edition, Boca Raton, FL: CRC Press Inc., 1990-1991., p. 04-54.
[51] Material Safety Data Sheet: Ranger Board Medium Density Fiberboard, West Pine MDF, West Fraser Mills Ltd., Quesnel (British-Colombia), Canada, 2013.